Materials Science & Engineering R 167 (2026) 101099

Contents lists available at ScienceDirect

Materials Science & Engineering R

journal homepage: www.elsevier.com/locate/mser

Antiviral molecularly imprinted polymers: Engineered precision for multifunctional therapeutic strategies

Xiaohan Ma [a,*,1], Latifa W. Allahou [a,b,c,1], Ren Yang [a], Yingqi Ma [a], Myrto Dimoula [a], David Y.S. Chau [a], Gareth R. Williams [c], Jonathan C. Knowles [a,d,e], Alessandro Poma [a,*]

[a] Division of Biomaterials and Tissue Engineering, University College London (UCL) Eastman Dental Institute, Royal Free Hospital, UCL Medical School, Rowland Hill Street, London NW3 2PF, UK
[b] Department of Pharmaceutics, Faculty of Pharmacy, Kuwait University, Kuwait City, Kuwait
[c] UCL School of Pharmacy, University College London, 29-39 Brunswick Square, London WC1N 1AX, UK
[d] Department of Nanobiomedical Science and BK21 PLUS NBM Global Research Center for Regenerative Med-icine, Dankook University, Cheonan 31116, South Korea
[e] UCL Eastman-Korea Dental Medicine Innovation Centre, Dankook University, Cheonan 31116, South Korea

ARTICLE INFO

Key words:
Viral infection
Molecularly imprinted polymer
Antiviral application

ABSTRACT

The pressing need for innovative antiviral therapies has accelerated the exploration of molecularly imprinted polymers (MIPs), which exhibit selective and specific biomimetic recognition capabilities. Although originally developed for chemical sensing and diagnostic applications, MIPs have shown considerable potential in antiviral contexts due to their structural adaptability, chemical stability, tunable physicochemical properties, and capacity for tailored target recognition that can rival natural antibodies in certain applications. This review provides a comprehensive overview of virological principles and the limitations of conventional antiviral strategies, followed by a rationale for employing MIPs in antiviral therapeutic applications. It briefly summarizes MIP fabrication methods and examines their antiviral potential across four strategic domains. These include inhibiting viral entry by recognizing intact virions or surface components, disrupting genome synthesis and replication by targeting structural and non-structural proteins as well as viral nucleic acids, enhancing immune responses by interfering with viral immune evasion and promoting immune-mediated clearance, and facilitating antiviral drug delivery through sustained-release carriers, stimuli-responsive platforms, and applications in pharmaceutical detection and purification. In addition to highlighting these applications, the review addresses critical translational challenges such as biocompatibility, off-target effects, large-scale manufacturing, and regulatory considerations, which remain key barriers to real-world deployment of antiviral MIP technologies. Future efforts should emphasize intelligent design tools, biosafety optimization, and standardization to support the safe and effective clinical translation of antiviral MIPs. Together, these insights position MIPs as a highly promising, multifunctional, and technologically adaptable platform that addresses key limitations of conventional therapies and paves the way for next-generation precision antiviral interventions.

1. Introduction

1.1. General virology

Viruses are found in all of our surroundings: the air, the ocean, the soil, rivers, streams, and ponds. They are present wherever life occurs, and it is thought that every living thing has a virus that infects it [1]. In particular, for humans, some of the most devastating human diseases have been or still are caused by viruses, such as smallpox, yellow fever, poliomyelitis, influenza, measles, and acquired immunodeficiency syndrome (AIDS). Viral infections can lead to life-threatening diseases that impact all organs, including the lungs, liver, central nervous system, and intestines. Viruses are responsible for approximately 20 % of the human cancer burden, and viral infections of the respiratory and gastrointestinal tracts kill millions of children in the developing world each year [2]. The coronavirus disease 2019 (COVID-19), caused by severe acute respiratory syndrome coronavirus 2 (SARS-CoV-2), is the most representative in recent years [3]. This rapidly evolving infectious respiratory

* Corresponding authors.
E-mail addresses: xiaohan.ma.21@ucl.ac.uk (X. Ma), a.poma@ucl.ac.uk (A. Poma).
[1] These authors contributed equally.

https://doi.org/10.1016/j.mser.2025.101099
Received 23 February 2025; Received in revised form 8 August 2025; Accepted 25 August 2025
Available online 5 September 2025

disease first emerged at the end of December 2019. Despite the full attention of the World Health Organization (WHO) and the international community toward controlling the spread, as of 11 May 2025, over 777 million confirmed cases and > 7 million deaths had been reported globally [4].

The fight against viruses or viral infections requires an understanding of their characteristics and mechanisms of action. The definitive properties of viruses are summarized as follows:

(i) viruses are infectious, obligate intracellular parasites, meaning that they are entirely dependent upon the internal environment of the host cell to create new infectious virus particles;

(ii) the viral genome comprises DNA or RNA (but not both), and directs the synthesis of viral components by cellular systems within an appropriate host cell;

(iii) infectious progeny virus particles, called *virions*, the typical sizes of which are 20–1000 nm in diameter, are formed by *de novo* self-assembly from newly synthesized components;

(iv) a progeny virion assembled during the infectious cycle is the vehicle for transmitting the viral genome to the next host cell or organism, where its disassembly initiates the next infectious cycle [2].

It has been argued extensively whether viruses are living organisms. Most virologists consider them non-living, as they do not meet all the criteria of the generally accepted definition of life, although they are intricately tied to the web of life here on Earth. It has also been argued, however, that viruses can be viewed as microbes that exist in two phases: an inanimate phase, the virion, and a multiplying phase in an infected cell [2].

Each virus possesses a protein capsid to protect its nucleic acid genome from a harsh environment. Virus capsids predominantly come in two shapes: helical and icosahedral [5]. Most viruses also have an envelope surrounding the capsid (Fig. 1).

The envelope is a lipid membrane derived from one of the cell's membranes, most often the plasma membrane, although the envelope can also come from the cell's endoplasmic reticulum, Golgi complex, or even the nuclear membrane, depending upon the virus. A virus that lacks an envelope is known as a "non-enveloped" or "naked" virus (Fig. 1). All viruses can be classified according to the nature of the nucleic acids in the virion (DNA or RNA), the symmetry of the protein shell (capsid), the presence or absence of a lipidic membrane (envelope), and the dimensions of the virion and capsid. They are commonly identified by genome type through the Baltimore classification system [2].

1.2. Current antiviral strategies and challenges

Vaccines and antiviral drugs are the two main armaments available to us to fight against viral diseases. The basic strategy behind vaccination is to present antigens to the immune system in such a way as to stimulate immunity against the fully virulent organism without causing disease [6]. Traditional vaccination strategies, based on inactivated viral preparations or live-attenuated strains, have successfully controlled extremely serious viral diseases (e.g., smallpox, polio, and measles). The eradication of smallpox is one of humankind's most outstanding achievements, thanks to massive vaccination worldwide [7, 8]. In addition to traditional vaccines, virus-vectored, subunit, viral-like particle, nucleic acid-based vaccines, and rational vaccine design provide innovative technologies to surmount existing vaccine development challenges.

On the other hand, antiviral drugs are agents [small or large molecule(s), synthetic or natural] that can decrease the morbidity and mortality related to the viral infection. They are designed to limit the survival and spreading of viruses by blocking any one or a combination of the stages of virus infection. Most are targeted to interfere with the replication of the viral genome. Besides these, other types of antiviral molecules include entry inhibitors, integrase inhibitors, protease inhibitors, interferons, immunomodulators, etc. [9] The antiviral drugs available to treat viral infections have saved tens of millions of human lives over the last decades, and they will continue to be a cornerstone for the treatment of current as well as (re)emerging viral infections [7].

While innovation continues, the development of vaccines and antiviral drugs still faces significant challenges. Pathogen genetic sequence variability remains a major impediment to vaccine development due to (i) tremendous genetic diversity among viral strains; (ii) antigenic drift, which involves minor, gradual mutations in viral genes encoding surface proteins, such as hemagglutinin and neuraminidase in influenza viruses. These mutations allow the virus to evade immune recognition over time, necessitating frequent updates to vaccines; (iii) antigenic shift, a more drastic process in which two or more viral strains combine to form a new subtype with a completely novel antigenic profile. Antigenic shift can lead to pandemics, as the immune system has no prior exposure to the new strain. Additionally, viruses with rapid mutation rates further complicate vaccine design [10]. Other barriers to vaccine development include host variability, vaccine safety concerns, environmental and geographical factors, and incomplete understanding of the mechanisms driving immunity [11]. Recent advances, such as the development of

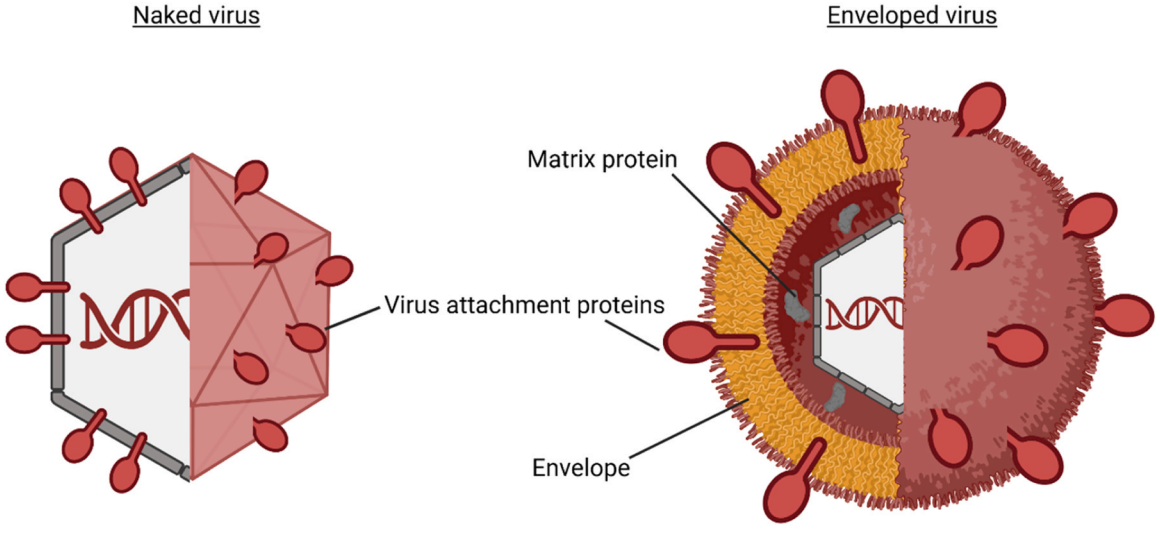

Fig. 1. Comparison Between a naked and enveloped virion: The capsid of an enveloped virion is wrapped with a lipid membrane derived from the host cell. Virus attachment proteins located in the capsid or envelope facilitate the binding of the virus to its host cell, adapted with permission from Louten [5]. Copyright 2016, Elsevier.

COVID-19 vaccines and the RSVpreF vaccine for respiratory syncytial virus (RSV), showcase the potential of vaccines to address major public health threats [12,13]. However, effective vaccines for pathogens such as human immunodeficiency virus (HIV), herpes simplex viruses (HSV-1 and HSV-2), and hepatitis C virus (HCV) remain elusive, reflecting the challenges posed by highly variable and immune-evasive viruses and highlighting the critical need for continued research and innovative approaches [14].

In terms of antiviral drug development, existing drugs are incapable of completely controlling viral infections. Since viruses rely primarily on the host cell's biosynthetic machinery for replication, only a limited number of virus-specific metabolic functions can be targeted by antiviral drugs without harming the host. The specificity of existing small molecule drugs is less than ideal, resulting in intrinsic toxicity during the treatment [15]. Their side effects (which include gastrointestinal tract reactions, hepatotoxicity, nephrotoxicity, cardiotoxicity, myelosuppression, etc.), hinder compliance with long-term medication usage and even result in discontinuation of treatment [16]. Furthermore, the high mutation rates of many virus strains lead to severe pharmacological resistance and, subsequently, to the loss of efficacy of current antiviral drugs [17]. For example, the retrovirus HIV uses reverse transcription to replicate its genome within the infected host cell. The reverse transcriptase is highly error-prone, resulting in high nucleotide substitution rates, increased population diversity and frequent resistance mutations during drug treatment [18]. Moreover, the physicochemical and pharmacokinetic shortcomings of existing antiviral drugs, such as low solubility, poor permeability, short circulation half-life, insufficient targeting ability, and low bioavailability, have restricted their efficacy [16]. Therefore, despite the vast diversity of human viruses (over 200 currently known), antiviral drugs are approved only for a handful of viruses, including HIV, HCV, influenza virus, RSV, hepatitis B virus (HBV), human papillomavirus (HPV), herpesviruses, and SARS-CoV-2 [9].

The intrinsic biological complexity and rapid adaptability of viruses have increasingly constrained the efficacy of existing antiviral strategies. Immune evasion, mutation-driven resistance, off-target toxicity, and poor pharmacokinetic profiles remain persistent barriers, undermining therapeutic outcomes and contributing to significant adverse effects. These multifactorial challenges highlight the urgent need for next-generation antiviral platforms with superior target selectivity, improved biostability, and adaptability to viral evolution.

1.3. Molecularly imprinted polymers (MIPs)

Molecularly Imprinted Polymers (MIPs) have emerged as a promising class of synthetic materials for antiviral therapy. They are engineered to exhibit selective molecular recognition toward specific viral targets, and their robust chemical and thermal stability ensures functionality under physiologically relevant or even harsh environmental conditions. Additionally, MIPs can be synthesized in a cost-efficient manner and structurally adapted to support a range of therapeutic applications, including viral neutralization, immune modulation, and controlled drug delivery. These properties make MIPs a distinctive and versatile platform for addressing key challenges associated with conventional antiviral approaches. The following sections will introduce the fundamental principles of MIPs, their fabrication techniques, and their emerging roles in antiviral applications.

1.3.1. Rationale of MIPs

MIPs are biomimetic synthetic materials that mimic natural antibody-antigen systems, featuring specific cavities that recognize and bind target molecules with high affinity and selectivity. MIPs are synthesized by copolymerizing functional monomers and cross-linkers in the presence of target molecules, known as templates [19,20]. Templates can range from small molecules, peptides, proteins, viruses, to even whole cells, including bacteria [21,22]. Depending on the application, either a single template or multiple templates may be chosen [23]. During polymerization, functional monomers form a complex with the template through interactions such as hydrogen bonding, electrostatic forces, van der Waals forces, or hydrophobic interactions in the case of non-covalent imprinting. In covalent imprinting, reversible covalent bonds are formed between the template and monomers before polymerization, which are later cleaved to create the recognition cavities. After the removal of template molecules, the resulting polymer exhibits complementary shape, size, and chemical functionality within the matrix, enabling it to bind target molecules via a "lock and key" mechanism (Fig. 2)[19,20,24].

Compared to natural antibodies (proteins), MIPs exhibit higher physicochemical robustness, resistance to elevated temperature and pressure and high inertness towards acids, bases, metal ions and organic solvents. In addition, they are also less expensive to be synthesized and can usually be stored for longer periods than natural biomolecules in absence of special environmental storage conditions [26].

1.3.2. Production of MIPs

The formation of MIPs typically relies on free radical polymerization (FRP) or controlled/living radical polymerization (CRP), using functional monomers (*e.g.*, acrylic or vinyl derivatives) and suitable crosslinkers to generate stable polymer networks with specific recognition sites. Depending on the nature of the template (size, structure, chemistry, *etc.*) and the intended application, MIPs can be designed and produced in diverse physical forms, such as monoliths, micro/nanoparticles, films, and nanocomposites (*e.g.* core–shell particles with inorganic cores like SiO_2 and Fe_3O_4) [27]. The overall design process involves three interrelated considerations: selecting a representative and stable template, choosing functional monomers with suitable binding affinity, and adopting a polymerization strategy that ensures effective site accessibility and recognition performance [28]. These factors collectively determine the imprinting efficiency, selectivity, and downstream applicability of antiviral MIPs. General design principles and systematic considerations for template and monomer selection are available in several comprehensive reviews [29–34]. In this section, we outline the main MIP preparation strategies and assess their respective advantages, limitations, and suitability for antiviral applications.

1.3.2.1. Bulk imprinting polymerization. Bulk imprinting polymerization is a standard imprinting method that has been widely used for the imprinting of small molecules. In this technique, the template is added directly into the monomer mixture to form a pre-polymerized complex which subsequently undergoes polymerization. This process generates interaction sites that are distributed both on the surface and throughout the entire bulk of the polymer matrix [35]. However, this approach has limitations, as many of the selective binding sites within the polymer matrix are only accessible through extended diffusion pathways, leading to unfavorable binding kinetics [36]. Particularly for macromolecules (*e.g.* viruses, proteins), their diffusion into the imprinted cavities buried inside a highly crosslinked MIP matrix is significantly hindered by their large size [37].

To overcome these issues, modified bulk systems have been developed. For instance, porous or flexible polymer matrices, hybrid organic-inorganic composites, and cryogel-based MIPs have been introduced to improve mass transfer and site accessibility [38]. Among these, hydrogels have gained particular attention. As hydrophilic, 3D polymer networks, they offer improved molecular diffusion, enhanced flexibility, and better binding kinetics compared to conventional dense matrices [36]. In addition, density fluctuations in the hydrogel network create regions or microgels of localized higher crosslinking, which contain an effective imprinting structure and proper rigidity to produce adequate specificity [39,40]. Furthermore, the 3D matrix of hydrogels offers a greater number of imprinted cavities that are complementary to the shape of the template. This makes hydrogels particularly well-suited for

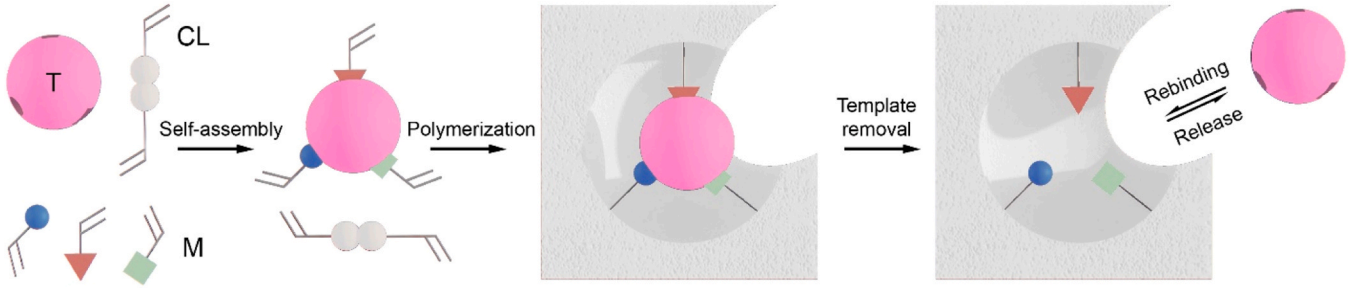

Fig. 2. Schematic illustration of the general principle of molecular imprinting. The process begins with the self-assembly of functional monomers (M) and cross-linkers (CL) around a template molecule (T), forming a pre-polymerization complex. Upon polymerization, a cross-linked polymer network is created with the template embedded in its matrix. Subsequent template removal leaves behind specific binding cavities that are complementary in shape, size, and chemical functionality to the original template. The final rebinding–release process allows selective recognition of the target molecule based on these imprinted sites. Adapted with permission from Haupt [25]. Copyright 2003, American Chemical Society.

the extraction of large quantities of templates, such as viruses [41]. Consequently, there are diverse examples using hydrogels for imprinting whole viruses (2.1.3) [42,43].

1.3.2.2. Surface imprinting polymerization. In contrast to bulk imprinting, which distributes recognition sites throughout the polymer matrix, surface imprinting strategically positions these sites predominantly on the polymer surface. This approach focuses on creating binding sites in a thin surface layer, improving accessibility and binding kinetics for large biomolecules such as proteins, viruses, and even cells [35]. The surface imprinting technique include soft lithography, template immobilization, emulsion polymerization, and electropolymerization [44]. Each method offers unique advantages in terms of the precision and efficiency of the imprinting process.

For example, soft lithography enables detailed patterning of surfaces, which is particularly useful for creating highly selective biosensors [45]. Template immobilization involves the attachment of the template molecule onto a solid support, which is then used to form the imprinted polymer surface. This method is particularly useful for creating recognition sites with high specificity while introducing properties of the support itself [46]. Emulsion polymerization is used to create uniformly sized imprinted particles, which are advantageous for industrial applications due to their reproducible binding characteristics [47]. Electropolymerization is another method under the surface imprinting umbrella, where polymerization is initiated by applying an electrical potential. This technique enables precise control over the thickness and morphology of the polymer layer, making it particularly suitable for creating thin MIP films on electrode surfaces for biomolecule detection and sensing [48,49].

Surface imprinting techniques enhance selectivity, mass transfer, and binding efficiency, making them ideal for peptides, proteins, and whole virus particles. Successful application, especially with macromolecular templates, requires effective template removal, as incomplete removal can reduce site accessibility and cause non-specific binding. Common methods include enzymatic treatment, surfactants or chaotropic agents, and pH or ionic modulation, chosen based on template and polymer stability [50]. Additionally, phase boundary effects at MIP-modified surfaces, such as hydration dynamics, diffusion barriers, and surface energy, can significantly influence recognition site performance [51]. Numerous examples of surface-imprinted MIPs targeting viral particles and proteins are presented throughout this review, highlighting their practical relevance in antiviral applications.

1.3.2.3. Solid-phase synthesis. Solid-phase synthesis involves immobilizing the template molecule on a solid support, followed by polymerization of monomers around the template. This is generally used for the synthesis of MIP nanoparticles (MIP NPs). After polymerization, the MIP NPs are released from the solid support. This method ensures the reliable reuse of molecular templates and maintains high affinity and specificity across multiple batches. Consequently, it is a cost-effective process, particularly for expensive templates like proteins and viruses [52,53]. While the overall yield of solid-phase synthesis may be lower than that of bulk imprinting due to limited template loading and additional separation steps, its ability to improve imprinting efficiency, reduce non-specific binding, and ensure batch-to-batch reproducibility supports its potential for scalable and high-specificity production in antiviral applications.

1.3.2.4. Comparative analysis of MIP preparation strategies. Although bulk, surface, and solid-phase imprinting each follow different synthesis pathways, their relative strengths and weaknesses become apparent when considering template size, recognition site accessibility, production scalability, and application context. Table 1 provides a side-by-side comparison of the three methods to guide their rational selection in antiviral MIP design.

In addition to the conventional synthesis strategies described above, recent advances have introduced computational modeling and artificial intelligence (AI)-based approaches to support the rational design of MIPs [56,57]. These emerging methods facilitate the selection of functional monomers, prediction of template–monomer interactions, and optimization of polymer architectures [58–60]. Such strategies are particularly useful for imprinting complex biological targets, including virus-derived proteins. While not the main focus of this review, these computational and AI-assisted approaches represent a growing trend in the production of MIPs and hold promise for improving the precision, efficiency, and adaptability of MIPs in biomedical applications.

1.3.3. Application of MIPs

MIPs have been widely applied in purification, separation science, and chemical/biological sensing [61–64]. Over the past decades, MIPs specifically designed for viral targets have also been primarily employed for detection purposes, aiming to meet the huge demand for diagnosing viral infections and determining trace amounts in virus-contaminated environments. Scientists have developed various types of MIP-based virus sensors including quartz crystal microbalance (QCM), electrochemical sensors (ECS), fluorescent sensors (FLS), resonance light scattering (RLS) methods, *etc.* [65,66]. Most of these methods are targeted at human viral pathogens, such as influenza virus [67,68], dengue virus [69–72], Japanese encephalitis virus (JEV) [46,73,74], HIV [75,76], hepatitis A virus (HAV) and HBV [77,78], virions of poliovirus [79], HPV [80], Zika virus [81], SARS-CoV-2 [48,82,83], *etc*. In addition, MIPs have also been developed for detecting viruses affecting plants and bacteria, expanding their application scope [84]. These MIPs target whole viruses or virus-associated proteins, such as bovine leukemia virus glycoproteins [85], the nucleoprotein and spike glycoprotein of SARS-CoV-2 [86–88], highlighting their capability to target complex

Table 1
Comparative MIP preparation methods.

Method	Advantages	Limitations	Representative Applications	References
Bulk imprinting	– Simple and widely used method – Scalable and cost-effective – Compatible with hydrogels and porous matrices, enabling improved diffusion and structural adaptability for large templates	– Limited accessibility of internal binding sites – Inefficient template removal – Particle grinding may damage recognition sites and cause heterogeneity	– Hydrogel-based MIPs for whole virus recognition and capture – High-yield applications with adaptable matrices	[41]
Surface imprinting	– High accessibility of recognition sites – Fast binding kinetics – Suitable for large biomolecular templates – Can be applied to a wide range of material surfaces (*e.g.*, SiO_2 and Fe_3O_4 NPs, electrodes)	– Template removal can be incomplete – Lower binding capacity per volume – Binding performance may be influenced by surface hydration layers and diffusion barriers	– MIPs for virus detection, protein recognition, biosensors – Antiviral capture platforms	[54]
Solid-phase synthesis	– High specificity and reproducibility – Efficient reuse of immobilized templates – Generates uniform MIP NPs with enhanced surface accessibility	– Requires template immobilization – Lower yield compared to bulk – More complex and time-consuming procedure	– MIP NPs for viral proteins and epitopes – Applications requiring precision, uniformity, and template conservation	[55]

viral components and supporting their application in virus diagnostics. Representative MIP-based virus detection platforms and their corresponding targets are summarized in Table 2.

Building upon their high specificity and selectivity, MIPs are increasingly being explored beyond detection purposes. They can be developed as "monoclonal-like" synthetic antibodies to target and block viral infection processes. Specifically, MIPs can act on the virus directly, either by recognizing and capturing viral particles or by binding to viral surface proteins, thereby preventing entry into host cells [99]. They can also be designed to target proteins and genetic materials essential for viral replication, disrupting the replication process. Additionally, MIPs may serve as tools to enhance the immune response against viral infections. Their drug-loading and controlled release capabilities further position MIPs as a promising platform for antiviral drug delivery systems. Moreover, as noted earlier, MIPs possess distinct advantages over natural antibodies, including superior stability, safety, low immunogenicity, reusability, independence from animal-based production, resistance to proteolytic degradation, and ease of synthesis [100]. These methods and advantages provide a highly promising pathway to overcome the current limitations of antiviral therapies [101]. Illustrative examples of their antiviral efficacy are provided in Table 3. The following sections will explore antiviral MIPs in detail.

2. MIPs for inhibiting viral entry into host cells

2.1. Catching whole viruses with MIPs

The most direct method of eliminating viral infections is to remove viral particles to block the virus-host cell interactions. Virus-imprinted MIPs offer a viable way to achieve this. They are prepared using whole viruses or pseudoviruses as templates and therefore have cavities that specifically catch the viral particles. The virus surface with the large number of functional groups available for the interaction with functional monomers can provide rich binding sites for the formation of imprinted cavities. These cavities could adsorb virus particles and reduce their contact with cells, thus inhibiting viral infection. Another potential benefit of whole virus imprinting is that the large number of binding sites ensures binding effectiveness, thus making MIPs less susceptible to failure by viral mutations. Ideal MIPs for virus removal are able to selectively and specifically remove one or more pathogenic viral species from specific environments, acting as "virus traps".

2.1.1. MIP-mediated virus capture and neutralization

MIP "virus traps" have demonstrated significant antiviral efficacy in research. Sankarakumar *et al.* developed antiviral MIP NPs using fr phages as templates and demonstrated that the specific adsorption is responsible for the viricidal action [102]. Phages are viruses that infect and replicate within bacteria, often serving as models or surrogates for human viruses due to shared structural and functional features. Fr phage, a small enteric phage targeting *Escherichia coli* (*E. coli*), is widely used in controlled studies to investigate antiviral mechanisms. The results of the anti-phage activity studies showed that the maximum reduction in phage titers was obtained for the imprinted NPs, with log reduction values of 1.14–3.25 times that of non-imprinted particles within 3 h. Additionally, adsorbed virus infectivity study showed that the viruses adsorbed by the imprinted particles lose their ability to infect the host cells. Similarly using bacteriophages (f2, T4, P1 and M13) as templates, Li *et al.* prepared virus-imprinted MIPs on poly-dopamine-coated silica particles through surface imprinting (Fig. 3) [94]. These MIPs exhibited remarkable dose-dependent and time-dependent inhibitory effects, achieving up to 90 % inhibition of viral infectivity at 40 mg/mL in the f2 model. Infectivity suppression was sustained for up to 12 h, and the MIPs showed consistent antiviral performance across multiple phage types. Moreover, they demonstrated biocompatibility, non-toxicity, and excellent stability, indicating their potential for *in vivo* applications in antiviral therapy.

To extend these findings to clinically relevant viruses, Graham *et al.* developed virus-imprinted hydrogel microparticles using purified and chemically inactivated porcine reproductive and respiratory syndrome virus (PRRSV-1) as the template [95]. The virus was obtained *via* ultracentrifugation through a sucrose cushion and inactivated with binary ethylenimine prior to imprinting. Three different functional monomers were tested to evaluate the influence of polymer composition on imprinting performance: acrylamide (AA), *N*-hydroxymethylacrylamide (NHMA), and *N*-isopropylacrylamide (NIPAM). Polymerization was conducted via aqueous FRP in the presence of whole PRRSV-1 particles. *N,N′*-methylenebisacrylamide was used as the cross-linker. The resulting MIPs formed from AA and NHMA exhibited rapid and potent virus neutralization, reducing PRRSV-1 titers by more than 4 $\log_{10}$ units within just 2.5 min, to levels below the assay's detectable threshold. Although no half maximal effective concentration (EC_{50}) or half maximal inhibitory concentration (IC_{50}) was reported, the dramatic reduction in infectious titer provides direct and robust evidence of neutralization. In contrast, their corresponding NIPs showed no significant antiviral activity. The MIPs also demonstrated virus selectivity, as no neutralization was observed against bovine viral diarrhea virus (BVDV-1). However, MIPs and NIPs formed from NIPAM showed similar activity levels, suggesting non-imprinting-related interactions, potentially due to non-specific adsorption or inherent polymer effects. These findings highlight the utility of virus-imprinted hydrogel microparticles for selective and efficient viral neutralization, while also emphasizing the importance of monomer selection and imprinting precision in achieving targeted antiviral performance.

These encouraging findings suggest that MIPs are effective tools for the selective capture and neutralization of viruses. However, their practical application, particularly in antiviral therapy for *in vivo* use and

Table 2
Representative MIP-based virus detection platforms and their corresponding targets.

Target Virus	Template	Type of MIP	Detection Platform	Results	References
Influenza virus	Whole virus (H5N1, H5N3, H1N1, H1N3, and H6N1)	MIP film on gold electrode	QCM	The limit of detection (LOD): 105 particles/mL; enabled clear subtype discrimination	[68]
	Whole virus (H5N1)	MIP film on gold electrode	QCM	Oseltamivir and antibodies reduced virus rebinding, indicating sensitivity to probe-induced conformational changes	[67]
	Whole virus (HK68)	MIP film on gold-coated glass substrate	FLS	LOD: 8 fM; capture in 1 min; 8-fold selectivity over newcastle disease virus (NDV)	[89]
Dengue virus	Non-structural protein 1 (NS1) epitope	MIP film on gold electrode	QCM	15 Hz frequency shift; positive in 86 % (18/21) of confirmed cases; no signal in 16 controls; correlation with enzyme-linked immunosorbent assay (ELISA) $r^2 = 0.73$	[69]
	Whole virus	MIP film on gold electrode	QCM	Imprinting factor 3.0, indicating practical sensor selectivity; reversible binding confirmed by signal recovery	[71]
	NS1 epitope	MIP film on gold electrode	QCM	LOD: 56.1 ng/mL; linear range: 0.2–10 μg/mL	[72]
JEV	Whole virus	MIP-coated magnetic silica microspheres	FLS	LOD: 0.32 nM; linear range: 2.5–45 nM; imprinting factor: 2.98	[74]
	Whole virus	MIP shell on fluorescent silica microspheres	FLS	LOD: 9.6 pM; linear range: 24–960 pM; imprinting factor: 2.12; recovery: 97.7–100.5 % in 2000-fold diluted serum	[73]
	Whole virus	MIP shell on metal-organic framework (MOF)–SiO_2 core–shell NPs	FLS	LOD: 13 pM; linear range: 50–1400 pM; imprinting factor: 4.3; detection in serum within 20 min	[90]
	Whole virus	MIP shell on magnetic Fe_3O_4@SiO_2 NPs	RLS	LOD: 1.3 pM; selective over other viruses; detection in 20 min	[46]
	Whole virus	MIP layer on dansyl-labeled SiO_2 microspheres	FLS	LOD: 0.11 pM; imprinting factor: 1.7; recovery: 96.3–100.6 % in 2000-fold diluted serum within 55 min	[91]
HIV	gp41 epitope	MIP film on gold electrode	QCM	LOD: 2 ng/mL; dissociation constant (K_D): 3.17 nM; comparable to ELISA; recovery: 86.5–94.1 % in urine	[75]
	HIV protease (PR) epitope	MIP film on gold electrode	QCM	LOD: 0.1 ng/mL; K_D: 78.5 pM for HIV protease; inhibition constant (Ki): 1.99 nM for nelfinavir; reusable sandwich assay for inhibitor screening	[76]
HAV	Whole virus	MIP shell on SiO_2@polydopamine NPs	RLS	LOD: 8.6 pM; selective over other viruses; detected in 20,000-fold diluted serum	[77]
	Whole virus	Quantum dot (QD)-based silica NPs with MIP layer	FLS	LOD: 88 pM for HAV; recovery: 96.7–101.6 % in spiked serum	[92]
	Whole virus	MOF-based MIP NPs	RLS	LOD: 0.1 pM in 20 min; recovery: 88–108 % in spiked serum	[93]
HAV and HBV	Whole virus	QD-based MIP NPs	FLS	LODs: 3.4 pM (HAV), 5.3 pM (HBV); detection in 20 min	[78]
Poliovirus	Carcinoembryonic antigen (CEA) and poliovirus (whole virus)	MIP film on gold electrode	ECS	Virus-induced potential shift saturated at 3.1×10^9 particles/mL	[79]
HPV	E7 protein	MIP film on carbon nanotube tip array	ECS	LOD: 0.2 pg/L; > 4-fold selectivity over HPV E6 and BSA	[80]
Zika virus	Whole virus	MIP–graphene oxide composite	ECS	LOD: 2×10^{-4} PFU/mL (1 RNA copy/mL) in PBS and 2×10^{-3} PFU/mL (10 RNA copies/mL) in 100-fold diluted serum	[81]
SARS-CoV−2	Whole virus	MIP hydrogel on screen-printed electrode	ECS	LOD: 4.9 $\log_{10}$ PFU/mL (88 fg/mL); 75 % agreement with loop-mediated isothermal amplification (LAMP) in 24 clinical saliva samples; detection in 10 min	[48]
	Nucleocapsid protein	Surface-imprinted poly(m-phenylenediamine)-based MIP film	ECS	LOD: 15 fM in lysis buffer; 27 fM in clinical nasopharyngeal swabs; validated in COVID−19 patient samples	[82]
	Spike protein subunit S1	MIP film on gold electrode	ECS	LOD:15 fM in buffer and 64 fM in patient swabs; completed within 15 min	[83]

in viral clearance strategies for *in vitro* systems, still faces several challenges. These include non-specific binding in complex biological environments, the need for efficient virus isolation and material recycling, and technical limitations related to virus template preparation and imprinting precision. Addressing these issues is essential to fully realize the therapeutic and prophylactic potential of MIPs.

2.1.2. *Capturing viruses from complex biological environments*

Despite the promise of virus-imprinted MIPs, their application in complex environments, particularly *in vivo*, is hindered by the issue of non-specific binding. The *in vivo* environment, including blood and tissue fluids, is composed of a complex mixture of electrolytes, metabolites, proteins, and other molecules that can interfere with the selective binding of MIPs to target viruses [103,104]. To address this challenge, various strategies have been developed, such as the use of self-assembled monolayers (SAMs) [105], PEGylation [106], and pre-adsorption of strongly adhering proteins [107]. These approaches aim to reduce unintended protein-surface interactions, thereby enhancing the selectivity and specificity of MIPs. By minimizing non-specific binding, MIPs can more effectively bind and neutralize target viruses, a critical requirement for their therapeutic use *in vivo*.

For instance, Mizaikoff *et al.* synthesized adenovirus-imprinted microparticles (VIPs) and coated their surfaces with a blocking agent, bovine serum albumin (BSA), to reduce non-specific interactions (Fig. 4) [108]. Their study showed that without a blocking agent, VIPs and NIPs exhibited similar virus-binding performance. However, with BSA, the virus binding of VIPs increased to 97 %, compared to less than 5 % for NIPs. This demonstrates the critical role of surface modification in improving the specificity of virus-imprinted MIPs in complex biological environments. Although subsequent studies exploring binary blocking agents (*e.g.,* Tween 20 and BSA/skim milk) yielded less pronounced differences, MIPs maintained their ability to adsorb substantial amounts

Table 3
Quantitative antiviral efficacy data of representative MIP systems. Summarizes virus types, MIP templates, inhibition rates, EC_{50}/IC_{50} values, and detection methods from key studies, to enable cross-system comparison of antiviral potency.

Virus	MIP Matrix	Template	Inhibition Rate	EC50 / IC50	Detection Method	Reference
f2 Phage	PDA-coated SiO_2 core–shell MIP microparticles	Whole virus	≈ 90 % at 40,000 μg/mL	Not directly reported	Plaque assays on host cells	[94]
PRRSV−1	Hydrogel-based MIP microparticles	Whole virus	Infectious titer below limit of detection (LOD)	Not directly reported	Virus neutralization assay via immunoperoxidase staining	[95]
SARS-CoV−2	MIP NPs	RBD of spike protein	99 ± 0.5 % at 20 μg/mL	Not directly reported	Virus replication (in Vero cells), RT-PCR	[96]
SARS-CoV−2	MIP NPs	RBD of spike protein	90 ± 0.9 % at 10 μg/mL; 80 ± 0.1 % at 20 μg/mL; 66 ± 0.5 % at 30 μg/mL	Not directly reported	Plaque reduction assay, quantification of PFU/mL.	[96]
HIV−1 tier 1 strain HXB2	SiO_2 core-shell MIP NPs	High-mannose glycans on HIV−1 gp120	≈ 90 % at 40 μg/mL	IC_{50} = 19.07 ± 2.88 μg/mL (3.90 ± 1.80 pM)	Luciferase reporter assays in TZM-bl cells	[97]
HIV−1 tier 1 strain 92RW (92RW020.2)	SiO_2 core-shell MIP NPs	High-mannose glycans on HIV−1 gp120	≈ 80 % at 40 μg/mL	IC_{50} = 29.34 ± 4.43 μg/mL (6.00 ± 0.42 pM)	Luciferase reporter assays in TZM-bl cells	[97]
HIV−1 tier 1 strain 25710	SiO_2 core-shell MIP NPs	High-mannose glycans on HIV−1 gp120	≈ 30 % at 40 μg/mL	IC_{50} = 42.93 ± 6.48 μg/mL (8.78 ± 1.24 pM)	Luciferase reporter assays in TZM-bl cells	[97]
HIV−1 tier 1 strain ZM197 (ZM197 M. PB7)	SiO_2 core-shell MIP NPs	High-mannose glycans on HIV−1 gp120	≈ 70 % at 40 μg/mL	IC_{50} = 26.56 ± 4.01 μg/mL (5.43 ± 0.34 pM)	Luciferase reporter assays in TZM-bl cells	[97]
HIV−1 tier 2 strain TRO11	SiO_2 core-shell MIP NPs	High-mannose glycans on HIV−1 gp120	≈ 60 % at 40 μg/mL	IC_{50} = 37.66 ± 5.68 μg/mL (7.70 ± 1.21 pM)	Luciferase reporter assays in TZM-bl cells	[97]
HIV−1 tier 2 strain SC422 (SC422661.8)	SiO_2 core-shell MIP NPs	High-mannose glycans on HIV−1 gp120	≈ 35 % at 40 μg/mL	IC_{50} = 47.09 ± 7.10 μg/mL (9.63 ± 1.65 pM)	Luciferase reporter assays in TZM-bl cells	[97]
HIV−1 tier 2 strain WITO (WITO4160.33)	SiO_2 core-shell MIP NPs	High-mannose glycans on HIV−1 gp120	≈ 70 % at 40 μg/mL	IC_{50} = 18.74 ± 2.83 μg/mL (3.83 ± 1.00 pM)	Luciferase reporter assays in TZM-bl cells	[97]
SARS-CoV−2 Wild-type	PEGylated silica-boronate MIP NPs	Mannose	90.2 % at 500 μg/mL	EC_{50} = 37.5 ± 7.3 μg/mL (0.75–1.04 nM)	Luciferase-based pseudovirus neutralization assay and RT-qPCR	[98]
SARS-CoV−2 D614G	PEGylated silica-boronate MIP NPs	Mannose	≈ 90 % at 400 μg/mL	EC_{50} = 45.7 ± 7.6 μg/mL (0.91–1.27 nM)	Luciferase-based pseudovirus neutralization assay and RT-qPCR	[98]
SARS-CoV−2 N501Y	PEGylated silica-boronate MIP NPs	Mannose	≈ 90 % at 400 μg/mL	EC_{50} = 49.3 ± 3.6 μg/mL (0.99–1.37 nM)	Luciferase-based pseudovirus neutralization assay and RT-qPCR	[98]
SARS-CoV−2 N439K	PEGylated silica-boronate MIP NPs	Mannose	≈ 90 % at 400 μg/mL	EC_{50} = 41.4 ± 6.7 μg/mL (0.83–1.15 nM)	Luciferase-based pseudovirus neutralization assay and RT-qPCR	[98]
SARS-CoV−2 Δ69–70	PEGylated silica-boronate MIP NPs	Mannose	≈ 90 % at 400 μg/mL	EC_{50} = 36.9 ± 4.9 μg/mL (0.74–1.02 nM)	Luciferase-based pseudovirus neutralization assay and RT-qPCR	[98]
SARS-CoV−2 Delta	PEGylated silica-boronate MIP NPs	Mannose	≈ 90 % at 400 μg/mL	EC_{50} = 44.2 ± 3.6 μg/mL (0.88–1.23 nM)	Luciferase-based pseudovirus neutralization assay and RT-qPCR	[98]
SARS-CoV−2 Omicron	PEGylated silica-boronate MIP NPs	Mannose	≈ 90 % at 400 μg/mL	EC_{50} = 43.7 ± 4.4 μg/mL (0.87–1.21 nM)	Luciferase-based pseudovirus neutralization assay and RT-qPCR	[98]
Lassa virus (LASV)	PEGylated silica-boronate MIP NPs	Mannose	95.5 % at 400 μg/mL	EC_{50} = 27.6 ± 1.3 μg/mL (0.55–0.77 nM)	Luciferase-based pseudovirus neutralization assay and RT-qPCR	[98]
HIV−1	PEGylated silica-boronate MIP NPs	Mannose	97.2 % at 400 μg/mL	EC_{50} = 18.9 ± 2.9 μg/mL (0.38–0.53 nM)	Luciferase-based pseudovirus neutralization assay and RT-qPCR	[98]

of adenovirus from complex matrices [109].

These findings emphasize the critical role of refining anti-fouling strategies. Advancements in this area highlight the potential of MIPs for complex biological applications, such as serving as antiviral agents for selective pathogen neutralization *in vivo*, as well as for blood filtration and viral diagnostics.

2.1.3. *Expanding virus capture capabilities*

Expanding the capacity of MIPs to capture viral particles enables the removal of large quantities of viruses from the environment. This not only directly blocks virus-cell interactions but also reduces the overall viral load, thereby mitigating the risks of infection and transmission. Unlike sensors designed to detect trace amounts of viruses, virus removal technologies focus on extracting as many particles as possible. As discussed in 1.3.2, hydrogels, with their adaptable network structures, enhance virus capture efficiency by providing accessible binding sites and supporting high-capacity removal.

Bolisay *et al.* demonstrated the potential of virus-imprinted hydrogels by developing one for tobacco mosaic virus (TMV). This hydrogel exhibited a high binding capacity for TMV (8.8 mg TMV/g polymer), significantly outperforming non-imprinted hydrogels (4.2 mg TMV/g polymer) [41]. Furthermore, the hydrogel's binding selectivity was evident: it showed much lower binding capacity for the spherical tobacco necrosis virus (TNV), comparable to that of the non-imprinted

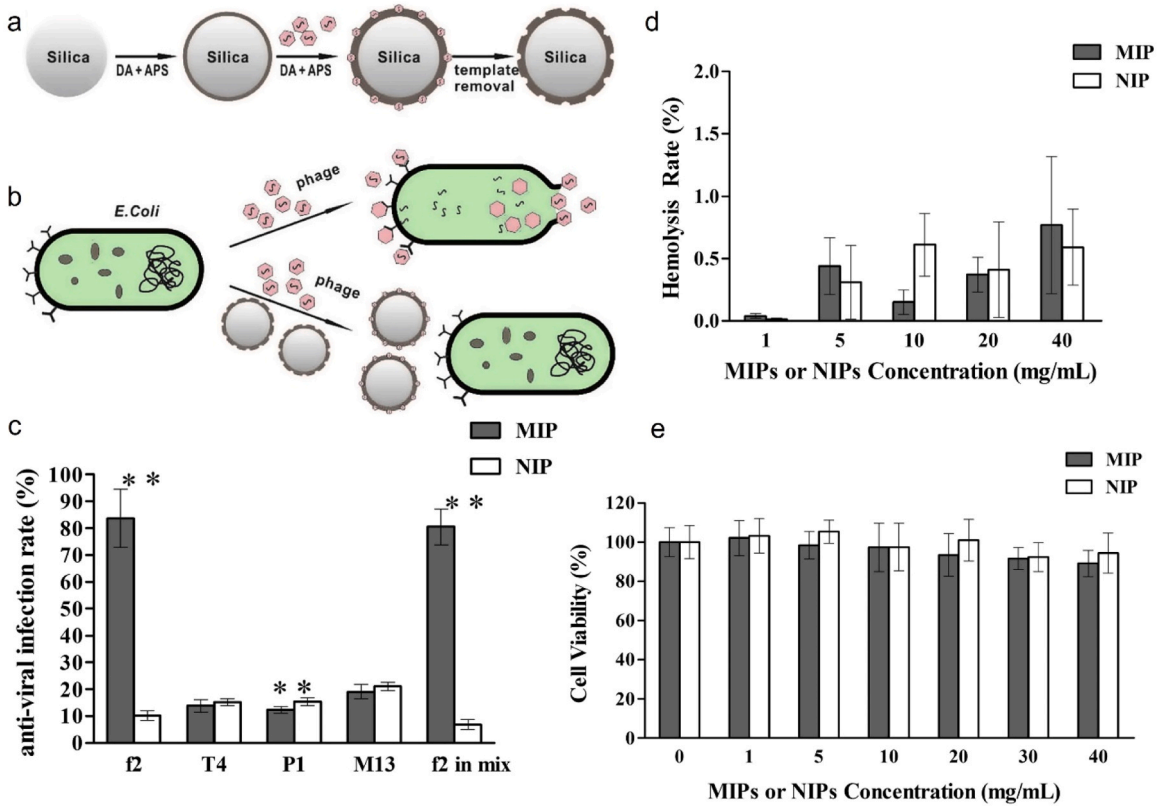

Fig. 3. a) Schematic illustration of the preparation process for virus-imprinted MIPs via surface imprinting on polydopamine (DA)-coated silica particles, using ammonium persulfate (APS) as the initiator. b) Mechanism of selective virus binding by MIPs, highlighting the prevention of phage infection in host cells. c) Antiviral efficacy of f2-imprinted MIPs against multiple viruses, presented as infection inhibition rates. d) Hemolysis rates observed for MIPs and non-imprinted polymers (NIPs), comparing their biocompatibility. e) HepG2 cell viability after 24-hour exposure to MIPs and NIPs, demonstrating cytocompatibility of the materials. Adapted with permission from Li *et al.* [94]. Copyright 2017, Elsevier.

hydrogel (4.0 mg TMV/g polymer), highlighting the role of geometric factors in target specificity. Subsequent optimization, including adjustments to the pre-polymerization mixture and template removal methods, led to a modest increase in the imprinting factor (IF, the ratio of virus binding capacity of imprinted and non-imprinted hydrogels) from 2.1 to 2.3 (Fig. 5) [110]. However, excessive swelling of the hydrogel in water was reported to enlarge the binding cavities, reducing their specificity for the target virus. Although the use of phosphate buffer (pH=7) mitigated some swelling and optimized binding conditions during batch rebinding assays, the residual instability in cavity size likely constrained further increases in IF, limiting the hydrogel's overall performance in practical applications [42].

Stimulus-responsive hydrogels show potential for addressing swelling-induced specificity issues by dynamically adjusting their binding cavity size, enabling efficient and selective virus capture while facilitating material reuse across diverse applications. For instance, hydrogels imprinted with influenza A virus (IAV) shrink upon virus binding due to increased cross-linking density from interactions between hemagglutinin (HA) on the virus surface and sialic acid (SA) on the hydrogel's molecular chains (Fig. 6) [111]. Immersing these hydrogels in diluted acid solution removes the virus, causing the hydrogel to swell back to its original size. Such reversible deformation preserves the size and shape of the binding cavities, which could potentially counteract the negative effects of swelling and improve virus capture specificity. Additionally, hydrogels containing gold nanoparticles (Au NPs) provide a visual indicator of IAV adsorption or removal through color changes (*e.g.,* purple to pink), attributed to the plasmonic properties of Au NPs. These hydrogels also exhibit mechanical reversibility, enabling them to maintain functionality over multiple cycles of virus binding and removal, thereby functioning as reusable "sponges" for virus capture with significant practical advantages.

A study on Apple Stem Pitting Virus (ASPV) further confirmed the feasibility of using shrink-responsive hydrogels to effectively imprint viruses (Fig. 6 **c**) [43]. These hydrogels, prepared with polymerizable aptamers, showed high specificity and avoided interference from impurities in virus extracts, eliminating the need for complex purification steps. Interestingly, some aptamer-based virus-imprinted hydrogels have been reported to swell rather than shrink upon virus binding, further expanding their application potential in virus capture [112].

In summary, virus-imprinted hydrogels, particularly those designed with stimuli-responsive properties, represent a versatile and effective platform for large-scale virus capture. By addressing challenges such as swelling-induced specificity loss, these advanced materials can contribute to significant progress in the prevention of viral transmission and the removal of infectious agents from various environments.

2.1.4. Managing captured viruses

The handling of virus-adsorbed MIPs after capture is a critical consideration, as it encompasses both the secure inactivation or isolation of captured viruses and the recycling of MIP materials. Effective post-capture management is essential to prevent viruses from reentering the environment or contacting host cells, especially in applications aimed at halting virus transmission.

Magnetic nanoparticle-based virus-imprinted MIPs offer a promising solution to this challenge. For example, Cai *et al.* developed magnetite (Fe_3O_4) NPs coated with a virus-imprinted MIP layer, specifically designed to target JEV (Fig. 7) [46,74]. These MIPs enable rapid and highly sensitive virus capture, followed by efficient magnetic separation to physically isolate the bound viruses. This approach not only enables the controlled removal of viruses from the environment but also allows

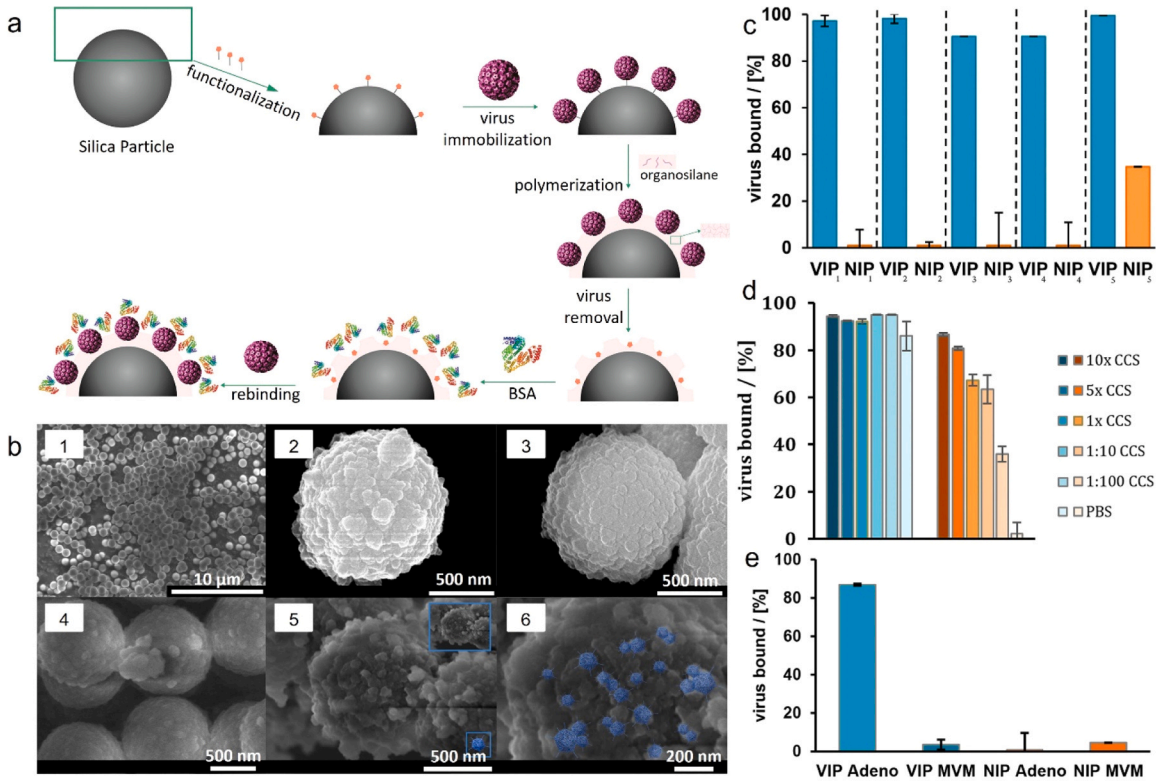

Fig. 4. a) Schematic of imprinting and passivation procedure. b) Scanning electron microscope (SEM) images comparison: (1) bare silica particles (scale bar = 10 µm), (2) VIP_{TAA} after imprinting (scale bar = 500 nm), (3) VIP_{TAA} after lysis (scale bar = 500 nm), (4) NIP_{TAA} (scale bar = 500 nm), (5) particles with rebound viruses (scale bar = 500 nm), (6) magnified view of rebound particles from (5) (scale bar = 200 nm). c) Multiple rebinding/regeneration cycles for VIP and NIP. Values normalized to the initially added virus amount. Rebinding performed in 105 µL with 480 µg imprinted beads, 77 µg BSA, and 1.00×10^5 IU virus in PBS buffer. Experiments repeated at least three times, measurements in duplicate. d) Influence of matrix components on rebinding for VIP and NIP. Columns show normalized amounts of adenovirus bound to imprinted particles. Typical rebinding in 105 µL with 480 µg imprinted particles, 77 µg BSA, and 1.00×10^5 IU adenovirus (AdV) in the medium. Experiments repeated at least three times, measurements in duplicate. e) Competitive rebinding study with templated AdV and nontemplated min virus of mice (MVM) to VIP and NIP. Columns show normalized values as a percentage of initial virus concentration. Studies in 105 µL with 77 µg BSA, 1.00×10^5 IU AdV, and 1.00×10^3 IU MVM in PBS buffer. Adapted with permission from Mizaikoff *et al.*[108]. Copyright 2018, American Chemical Society.

MIPs to be collected and safely treated to remove bound viruses before being reused under secure conditions.

In addition to enabling efficient separation, Fe_3O_4 NPs exhibit a range of physical and chemical properties that enhance their antiviral efficacy. When exposed to an alternating magnetic field (AMF), they generate localized heat through Néel and Brownian relaxation mechanisms, leading to a temperature increase around the NPs [113]. This localized heating causes viral protein denaturation, disruption of the viral envelope, and degradation of the viral genome, thereby effectively inactivating viruses. Furthermore, the unique rotational and surface effects of Fe_3O_4 NPs under AMF exposure may induce additional mechanical and chemical impacts on viral particles, enhancing the inactivation process [114]. These combined effects make AMF treatments more effective than water baths at similar temperatures, as demonstrated in the inactivation of pseudoparticles containing the SARS-CoV-2 spike protein (Fig. 8). This study highlights the potential for Fe_3O_4 NPs coated with a virus-imprinted MIP layer to serve as multifunctional tools, combining virus adsorption, separation, and inactivation in a single process. Such a strategy offers significant promise for antiviral applications including air purification systems, hospital wastewater treatment, and reusable antiviral coatings, addressing both clinical and environmental needs.

2.1.5. *Virus template preparation and imprinting process considerations*

The development of virus-imprinted MIPs relies heavily on the effective preparation and use of whole viruses as templates. While these MIPs show immense promise in capturing and neutralizing viruses, the processes of virus preparation, purification, and imprinting remain major bottlenecks due to the inherent complexity of viruses and the demanding technical requirements.

2.1.5.1. Virus preparation and purification. Preparing high-purity and high-concentration virus templates is critical to ensuring effective imprinting [41]. Typically, viruses must be propagated through cell culture systems, which require controlled conditions to achieve high titers. Post-propagation, the harvested viruses must undergo rigorous purification steps, such as ultracentrifugation, filtration, and chromatography, to remove cellular debris and other contaminants [115]. These steps are essential to prevent impurities from interfering with the imprinting process, as contamination could lead to non-specific binding sites and reduced MIP selectivity. However, these processes are time-consuming, labor-intensive, and involve significant biosafety risks, particularly when working with highly pathogenic viruses. Specialized equipment, such as high biosafety-level facilities and advanced separation systems, is often required, further increasing the complexity and cost [116].

Pseudoviruses, as non-infectious virus-like particles, mimic the structural and surface characteristics of real viruses, offering a safer and more practical alternative for imprinting [117]. Their use minimizes biosafety concerns while simplifying template handling, advancing MIP development for diagnostic and therapeutic applications. Furthermore, advances in virus purification techniques, such as affinity chromatography and novel filtration methods, have improved the efficiency of obtaining high-purity virus templates [118–120]. These methods reduce the time and cost associated with traditional purification processes

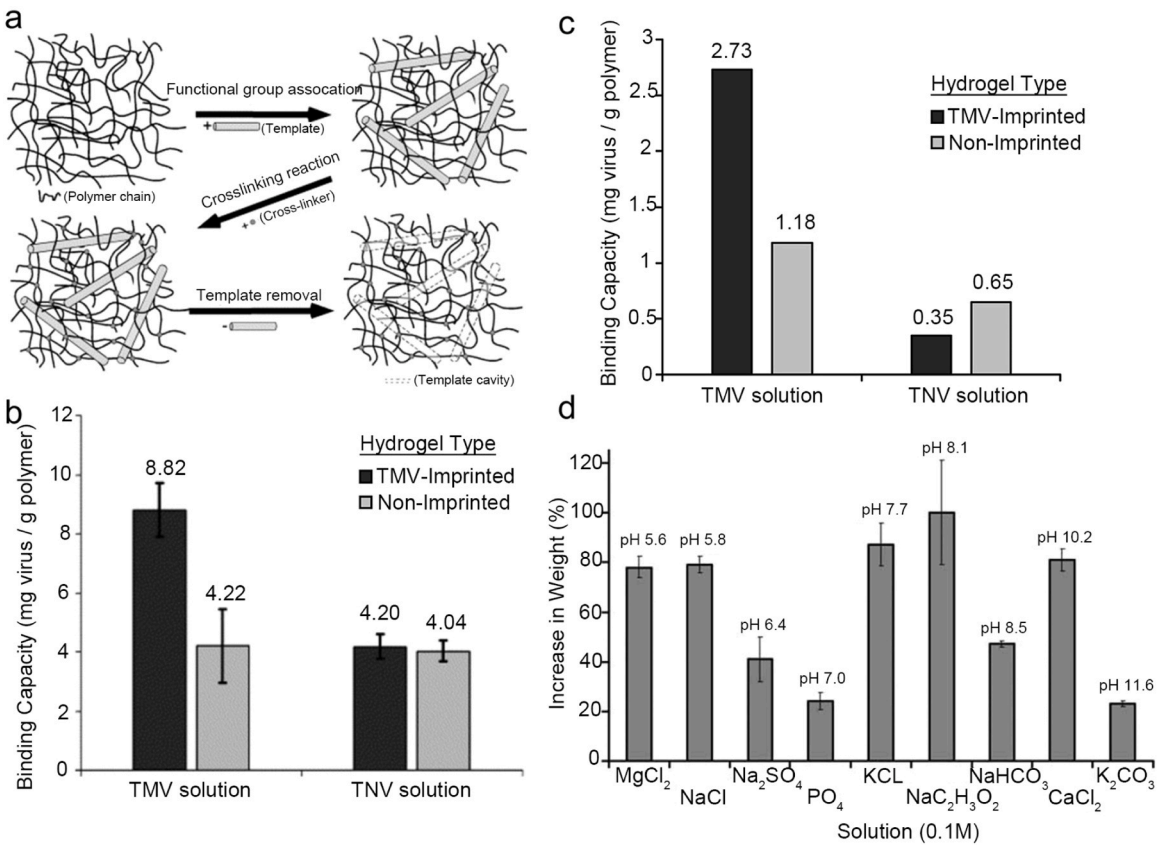

Fig. 5. a) Schematic of the imprinting processes for cylindrical TMV virus [41]. b) Virus-binding capacity of TMV-imprinted hydrogels compared to non-imprinted control hydrogels (IF=2.1) [41]. c) Virus-binding capacity of optimized TMV-imprinted hydrogels (IF=2.3) [110]. d) Swelling ratio of TMV-imprinted hydrogels in different 0.1 M ionic solutions. Adapted with permission from Bolisay & Kofinas [42]. Copyright 2010, Wiley.

while maintaining the quality necessary for effective imprinting.

In addition to using pseudoviruses and purified templates, researchers have explored alternative strategies to mitigate the dependency on high-purity viral preparations. For instance, as previously discussed in 2.1.3, aptamer-functionalized monomers in MIP synthesis enhance binding specificity and enable the use of less-purified or crude virus preparations [43]. Moreover, solid-phase synthesis has emerged as a promising approach for virus-imprinting, wherein viral particles are immobilized on solid supports, such as glass beads, during the polymerization process [121]. This approach has potential to minimize template aggregation in pre-polymerization mixtures, thereby ensuring the imprinting quality and maintaining the affinity and selectivity of the resulting MIPs [36]. Additionally, the Immobilized virus templates can be reused across multiple synthesis cycles, effectively reducing production costs [52].

These innovations collectively can potentially address the technical and economic hurdles associated with virus-imprinting processes. By integrating strategies such as pseudoviruses, advanced purification techniques, aptamer-functionalized monomers, and solid-phase synthesis, MIPs could enable breakthroughs in personalized medicine, rapid diagnostics, and scalable vaccine manufacturing.

2.1.5.2. Technical barriers in whole virus imprinting. Unlike small molecules or proteins traditionally used as MIP templates, viruses present unique challenges due to their size, structural complexity, and sensitivity to environmental conditions. As Gast highlighted, their large size and compositional complexity can hinder their movement into and out of recognition cavities, leading to poor mass transport and reduced imprinting efficiency [36]. Additionally, the uneven distribution of functional binding sites on the virus surface increases the risk of cross-reactivity and non-specific binding, undermining the selectivity of the resulting MIPs [122].

Further complicating the imprinting process, viruses are highly sensitive to non-physiological polymerization conditions, such as extreme temperatures, pH, or ionic strength. These conditions can cause virus aggregation, conformational changes, or denaturation, severely impacting their structural integrity and reducing the specificity of the imprinted polymers [42,123]. Moreover, the aqueous systems required to maintain virus stability further constrain the process by limiting functional monomer choices and disrupting template-monomer hydrogen bonding, reducing imprinting specificity.

Addressing these barriers requires careful optimization of the imprinting environment to balance virus stability with polymerization efficiency. In light of these challenges, researchers are also exploring imprinting strategies that target specific viral surface components rather than the entire virus, which will be discussed in the following section.

2.2. *Targeting viral surfaces with MIPs*

While whole virus imprinting provides a feasible approach for virus capture and neutralization, it is not the only strategy to inhibit viral entry into host cells. Focusing on specific viral surface components, such as proteins, binding domains, epitopes, and glycans, offers a more precise understanding of viral entry mechanisms and facilitates the development of highly specific antiviral agents. Additionally, these localized imprinting strategies address challenges inherent in whole virus imprinting, such as the complexities of virus preparation and purification, and the mass transport limitations posed by the size and structure of the virus.

This section explores four progressively refined strategies for targeting viral surfaces: imprinting entire surface proteins, focusing on binding domains, leveraging epitopes, and, as a recent advancement,

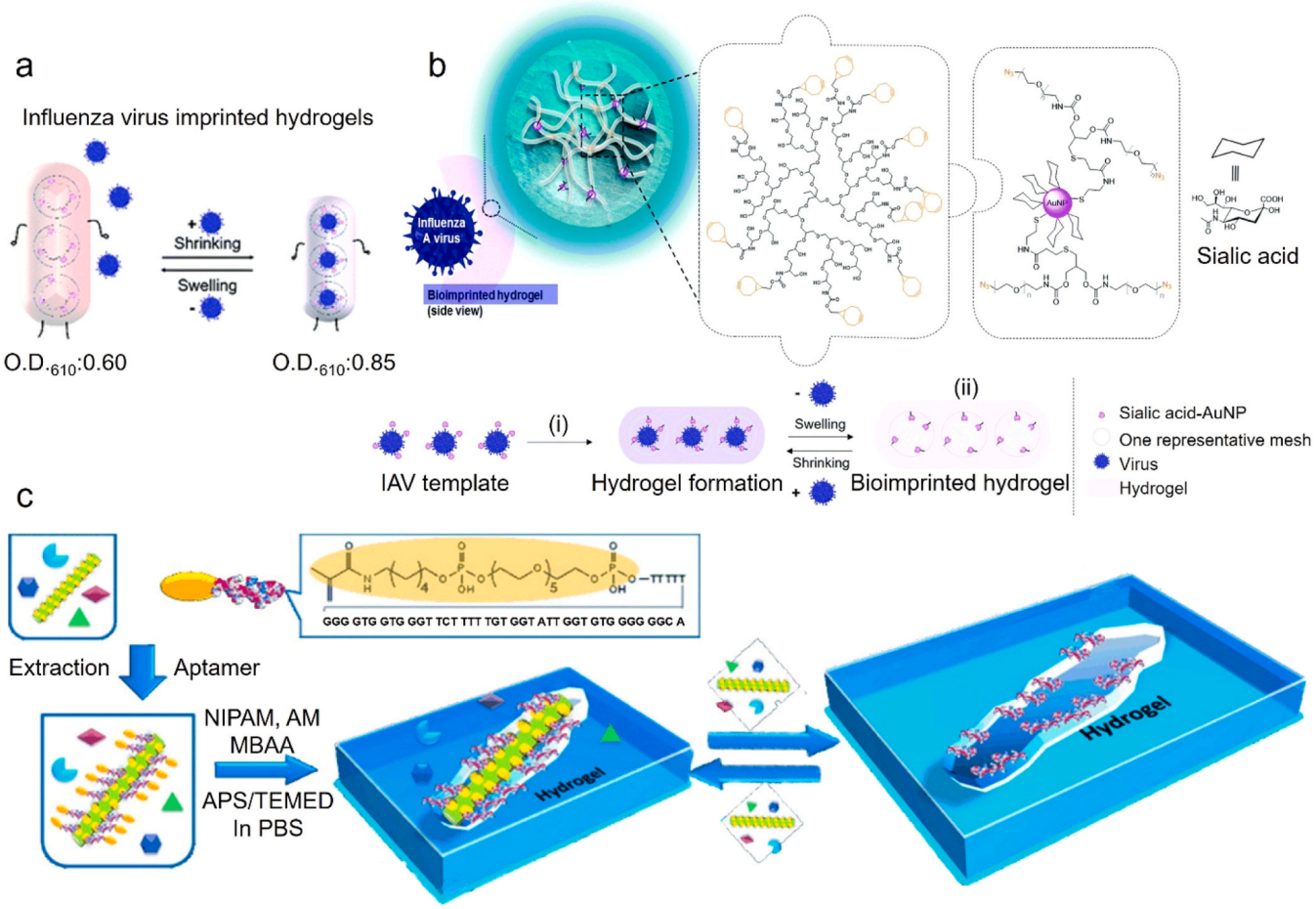

Fig. 6. a) Schematic of virus-responsive hydrogels interacting with IAV. b) Hydrogel structure and IAV imprinting process: IAV, serving as a template, is mixed with sialic acid-functionalized Au NPs and added to (i) a hydrogel precursor mixture of dPG-C and PEG-DIA. The hydrogel forms through click chemistry. IAV is subsequently removed using 3.7 % HCl, resulting in (ii) an IAV-responsive hydrogel that exhibits optical and mechanical changes when IAV is added or removed. Copyright 2020, Royal Society of Chemistry (RSC). c) Outline of the bioimprinting process used to create virus responsive super-aptamer hydrogels. NIPAM (N-isopropylacrylamide), AM (acrylamide), MBAA (*N,N'*-methylene bisacrylamide), APS (ammonium persulfate), TEMED (*N,N,N',N'*-tetramethylethylendiamine), PBS (phosphate-buffered saline). Copyright 2014, Wiley.
(a) Adapted with permission from Randriantsilefisoa *et al.* [111]. (b) Adapted with permission from Bai and Spivak [43].

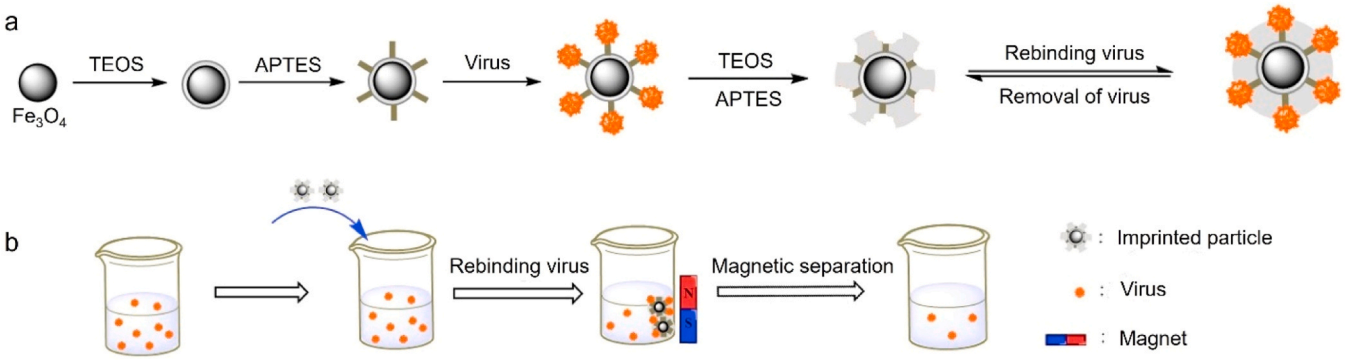

Fig. 7. a) Schematic illustration of the preparation process for JEV-imprinted particles. b) Depiction of the magnetic separation process used for virus isolation. Adapted with permission from He *et al.* [74]. Copyright 2016, Elsevier.

targeting viral glycans. These approaches demonstrate the potential of MIPs to serve as advanced antiviral tools by improving specificity, reducing production barriers, and enhancing practical applicability in diagnostics and therapeutics.

2.2.1. *Viral surface proteins*

Both naked and enveloped viruses rely on surface proteins for host cell interactions and entry, making these proteins critical targets for molecular imprinting [124]. Naked viruses, such as human adenovirus type 5 (hAdV5), display capsid proteins like hexon, while enveloped viruses, including HCV and SARS-CoV-2, utilize glycoproteins such as

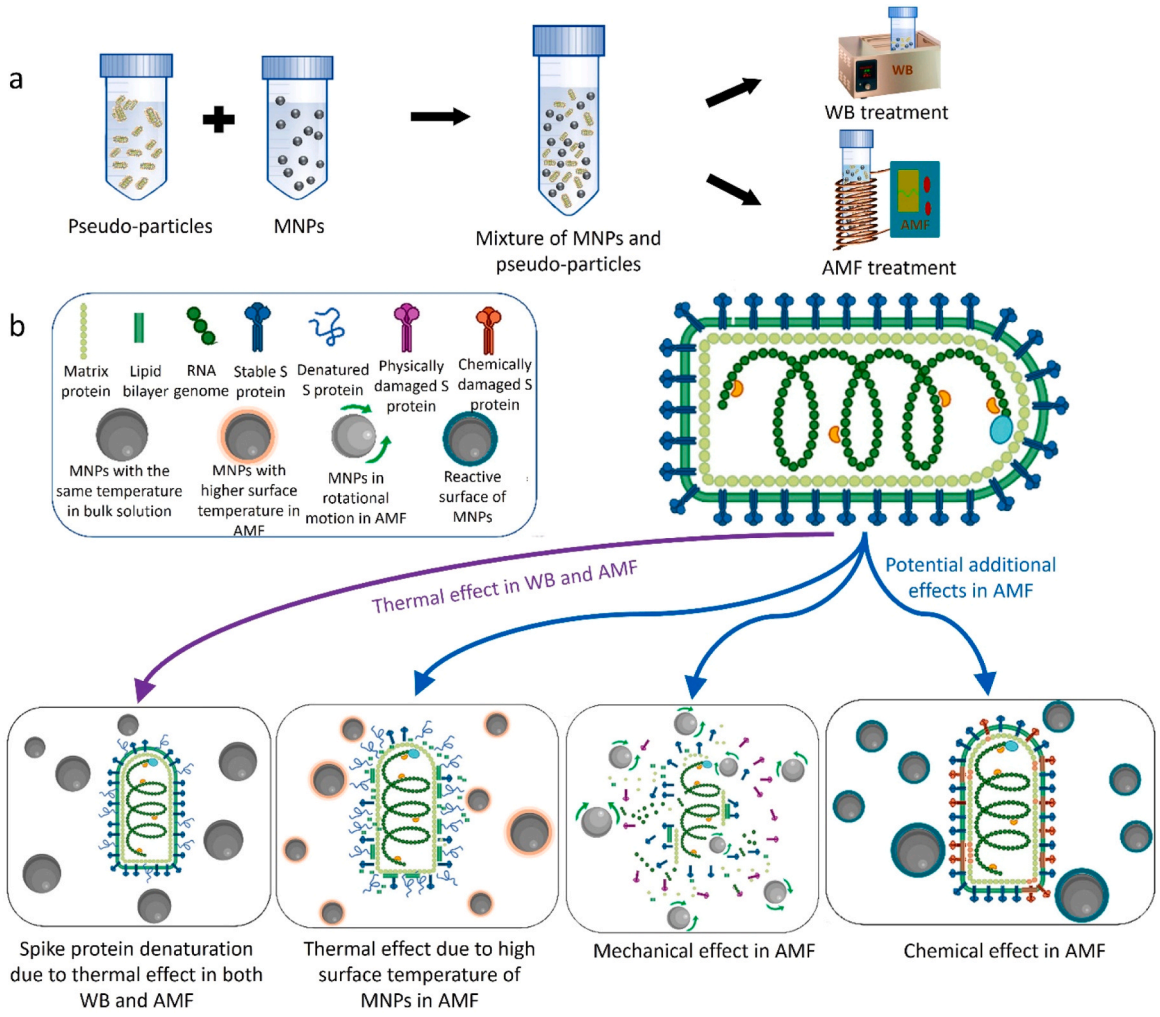

Fig. 8. a) Schematic representation of the treatment of magnetic nanoparticles (MNPs) using a water bath (WB) and an AMF for the inactivation of pseudoparticles containing the SARS-CoV-2 spike S protein. b) Illustration of the mechanism behind pseudoparticle inactivation during exposure to a water bath and AMF in the presence of MNPs. Adapted with permission from Paul *et al.* [114]. Copyright 2022, American Chemical Society.

HCV surface viral antigen (E2) and spike (S) proteins for receptor binding and fusion [125]. These surface proteins play indispensable roles in viral infection and serve as promising targets for antiviral strategies and vaccine development.

A recent study demonstrated the effectiveness of using the hexon protein of hAdV5 as a template for MIPs (Fig. 9) [126]. These hexon-imprinted polymer beads (HIPs) showed over 83 % selective binding to hAdV5 in competitive assays against the Minute Virus of Mice (MVM), a non-target virus with a significantly smaller diameter of 26 nm. Under optimal conditions (88 μg BSA as a blocking agent), the HIPs bound more than 90 % of the target virus at high viral loads, while NIPs exhibited minimal binding. This study highlights the utility of hexon-targeted MIPs for specific viral capture, offering a safer and scalable alternative by eliminating the need for live infectious viruses during imprinting.

This approach has also been extended to HCV, a significant human pathogen. HCV relies on its envelope glycoproteins E1 and E2 for host cell entry, with E2 specifically binding to receptors on host cells, such as Cluster of Differentiation 81 (CD81) and scavenger receptor class B type I (SR-BI) [127,128]. A study by Antipchik *et al.* developed a highly selective MIP film using the E2 protein as a template [129]. The optimized MIP exhibited strong binding affinity to free E2 and E2 incorporated within HCV-mimetic particles in human plasma. Importantly, it demonstrated high selectivity for E2 compared to other proteins with similar molecular weight and isoelectric points, such as human plasma albumin (HSA), immunoglobulin G (IgG), and CD81. This selective binding indicates that E2-targeted MIPs have the potential to block HCV entry into host cells and prevent infection.

Similarly, the S protein of SARS-CoV-2, a glycoprotein integral to viral entry, has been identified as a key target for MIP-based strategies [130]. The S protein is composed of two subunits: S1, which contains the receptor-binding domain (RBD) responsible for binding to the angiotensin-converting enzyme 2 (ACE2) receptor, and S2, which anchors the protein to the host cell membrane and facilitates viral fusion (Fig. 10). Blocking the interaction between the S protein and ACE2 is critical to preventing SARS-CoV-2 entry into host cells [131]. For this reason, the S protein has become a promising template for MIP development [132].

A recent example involved imprinting the S1 subunit using reversible covalent interactions between boronic acid groups on functional monomers, such as 3-aminophenylboronic acid (APBA), and the 1,2-diols of the glycosylated S1 protein (Fig. 11) [83]. These MIPs exhibited specific recognition of the S1 subunit with an IF of 4.3, significantly outperforming NIPs under optimal conditions. Competitive assays further demonstrated their selectivity, as MIPs showed a strong binding preference for the S1 subunit over non-target proteins such as nucleocapsid protein (ncovNP), HSA, and IgG, even in complex environments like nasopharyngeal samples from COVID-19 patients. These MIPs demonstrated specific recognition of S1 in both PBS and nasopharyngeal samples from COVID-19 patients. While this research primarily focused

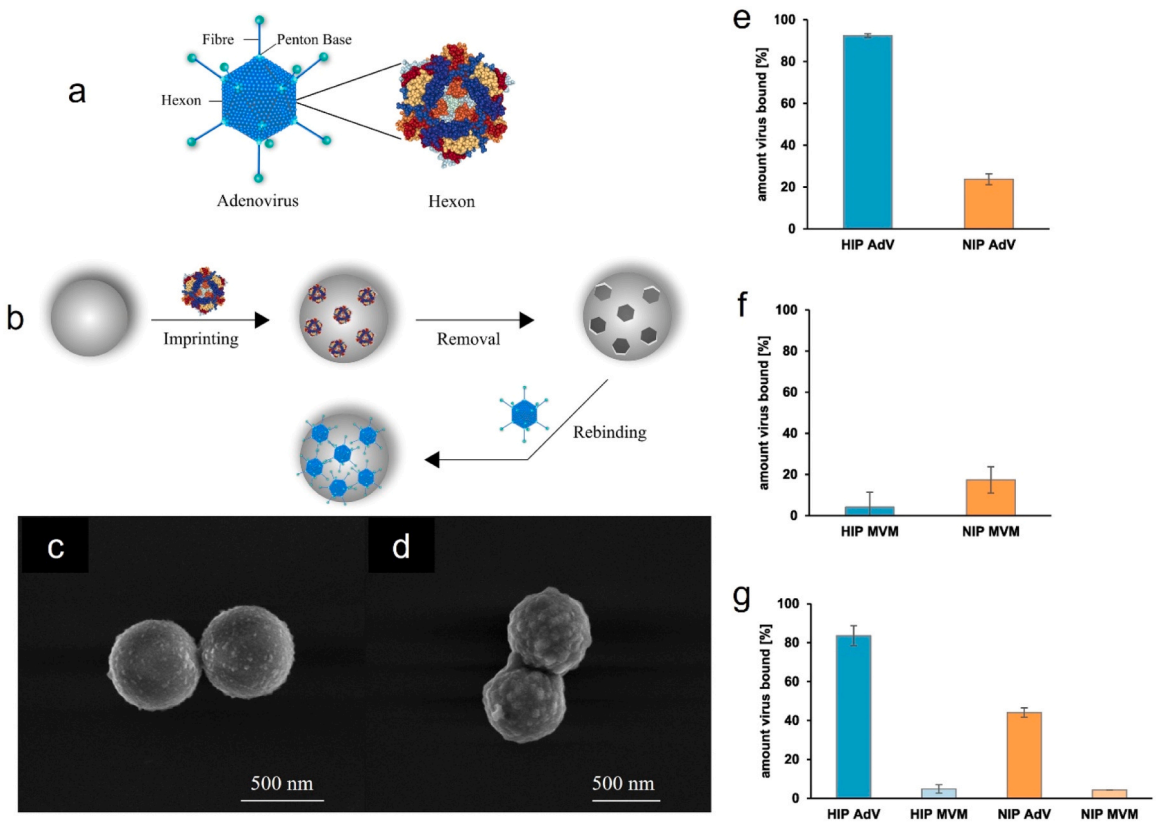

Fig. 9. a) Structure of Adenovirus and hexon protein; b) Schematic illustration of HIP production process. Scanning electron microscopy images of c) HIPs and d) NIPs after imprinting and template removal. Scale bars represent 500 nm. Rebinding studies conducted in simplex experiments with e) hAdV5 and f) Minute Virus of Mice (MVM), as well as g) duplex experiments with both viruses. The experiments were performed using hexon-imprinted beads (3 h) in the presence of 88 μg BSA, with 1E5 IU hAdV5 or 1E3 IU MVM for 30 min in 105 μL PBS. Adapted with permission from Gast *et al.* [126]. Copyright 2019, Elsevier.

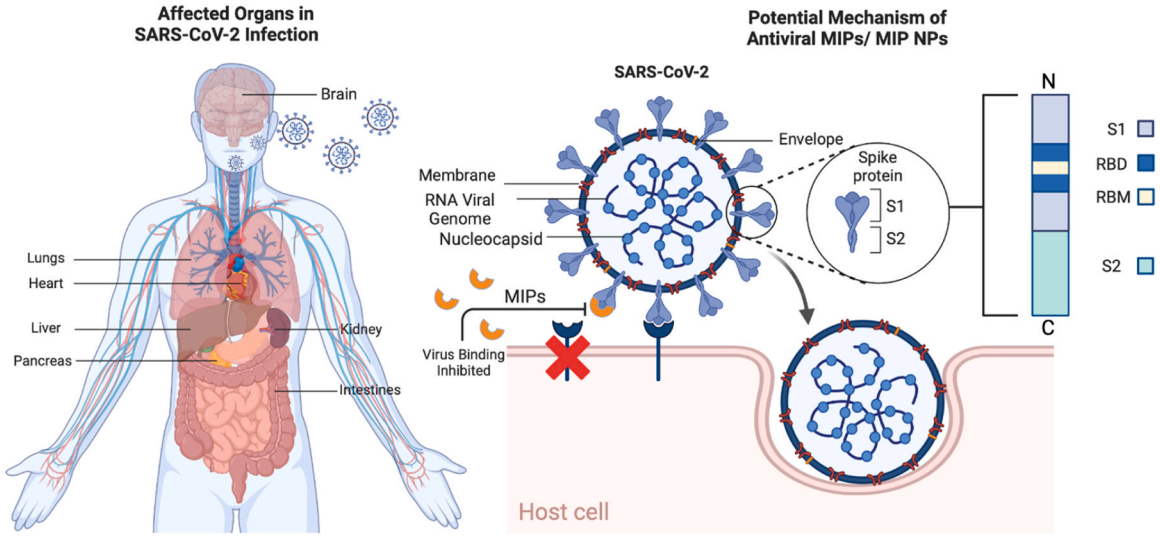

Fig. 10. Schematic diagram of the SARS-CoV-2 coronavirus particle and its structural components. Viral entry is facilitated by the S protein on the SARS-CoV-2 surface which binds the ACE2 receptor. The S protein is subdivided into two subunits: S1, which contains the RBD and its receptor-binding motif (RBM), and S2. Once cell-free, the macrophage-phagocytosed virus can lead to multi-organ damage by spreading and infecting other organs that contain ACE2 expressing cells. The interaction between the spike protein and the ACE2 receptor on host cells and the subsequent uptake of the virus into cells can be blocked by MIPs and MIP NPs that can bind the spike protein. Created by using Biorender.com.

on detection, the high selectivity of these MIPs suggests their potential to inhibit SARS-CoV-2 infection by blocking the critical interaction between the S protein and host cells.

Targeting entire viral surface proteins, such as hexon and E2, or larger subunits like the S1, has shown significant promise for preventing viral entry. However, focusing on smaller, functionally critical domains, such as RBDs, allows for even greater precision and efficiency. The next section examines the potential of targeting these binding domains to

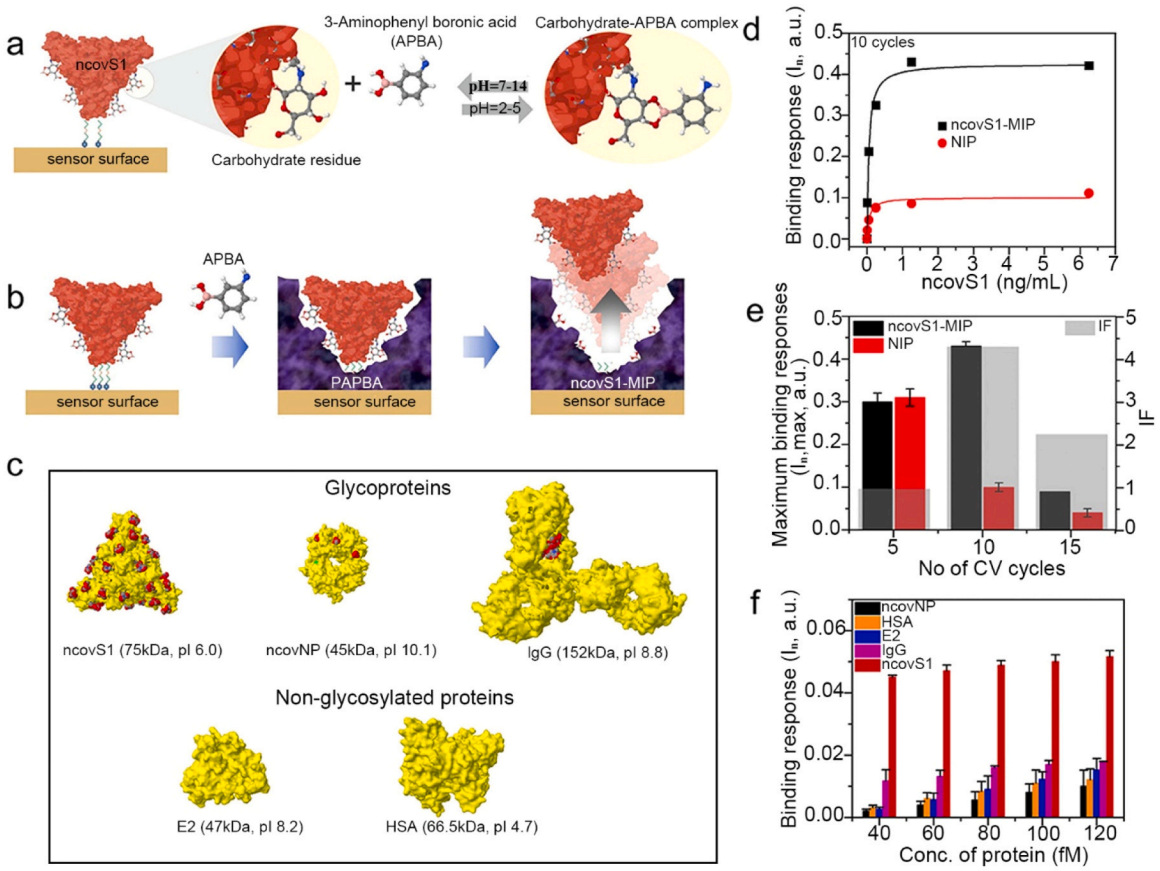

Fig. 11. a) Schematic representation of the covalent interaction between carbohydrate groups (red spheres) on glycosylated S1 subunit (ncovS1) and the boronic acid group of APBA. b) Formation of ncovS1-MIP on the sensor surface through the electropolymerization of APBA, followed by the removal of ncovS1 to create selective binding cavities in the poly(3-aminophenylboronic acid) (PAPBA) matrix. c) 3D structures of ncovS1, ncovNP, IgG, HSA (monomeric form), and E2 proteins, highlighting oxygen atoms (red spheres) in carbohydrate residues present in glycosylated proteins. d) Adsorption isotherms showing the binding responses of ncovS1-MIPs and NIPs after 15 min of incubation with increasing concentrations of ncovS1 (0.01–6.25 ng/mL) in PBS, under optimal conditions with 10 CV cycles. e) Maximum binding responses ($I_{n,max}$) of ncovS1-MIPs and NIPs prepared using 5, 10, and 15 CV cycles, with IFs calculated as the ratio of In,max for ncovS1-MIPs to NIPs. f) Selectivity of ncovS1-MIPs tested against various proteins (ncovNP, HSA, E2, IgG, and ncovS1), demonstrating differential responses at increasing protein concentrations (40–120 fM) in PBS. Adapted with permission from Ayankojo *et al.* [83]. Copyright 2022, Elsevier.

enhance MIP specificity and antiviral applications.

2.2.2. *Binding domains of viral surface proteins*

Focusing on specific binding domains of viral surface proteins, such as RBD within the SARS-CoV-2 S1 subunit, provides a more precise approach to inhibit viral entry than targeting entire proteins. This precision arises because binding domains are the specific functional regions directly involved in receptor interactions, whereas entire surface proteins often include non-essential regions that could dilute the targeting efficiency of MIPs [133]. The RBD contains the critical residues responsible for ACE2 receptor binding in SARS-CoV-2 infection, making it an ideal target for MIPs [134–137].

Recent studies have shown the efficacy of RBD-targeted MIPs. Parisi *et al.* developed MIP NPs that selectively bind to the SARS-CoV-2 RBD, achieving a significantly higher binding capacity (29.3 ± 1.1 %) compared to NIPs (3.7 ± 0.6 %) [138]. Selectivity assays showed minimal cross-reactivity of MIP NPs with the SARS-CoV RBD (0.68 ± 0.03 %), highlighting their specificity. Hemocompatibility tests revealed a hemolysis rate of 3.9 %, which is considered within a generally accepted safety range for biomedical applications (below 5 %) [139,140], supporting their potential for therapeutic use. These findings highlight the promise of RBD-imprinted MIPs as synthetic antibodies with high specificity and safety for antiviral strategies.

Further optimization of RBD-targeted MIPs by Parisi *et al.* incorporated molecular docking and quantum chemical calculations to select functional monomers that maximally covered the RBD surface area [96]. The resulting MIP NPs (MISMAs) achieved a higher adsorption capacity for the SARS-CoV-2 RBD (3.46 mg/g) compared to NIPs (1.47 mg/g). Importantly, MISMAs demonstrated the ability to inhibit ACE2-RBD interaction in a concentration-dependent manner, with a maximum inhibition rate of 99 ± 1 % at a polymer concentration of 20 ng/μL (Fig. 12). This inhibition effect emphasizes the high efficacy of the MIP NPs in antiviral applications, further validated by their negligible activity against non-target viral RBDs, confirming their selectivity.

Building on the promise of RBD-targeted MIPs, Dattilo *et al.* developed MIP NPs specifically targeting the SARS-CoV-2 Omicron RBD to address challenges from viral mutations [141]. These MIPs demonstrated strong selectivity (K_D = 9.5 nM for Omicron RBD vs. K_D = 21 nM for HSA) and effectively inhibited RBD-ACE2 binding in a concentration-dependent manner, achieving over 80 % inhibition at 500 ng/μL, while NIPs showed no significant effect. Cytotoxicity tests on BALB/3T3 cells confirmed their biocompatibility, and the absence of sensitization was validated by measuring the expression of co-stimulatory molecules CD86 and CD54 in THP-1 human leukemia monocytic cells. These findings affirm the potential of MIPs as safe and highly effective tools against emerging viral variants.

Compared to whole-protein imprinting, targeting binding domains offers significant advantages in specificity and functionality. Furthermore, recent advances, such as the development of MIPs tailored for the Omicron variant RBD, demonstrate the adaptability of this approach,

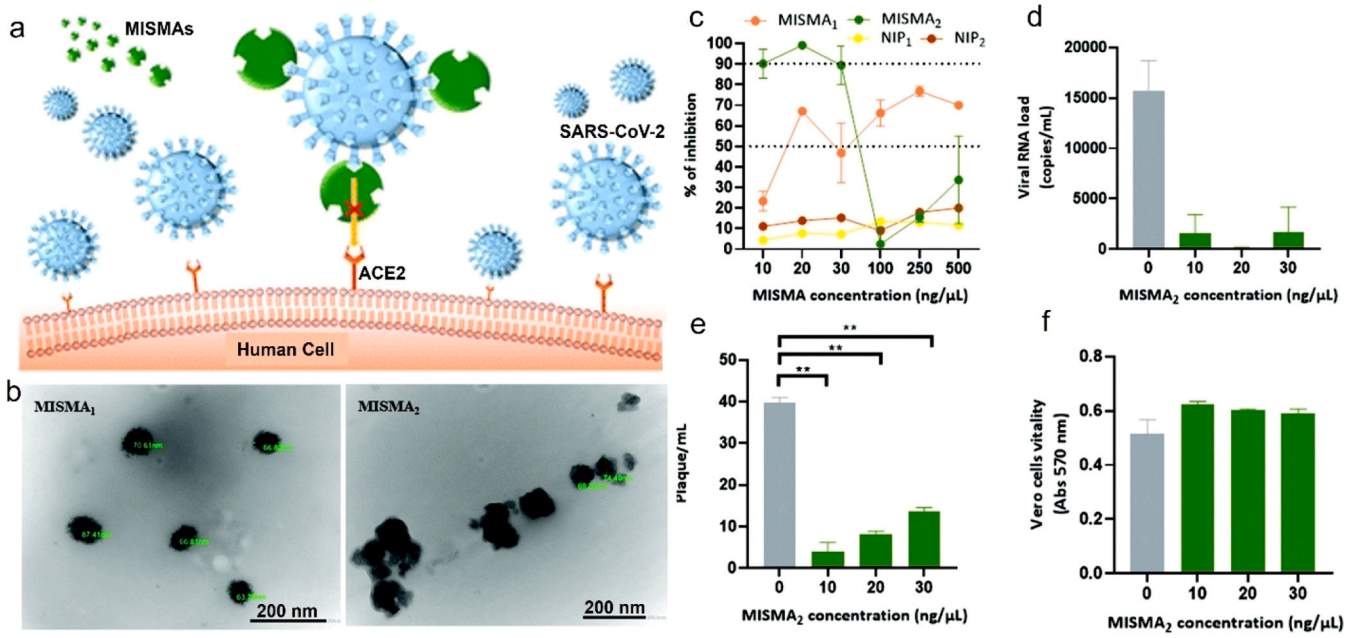

Fig. 12. a) Schematic diagram of MIP-based "monoclonal-type" plastic antibodies interacting with the SARS-CoV-2 virus. b) TEM micrographs of $MISMA_1$ and $MISMA_2$. c) molecularly imprinted synthetic material antibodies (MISMAs) inhibition activity on SARS-CoV-2 infectivity *in vitro*, $MISMA_1$ and $MISMA_2$ were synthesized using acrylamide and a mixture of acrylic acid and acrylamide as functional monomers, respectively. The inhibition of viral replication in Vero cells by both MISMAs was measured as the decrease in viral load in culture supernatant. Dotted lines indicate 50 % and 90 % inhibition of viral transmission. d) Detection of viral production by RT-PCR with and without $MISMA_2$. The mean and SD of triplicate from one experiment are displayed. e) The Inhibition of SARS-CoV-2 replication was measured *via* a plaque assay on Vero cells. The mean and SD of triplicate from two independent experiments are displayed. ** indicate $p < 0.005$ as calculated using the Mann–Whitney test. f) Cell vitality was measured *via* the Crystal Violet assay in Vero cells treated with $MISMA_2$. The mean optical density values and SD of one representative experiment performed in triplicate are displayed. Adapted with permission from Parisi *et al.* [96]. Copyright 2021, Royal Society of Chemistry (RSC).

highlighting its potential to address emerging viral mutations. Ongoing efforts continue to refine this strategy. As discussed in the next section, further focusing on minimal essential virus-host interaction sites, such as epitopes, holds promise for achieving even greater precision.

2.2.3. *Epitopes of viral surface proteins*

Epitopes are among the smallest functional and structural units of viral surface proteins, often representing the minimal sites necessary for virus-host interactions [142]. Unlike larger domains such as RBDs or entire surface proteins, epitopes are small, solvent-exposed fragments consisting of only a few to tens of amino acid residues, making them ideal targets for highly selective molecular imprinting (Fig. 13) [133, 143]. Using epitopes as templates not only improves specificity and reduces cross-reactivity but also addresses challenges associated with the stability and complexity of full-length proteins [133]. Synthesizing short peptide fragments is simpler, less expensive, and avoids the

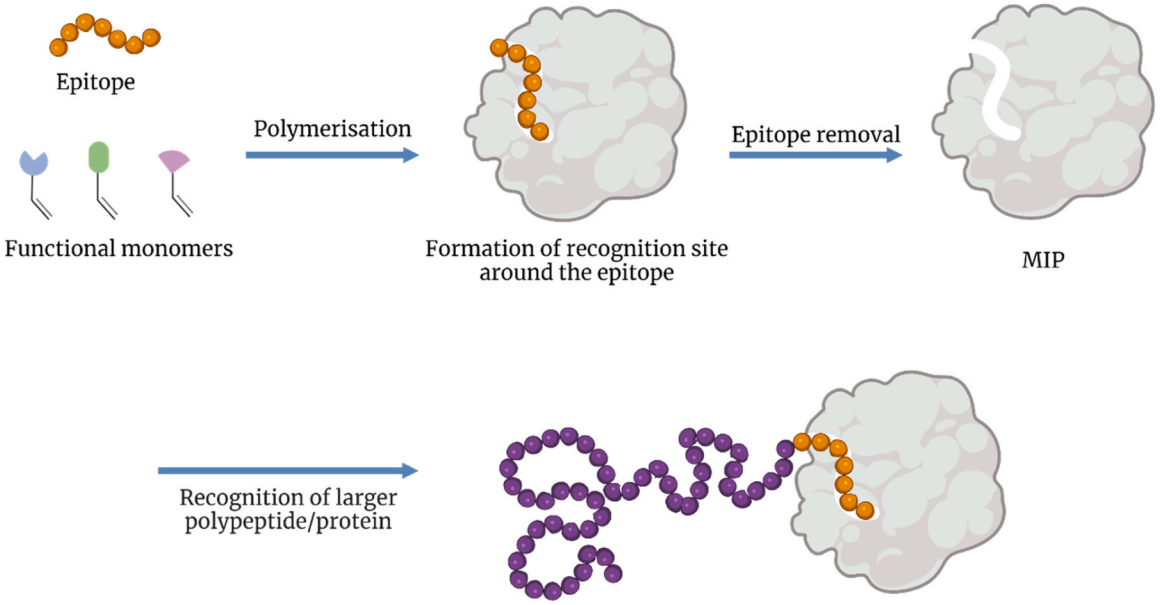

Fig. 13. Schematic representation of the epitope approach whereby an epitope imprinted cavity is formed in a MIP matrix which can selectively recognize its macromolecular counterpart.

variability often seen with larger protein structures [144]. By focusing on these minimal sites, MIPs achieve uniform, high-affinity binding while lowering production costs and complexity. This epitope-based approach provides a cost-effective and scalable strategy for therapeutic and diagnostic applications targeting critical virus-host interaction sites. Table 4 lists MIPs that target viral epitopes.

The specificity and efficiency of epitope-based MIPs have been exemplified in studies on SARS-CoV-2. For instance, Fresco-Cala *et al.* employed the FNCYFPLQSYGFQPTNG epitope from the SARS-CoV-2 RBD to develop magnetic MIPs (MMIPs) *via* dopamine self-polymerization [149]. Computational docking identified dopamine as the optimal monomer, forming strong multi-point interactions across the epitope, with a binding energy of −3.4 kcal/mol. These MMIPs exhibited significantly enhanced binding capacity and selectivity for the SARS-CoV-2 epitope, with IF reaching 5.48, compared to magnetic non-imprinted polymers (MNIPs). This selectivity allowed efficient distinction of SARS-CoV-2 from other viral sequences, such as those of Zika virus. Similarly, Batista *et al.* developed silica-based core-shell MIPs using the same epitope, designed to mimic ACE2 receptor binding [152]. The MIPs leveraged π–π and π–alkyl interactions between phenyltriethoxysilane (PTES) and aromatic residues of the epitope, resulting in superior binding performance. Infection assays using SARS-CoV-2 S protein pseudoviruses revealed that these MIPs significantly reduced residual infectivity in VeroE6 cells, demonstrating their antiviral potential (Fig. 14). Together, these studies illustrate the feasibility of epitope-based imprinting to inhibit viral entry with high specificity and functional precision.

Beyond SARS-CoV-2, epitope-based MIPs have been successfully applied to other viral targets, such as HIV-1. A notable example involves the fusion-mediating gp41 protein, a transmembrane subunit critical for HIV entry *via* host cell fusion. Using a synthetic peptide corresponding to residues 579–613 of gp41, researchers developed MIPs with a high binding affinity (K_D = 3.17 nM), comparable to monoclonal antibodies [75]. These MIPs also displayed exceptional specificity, with recognition levels to the full gp41 protein 6-fold higher than those for control peptides or BSA. Furthermore, Xu *et al.* imprinted another gp41 epitope to develop synthetic antibodies with immunoprotective potential, further highlighting the versatility of epitope-based MIPs in therapeutic applications [148]. The immune-enhancing aspects of this strategy will be discussed in 4.1.

2.2.4. *Viral surface glycans*

Glycans are carbohydrate structures ubiquitously found on the surface of viral envelope glycoproteins, where they play critical roles in facilitating viral entry. Glycans stabilize and modulate the conformation of key functional regions, such as RBDs or fusion peptides, facilitating efficient interactions with host cell receptors and enabling viral entry. Unlike proteins, which exhibit high mutation rates under selective pressures, viral glycans are host-derived and tend to maintain conserved structural features. This makes glycans both indispensable for viral infectivity and an appealing target for MIPs [153].

Zhou *et al.* explored this potential by developing glycan-imprinted MIPs (GINPs) to target high-mannose glycans on the HIV-1 envelope glycoprotein gp120 (Fig. 15) [97]. These conserved glycans are essential for viral binding to host CD4 receptors, a critical step in the HIV-1 infection process [154]. In this study, glycans enzymatically extracted from HIV-1 virions were used as templates for surface imprinting on SiO_2 NPs. A boronic acid–functionalized monomer system enabled reversible covalent interactions with the cis-diol groups of glycans during polymerization, facilitating the formation of a thin, site-specific

Table 4
Applications of MIPs targeting viral epitopes.

Targeted virus	Template used	Template sequence	MIP morphology and size	Application	Reference
Dengue virus (DENV)	Epitope from NS1 of DENV serotype 1	^{28}WTEQYKFQA^{36}	MIP film (17.51 nm thickness)	Detection of DENV NS1 protein in biosensors.	[145]
	Dengue NS1 epitope	Ac-VHTWTEQYKFQ-NH_2	MIP film (15 nm thickness)	Detection of dengue NS1 protein using a QCM-based sensor for early diagnosis of dengue infection.	[72]
	Dengue NS1 epitope	TELRYSWKTWGKAKM	MIP film (70 nm thickness)	Detection of Dengue NS1 protein.	[70]
HAV	Epitope from HAV receptor (HAVCR- 1)	CEHRGWFNDC-K(N_3)	MIP nanogels (48 nm size)	Recognition of HAVCR−1 for antiviral therapy.	[146]
hAdV5	Epitope from the fiber knob of the HAdV capsid	AKLTLVLTKCGSQILATVSVLA	MIP NPs (71.8 ± 8.12 nm diameter)	Detection of HAdV in water and human serum using a QCM-based sensor.	[147]
HIV	Epitope from the HIV protease (HIV PR) protein	IGRNLLTQIG	MIP film	Detection of HIV protease and screening for its inhibitors, such as nelfinavir, with potential applications in antiviral drug development.	[76]
	Epitope derived from the 3S motif of glycoprotein 41 (gp41)	CGSWSNKSC	MIP NPs (65 ± 4 nm diameter)	Recognition and blocking of the 3S motif on gp41, with the aim of preventing HIV-induced CD4$^+$ T cell depletion.	[148]
	Epitope derived from the gp41 fragment (residues 579–613)	RILAVERYLKDQQLLGIWGCSGKLICTTAVPWNAS	MIP film	Detection of HIV−1 gp41 in real samples (*e.g.*, human urine) for diagnostic purposes.	[75]
SARS-CoV−2	Epitope from RBD of the SARS-CoV−2 spike protein.	FNCYFPLQSYGFQPTNG	MIP NPs (45.57 nm diameter)	Detection of SARS-CoV−2 spike protein for potential use in virus detection systems.	[149]
	Epitope from RBD of the SARS-CoV−2 spike protein	-	MIP NPs (68.8 ± 0.6 nm diameter)	Thermal detection of SARS-CoV−2.	[150]
	Epitope from RBD of the SARS-CoV−2 spike protein	GFNCYFPLQ	MIP film (10 nm thickness)	Detection of the SARS-CoV−2 RBD using a surface plasmon resonance imaging (SPRi) platform for rapid screening and diagnostics.	[151]
	Epitope from RBD of the SARS-CoV−2 spike protein	FNCYFPLQSYGFQPTNG	Core/shell silica NPs with MIP film (500 nm diameter)	Selective binding of the SARS-CoV−2 spike protein, mimicking the ACE2 receptor for potential therapeutic applications.	[152]

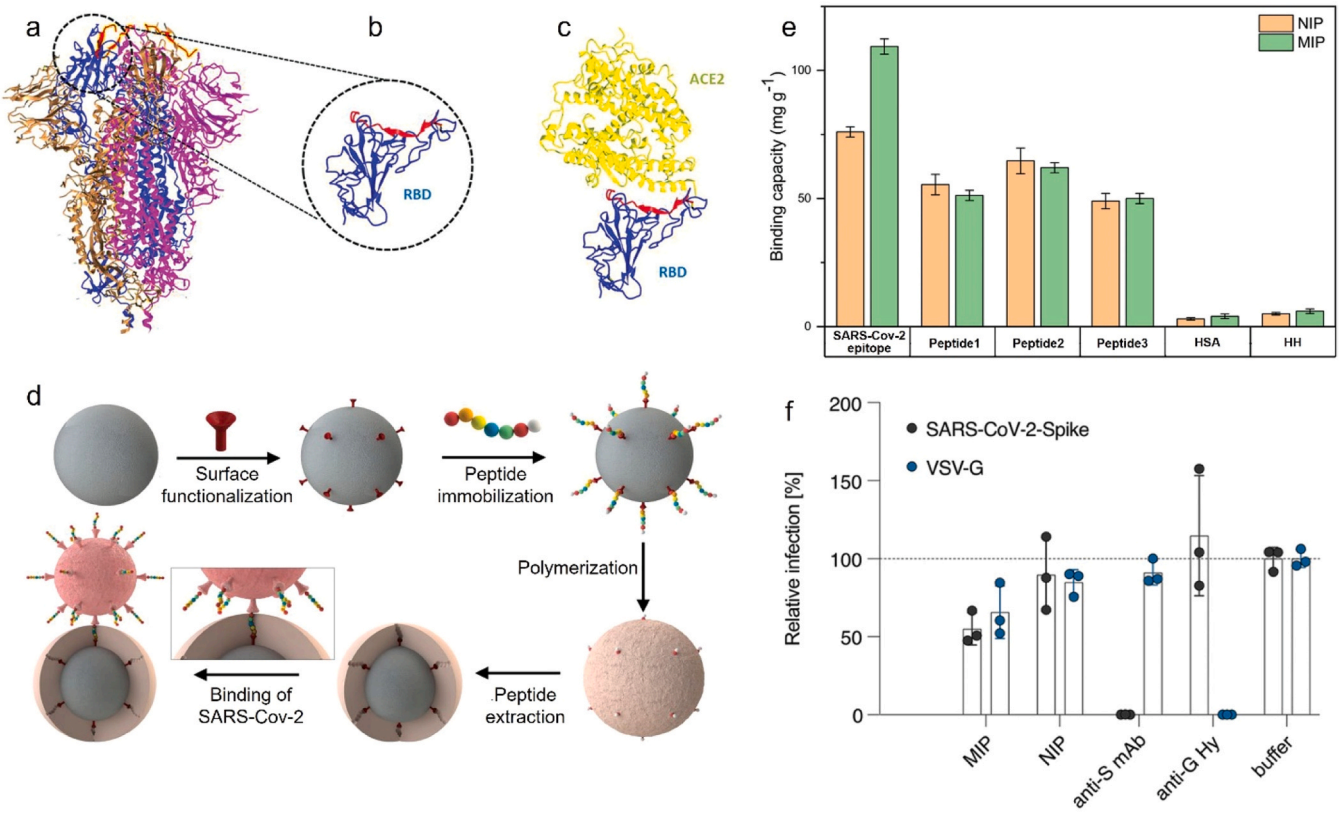

Fig. 14. a) Complete structural representation of the SARS-CoV-2 spike protein (PDB ID: 6VXX). b) Close-up view of the RBD, with the selected epitope marked in red. c) Illustration of the RBD in complex with the ACE2 receptor (PDB ID: 6M0J). d) Schematic outline of the synthesis process for core/shell particles imprinted with the SARS-CoV-2 epitope. e) Comparison of the binding capacities of MIPs and NIPs for the SARS-CoV-2 epitope and other peptides of comparable length. Peptide 1: MIVNDTGHETDENRA, peptide 2: TECSNLLLQYGSFCTQL, peptide 3: KLPDDFTGCV, HAS: human serum albumin, HH: human hemoglobin. f) Relative infection levels in the supernatant post-incubation with MIP, NIP, and neutralizing agents (anti-S mAb and anti-G Hy), where relative infection denotes luciferase activity measured in VeroE6 cells inoculated with pseudoviruses and treated with each sample, normalized to those treated with PBS alone. Infections were conducted in triplicate, with error bars indicating standard deviation (SD). Adapted with permission from Batista *et al.* [152]. Copyright 2022, Wiley.

MIP shell upon template removal.

GINPs bound HIV-1 with high affinity (K_D = 36.7 nM), comparable to broadly neutralizing antibodies, and exhibited low cross-reactivity with unrelated viruses such as influenza A, rabies, and adenovirus (<4 %). Flow cytometry and confocal imaging confirmed selective recognition of HIV-infected H9 cells and envelope-expressing 293T-gp160 cells. In pseudovirus assays, GINPs achieved potent neutralization across seven HIV-1 strains, including tier 2 viruses, with IC_{50} values at the low pM level. Long-term inhibition was sustained in infected T lymphoblastic cell line CEM-SS cultures for at least 9 days, achieving more than 95 % suppression of viral replication along with stable NPs dispersion. Cytotoxicity remained negligible at therapeutic concentrations.

While glycans extracted from HIV-1 virions provide biologically accurate templates, their low yield, batch-to-batch variability, and biosafety requirements pose limitations for scalable synthesis. To address this, the authors employed recombinant HIV-1 envelope glycoprotein trimers as alternative templates. Specifically, they used the BG505 SOSIP.664 construct, which faithfully mimics native glycan presentation and can be expressed in mammalian cells. GINPs prepared using this approach showed comparable binding performance and antiviral activity, while offering improved reproducibility and production feasibility.

Glycan-targeting strategies leverage structurally conserved and mutation-resistant features of viral surfaces, but protein-targeting MIPs remain equally important. In enveloped viruses, glycan shields do not fully obscure all functionally critical regions, allowing access to protein epitopes. In contrast, non-enveloped viruses such as adenoviruses lack glycan shielding altogether, making capsid proteins fully exposed and accessible to imprinting. This structural diversity highlights the complementary roles of glycan- and protein-targeted MIPs in broad-spectrum antiviral design.

2.3. *Challenges of MIPs for inhibiting viral entry*

The application of MIPs to inhibit viral entry into host cells presents both opportunities and challenges. While MIPs designed to capture whole viruses or target viral surfaces have demonstrated potential in reducing viral infection rates, several critical challenges remain to be addressed before these systems can be translated into clinical or environmental applications. The key challenges include specificity issues in complex biological environments, stability and durability in practical use, and biocompatibility when applied *in vivo*.

2.3.1. *Specificity challenges*

One of the primary challenges in using MIPs to inhibit viral entry is achieving high specificity while minimizing non-specific binding, particularly in complex biological environments. As discussed in 2.1.2, *in vivo* applications expose MIPs to bodily fluids containing a wide range of proteins, glycoproteins, lipids, and other biomolecules, which can interfere with the selective binding of MIPs to viral particles, leading to non-specific adsorption. Although strategies such as anti-fouling surface modifications (*e.g.*, PEGylation and SAM coatings) have been employed to mitigate these effects, the specificity problem becomes more nuanced when MIPs are designed to target specific viral surface components rather than whole viruses.

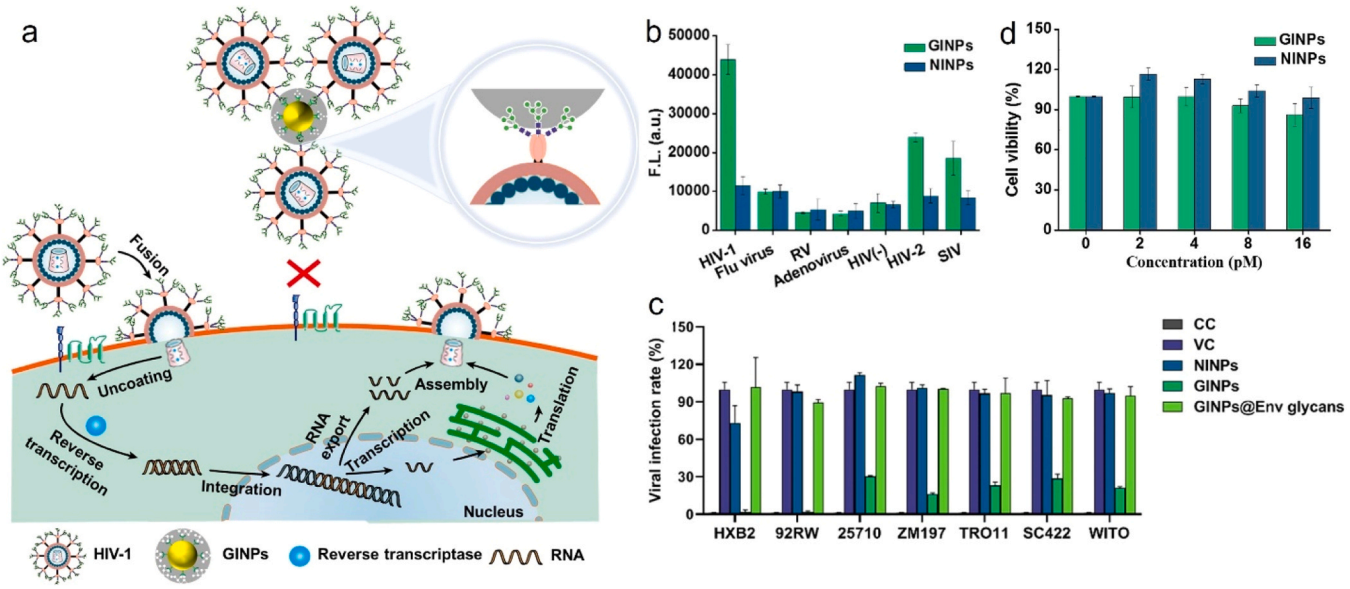

Fig. 15. a) Schematic representation of GINPs inhibiting HIV-1 infection by blocking envelope glycans. b) Adsorption selectivity of GINPs for various viruses, including influenza A virus (Flu, A/PR/8/34), rabies virus (RV), and simian immunodeficiency virus (SIV), *etc.* c) Broad neutralization effects of 16 pM GINPs on pseudoviruses with Env proteins from diverse HIV-1 strains. Tested strains include four tier 1 strains (HXB2, 92RW020.2, 25710, and ZM197 M.PB7) and three tier 2 strains (TRO11, SC422661.8, and WITO4160.33). Experimental groups: CC (negative control, no virus), VC (positive control, virus without NPs), NINPs (virus incubated with non-imprinted NPs), GINPs (virus incubated with glycan-imprinted NPs), and GINPs@Env glycans (virus incubated with GINPs pre-blocked by HXB2 envelope glycans). All groups were incubated for 30 min. d) Cytotoxicity assessment of NPs using Cell-Titer Glo assay. Error bars indicate the standard deviation of three independent experiments. Adapted with permission from Zhou *et al.* [97]. Copyright 2024, American Chemical Society.

In such cases, the choice of target region becomes critical, as it affects not only binding efficiency but also potential immunological interference. Targeting highly immunogenic regions, particularly those essential for host immune recognition, may inadvertently mask these sites and hinder immune surveillance, potentially promoting immune evasion. To maximize antiviral efficacy without compromising host immunity, MIPs should preferably bind to regions that are functionally important for viral entry yet exhibit relatively low immunogenicity. This approach enables a balance between molecular recognition precision and immunological compatibility, especially in prophylactic or therapeutic applications.

Viral surface proteins, especially in rapidly evolving viruses like SARS-CoV-2 and influenza, often undergo mutations that alter key binding regions, compromising the specificity of MIPs targeting these variable targets [155,156]. While some MIPs have been developed for specific variants, such as SARS-CoV-2 Omicron, the rapid evolution of viruses often leads to a lag between variant emergence and MIP adaptation. A more robust strategy is to focus on conserved epitopes that maintain structural stability across different viral strains, such as the S2 subunit of coronaviruses, to improve binding stability despite antigenic variation. Additionally, multi-target imprinting strategies that simultaneously recognize conserved protein epitopes and stable structural features, such as glycans, are expected to enhance the adaptability and recognition capacity of MIP-based virus capture.

Moreover, AI-driven techniques, including AlphaFold-assisted structural prediction and machine learning-based mutation analysis, enable researchers to identify mutation hotspots and predict how these changes may impact viral protein structure and binding interactions [157,158]. Integrating AI predictions with real-time viral evolution data enhances the resilience of MIP design against antigenic drift and shift, supporting rapid adaptation to emerging variants and improving the long-term applicability of MIP-based antiviral strategies [159,160].

In summary, optimizing MIP specificity requires a multi-faceted approach: incorporating anti-fouling surface modifications, targeting conserved regions with relatively low immunogenicity, using multi-target imprinting strategies, and leveraging AI-driven prediction tools. Addressing challenges related to non-specific binding and viral mutations remains critical for fully realizing the potential of MIPs in antiviral applications.

2.3.2. *Stability and durability*

Maintaining stability and durability is crucial for antiviral MIPs in specific applications. Potential environmental uses, such as air filtration, wastewater treatment, and blood purification, require MIPs to maintain virus capture and neutralization efficiency while enduring fluid dynamics and chemical exposure.

To enhance stability, particulate MIPs can be covalently grafted onto substrate surfaces or directly polymerized in situ to form MIP films, ensuring strong adhesion even under fluid stress. Increasing surface roughness further reinforces the mechanical interlocking between the substrate and the MIP layer [161]. Using chemically stable, non-degradable monomers and cross-linkers can improve resistance to degradation, while higher cross-linking density enhances structural integrity [162]. This approach contrasts with MIPs designed for *in vivo* applications, which prioritize biodegradability. Additionally, some MIPs incorporate regeneration mechanisms, such as the reusable, stimuli-responsive hydrogel "sponges" previously described (2.1.3), and MIPs based on Fe_3O_4 NPs for virus adsorption, magnetic separation, and inactivation (2.1.4). Implementing these strategies helps maintain the stability and durability of MIPs across diverse environmental applications, ensuring long-term reliable performance.

2.3.3. *Biocompatibility and safety*

Biocompatibility is a critical consideration for the *in vivo* application of MIPs. Due to their synthetic nature, MIPs may present potential risks such as cytotoxicity, immune activation, blood incompatibility, and long-term stability issues. To address these challenges, it is essential to optimize material composition, particle size, surface properties, and degradability to ensure safety while maintaining antiviral activity [163].

The cytotoxic risk of MIPs primarily stems from the monomers and cross-linkers used in their synthesis. For example, commonly used

monomers and cross-linkers such as methacrylic acid (MAA) and ethylene glycol dimethacrylate (EGDMA) may leave unreacted residues within the polymer matrix that leach out and cause acute toxicity [164,165]. This acute toxicity mainly manifests as oxidative stress and disruption of cell membrane integrity, especially in sensitive mucosal tissues [166]. Specifically, residual MAA can induce reactive oxygen species (ROS) generation, leading to membrane damage and cell death [164]. Optimizing the polymerization process to ensure complete monomer conversion is a key measure to reduce residual toxicity. To further remove unreacted chemicals from MIP synthesis and improve polymer purity and biocompatibility, advanced purification methods such as Soxhlet extraction or supercritical fluid extraction (SFE) can be employed [167]. These optimizations are particularly suitable for short-exposure applications with rapid natural metabolism or direct elimination, such as nasal sprays, oral rinses, and topical skin dressings. In such scenarios, MIPs are primarily used for rapid virus capture and clearance, acting in localized areas with short residence time, thus posing a low risk of bioaccumulation and exhibiting high safety.

However, for injectable formulations or MIPs designed for intravascular use, even low-concentration long-term exposure may lead to chronic toxicity, which is closely related to the structural stability, biodegradability, surface properties, and size of MIPs [168]. Due to their highly cross-linked rigid structure, MIPs are not easily degraded and may accumulate in the liver and spleen over time, causing macrophage aggregation, fibrotic encapsulation, and loss of tissue function [169]. MIPs with high rigidity and rough surfaces may also damage red blood cell membranes through mechanical stimulation in blood vessels, resulting in hemolysis [170,171]. In addition, the surface properties of MIPs determine their blood compatibility and immune response *in vivo*. Specifically, hydrophobic surfaces or those bearing negative charges are prone to non-specific adsorption of zwitterionic plasma proteins such as fibrinogen, thereby inducing platelet adhesion and aggregation, increasing the risk of thrombosis [172,173]. Once a protein corona forms on the MIP surface, it can be readily recognized by immune cells (such as macrophages or dendritic cells), triggering immune activation and acute inflammatory responses. Under long-term use or repeated exposure, this immune response may lead to chronic inflammation or decreased immune tolerance [174,175]. Moreover, MIPs with larger sizes (>200 nm) tend to persist *in vivo* and may provoke clearance by immune organs, while smaller MIPs (<100 nm) have higher surface reactivity, increasing the likelihood of protein corona formation and immune recognition [174,176].

To systematically address the above biocompatibility challenges, material selection for MIPs should prioritize building blocks with good biodegradability and immune inertness [177]. It is particularly recommended to incorporate Generally Recognized As Safe (GRAS) and naturally degradable polymers such as polydopamine, chitosan, and gelatin, or aliphatic polyesters synthesized via ring-opening polymerization, including polylactide (PLA), polyglycolide (PGA), and polycaprolactone (PCL) [178]. These materials not only reduce risks of long-term retention and immune activation but also enable a balance between recognition performance and in vivo degradability through modulation of cross-linking density, thereby providing a safer material foundation for injectable and intravascular MIP applications [179].

On this basis, surface modification is a key strategy to improve the blood compatibility and immune inertness of MIPs. Common hydrophilic strategies include PEGylation and zwitterionic polymer coatings, both of which can significantly reduce protein adsorption and immune recognition by forming stable hydration layers. PEGylation effectively shields surface sites and inhibits phagocytosis, while zwitterionic coatings neutralize surface charges to suppress platelet activation and thrombosis formation, and exhibit higher stability in long-term *in vivo* environments [180,181]. Furthermore, cell membrane coatings have shown promise in enhancing immune evasion and may offer a biomimetic strategy applicable to MIPs in future applications [182]. Notably, these modification strategies not only improve biocompatibility but also serve as antifouling layers, as previously mentioned, thereby enhancing MIPs' targeting specificity and recognition efficiency in complex biological environments while improving safety.

In addition, as viral entry inhibitors, the particle size of MIPs should be precisely tuned according to the administration route [183]. For injectable formulations, a particle size range of 50–200 nm is recommended to prolong circulation time, reduce liver and spleen accumulation, and enhance controllability of excretion [184,185]. For local and short-term applications such as nasal, oral, or dermal administration, size requirements can be relaxed, focusing instead on optimizing adhesion and residence time to enhance local antiviral effects while minimizing systemic exposure [186].

In summary, the biocompatibility of MIPs for *in vivo* use depends on material composition, size control, and surface modification strategies. Through rational structural design, size optimization, and the introduction of low-immunogenic modifications, MIPs can achieve both antiviral efficacy and reduced toxicity or immune risk, laying a foundation for safe use across various administration scenarios.

3. MIPs preventing virus genome synthesis and replication

Inhibiting viral genome synthesis and replication represents a critical strategy for halting the progression of viral infections. These processes rely on the coordinated activity of structural proteins, non-structural proteins, and the viral genome itself, all of which serve as potential molecular targets. MIPs offer a versatile platform to interfere with these processes, providing both diagnostic and therapeutic applications. This section discusses how MIPs are applied to three key targets: structural proteins involved in genome encapsulation, non-structural proteins critical for replication, and viral genetic material itself. By leveraging MIPs' unique properties, such as high specificity, stability, and adaptability, researchers aim to develop innovative strategies to disrupt viral replication while addressing the practical challenges associated with these approaches.

3.1. MIPs targeting viral structural proteins involved in genome synthesis and replication

Structural proteins are indispensable to the viral lifecycle, providing both structural integrity and functional regulation. These proteins can be broadly categorized into surface structural proteins, which mediate viral entry and have been extensively discussed in 2.2, and internal structural proteins, which are shielded within the viral capsid or envelope and play pivotal roles in intracellular processes. Internal structural proteins, such as the nucleocapsid (N) protein, are released upon entry into the host cell, where they stabilize viral RNA or DNA, facilitate replication, and assemble progeny virions. Unlike surface proteins, which primarily interact with extracellular host factors, such as receptors, internal proteins interact directly with the viral genome and host replication machinery, making them compelling targets for MIPs aimed at disrupting viral proliferation.

Among internal structural proteins, the N protein of SARS-CoV-2 has emerged as a particularly attractive target due to its multifaceted role in viral replication. This protein encapsulates viral RNA into a stable ribonucleoprotein complex, enabling the transcription and replication of the viral genome (Fig. 16) [187]. Furthermore, the N protein actively suppresses host antiviral responses, including RNA interference (RNAi) pathways, through direct RNA binding, thereby facilitating immune evasion and viral persistence [188]. Inhibiting the N protein could simultaneously block viral replication and restore host immune defense, showing its significance as a therapeutic target.

Recent advancements in MIPs have demonstrated their potential to selectively target the N protein with high specificity and affinity. For example, Raziq *et al.* developed a MIP film that achieved precise recognition of the SARS-CoV-2 N protein, demonstrating linear

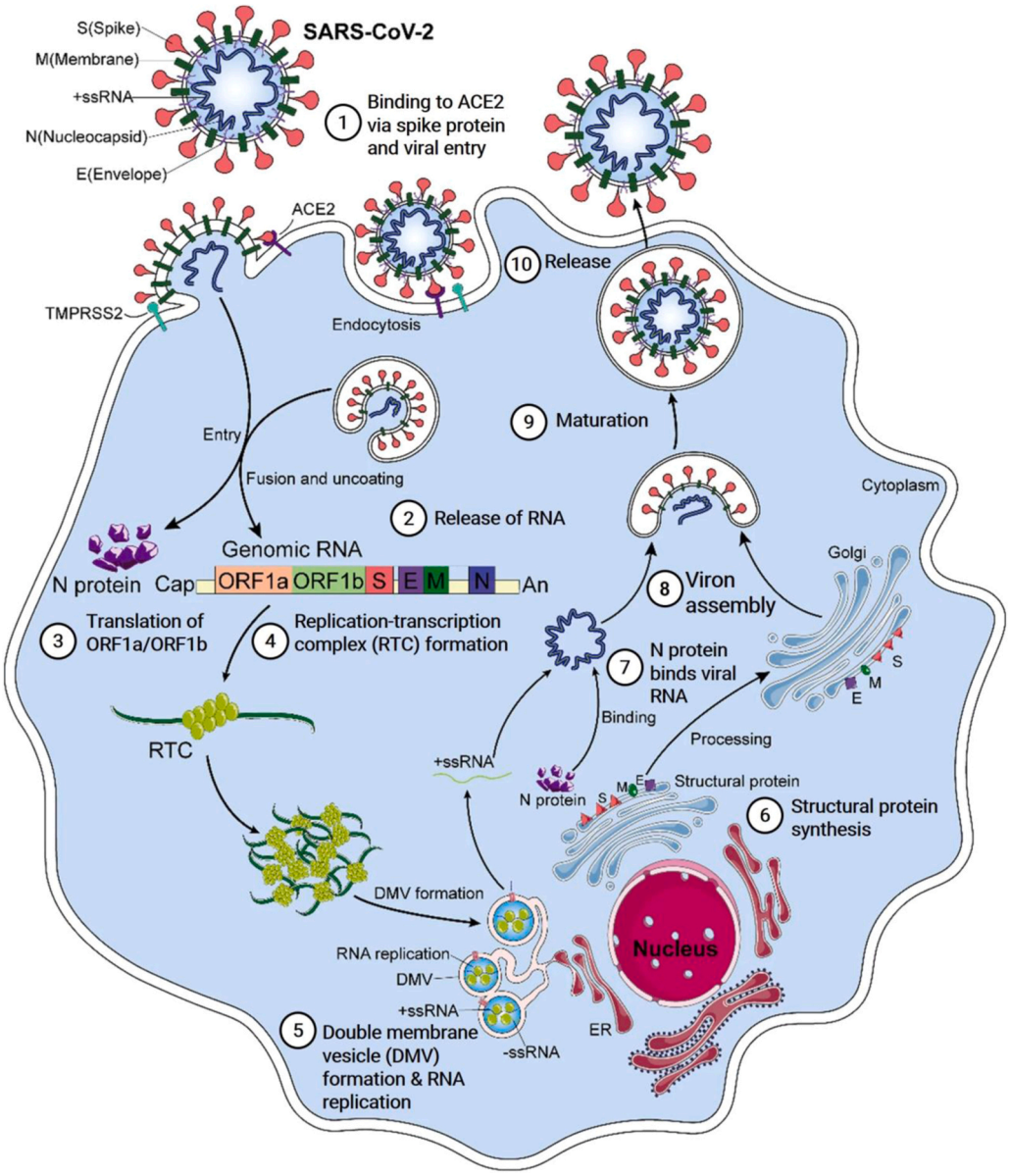

Fig. 16. Schematic illustration of the SARS-CoV-2 life cycle. The virus binds to the ACE2 receptor on target cells, and the S protein is cleaved by proteases like TMPRSS2, facilitating fusion with the plasma membrane. SARS-CoV-2 can also enter cells *via* endocytosis. The N protein dissociates from the positive strand viral RNA genome, which is then translated into polyproteins pp1a and pp1ab. These are processed and translated into NS proteins nsp1–16, which form replication and transcription complexes (RTCs) and reshape the cell membrane to create replicating organelles (DMVs). The organelles form a continuum with the endoplasmic reticulum (ER) and viral RNA replication occurs mainly in DMVs. The new viral RNA vacate the DMVs *via* transmembrane pores for translation or virion assembly. These translated structural proteins are transported to the ER membrane and move through the ER-to-Golgi intermediate compartment (ERGIC). The positive-strand viral RNA of the genome, wrapped by N protein, assembles with structural proteins S, M, and E, forming new virions that bud into the ERGIC lumen. Finally, progeny virions are released from the host cell. Adapted from Wu *et al.* [187] under the terms of the Creative Commons CC BY license.

detection up to 111 fM and successful identification in nasopharyngeal swabs from COVID-19 patients [82]. Drobysh *et al.* further advanced this approach by employing polypyrrole-based MIPs in combination with gold nanostructures, enhancing both specificity and binding strength while minimizing non-specific interactions [189]. Zhang *et al.* introduced a poly-arginine-functionalized gold/graphene nanohybrid MIP, leveraging the material's high surface area and conductivity to achieve ultra-sensitive detection of the N protein [190]. Originally designed for diagnostic purposes, these MIPs exhibit selective binding capabilities that highlight their therapeutic potential in targeting replication-associated N proteins. While these thin-film MIPs are optimized for detecting replication-associated N proteins in diagnostic applications, transitioning to therapeutic use requires re-engineering them into nanosystems capable of intracellular delivery. Such a transformation could enable these MIPs to go beyond detection and directly disrupt viral replication processes. This concept will be explored in detail in Section 3.4.

In addition to N proteins, other internal structural proteins, such as the matrix (M) protein, also play vital roles in the viral lifecycle and represent promising future targets for MIP development. The M protein, which coordinates the assembly of viral components into infectious virions, is essential for the structural and functional integrity of many enveloped viruses [191]. Developing MIPs against the M protein could expand the scope of antiviral applications by targeting additional stages of the viral replication cycle.

MIPs targeting internal structural proteins, particularly the N

protein, represent a novel and effective approach to inhibiting viral replication by selectively binding to components critical for genome stability and transcription. Although primarily explored for diagnostic purposes, the high specificity and affinity of these MIPs suggest significant therapeutic potential, laying the groundwork for theranostic tools that integrate antiviral treatment and real-time detection. Future efforts to develop MIPs targeting other internal proteins, such as the M protein, could further diversify antiviral strategies and enhance the applicability of this technology across different viral pathogens.

3.2. MIPs targeting viral non-structural proteins

Beyond structural proteins, viral non-structural (NS) proteins represent another critical class of targets for MIP-based intervention. These proteins are essential to the viral lifecycle, mediating processes such as genome replication, transcription, and immune evasion [192]. Unlike structural proteins, which form the physical framework of the virus, NS proteins are not incorporated into the virion but are instead transiently expressed within infected host cells [193]. By selectively binding and inhibiting these proteins, MIPs can disrupt key stages of viral replication, offering a novel approach to limit viral spread and enhance therapeutic outcomes.

One significant application of MIPs targeting NS proteins involves the HPV E6 and E7 oncoproteins, which are pivotal in HPV-mediated carcinogenesis. E6 and E7 proteins interfere with tumor suppressors p53 and Rb, respectively, driving malignant transformation in infected cells [194]. Cai *et al.* synthesized MIPs with a non-conductive polymer coating specific to HPV E7 (type-16), achieving exceptional sensitivity at sub-picogram levels [80]. These MIPs demonstrated outstanding selectivity, binding exclusively to E7 while excluding E6, as validated through computational docking analyses. This precise targeting illustrates the potential of MIPs in HPV-related therapeutic applications, particularly in addressing malignancies linked to high-risk HPV types.

For the DENV, the NS1 protein plays a dual role in supporting viral replication and facilitating immune evasion. NS1 forms complexes critical for RNA synthesis and packaging, while also modulating host immune responses to promote vascular permeability and inflammatory cytokine production (Fig. 17) [195]. Arshad *et al.* developed MIPs targeting the full NS1 protein using screen-printed carbon electrodes (SPCE) modified with polysulfone nanofibers and polydopamine coatings [196]. This innovative design preserved NS1's structural integrity and enabled highly specific binding, even in complex biological samples. By disrupting NS1 function, these MIPs could interfere with both replication and immune evasion, demonstrating their therapeutic potential in mitigating severe dengue pathogenesis.

Moving beyond targeting entire NS proteins, epitope imprinting

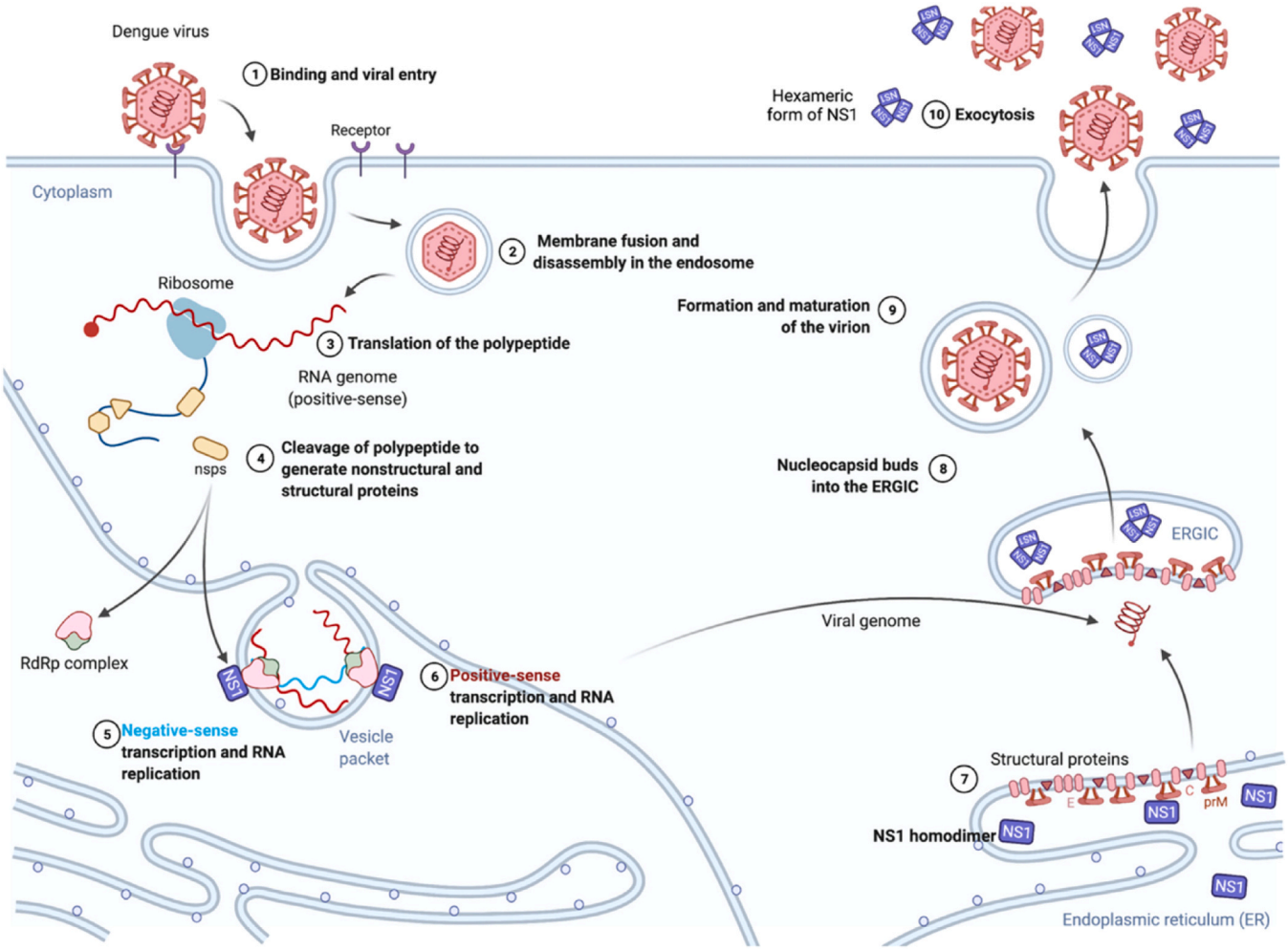

Fig. 17. The role of the DENV NS1 protein in the viral lifecycle, performing various critical functions. Following its cleavage from the polyprotein, NS1 forms homodimers that bind to viral RNA complexes and facilitate viral morphogenesis through interactions with prM and E proteins. Owing to its hydrophobic characteristics and membrane affinity, NS1 contributes to the creation of vesicle packets, which are crucial structures for hosting the viral replication machinery. Notably, among non-structural proteins, NS1 is unique as its soluble hexameric form circulates in infected individuals, necessitating transport into the ER-Golgi intermediate compartment for release. Adapted from Lebeau *et al.* [197] under the terms of the Creative Commons CC BY license.

offers a more precise strategy by focusing on minimal functional regions within these proteins. Liang *et al.* synthesized MIPs tailored to bind a specific peptide sequence from DENV NS1 using a click chemistry approach to create functional monomers with hydrophobic, positively charged, and negatively charged groups (Fig. 18) [198]. The resulting MIPs demonstrated an adsorption capacity of 1.62 mg/g for the NS1 peptide, nearly tripling the capacity of NIPs, which had an adsorption capacity of 0.55 mg/g. This IF of 2.93 highlights the superior specificity and selectivity of the MIPs compared to NIPs, suggesting their potential to disrupt NS1's role in viral replication. Furthermore, these MIPs demonstrated stable adsorption across multiple cycles, highlighting their potential for long-term antiviral applications.

Building on this epitope-targeting approach, Tai *et al.* employed a linear 15-mer peptide epitope from DENV NS1 as a template for MIP synthesis [70]. These MIPs demonstrated high affinity not only for the peptide epitope but also for the intact NS1 protein, providing a streamlined alternative to full protein imprinting while enhancing specificity. The same epitope-based MIPs were adapted for serological assays, enabling clinical detection of dengue viral markers in patient samples and highlighting their diagnostic potential in detecting viral infections [69]. Buensuceso *et al.* designed electropolymerized MIPs (E-MIPs) using another DENV NS1 peptide epitope as the template and polyterthiophene as the primary monomer [72]. The resulting MIPs featured well-defined binding cavities optimized for the target peptide, achieving a threefold increase in binding capacity compared to NIPs. This enhanced binding capacity, coupled with high stability, demonstrates the potential of E-MIPs to serve as both diagnostic tools and models for antiviral therapeutic applications.

Epitope imprinting enhances the specificity of MIPs; however, not all epitopes are suitable for therapeutic applications. Silva *et al.* developed MIPs targeting the heat-denatured dengue virus NS1 protein, exposing hidden epitopes that were otherwise inaccessible in the native conformation [145]. These MIPs effectively distinguished dengue NS1 from Zika NS1 and other proteins, demonstrating their potential in differential diagnosis. However, the dependency on denatured protein structures confines their use to diagnostics, as NS1 adopts a native conformation in natural infections. This highlights the utility of epitope-imprinted MIPs in controlled diagnostic settings, while their therapeutic relevance remains constrained.

MIPs targeting viral NS proteins represent a highly versatile strategy for disrupting viral replication and pathogenesis. By focusing on both entire NS proteins and their critical functional regions, MIPs achieve high specificity and stability while addressing the practical challenges associated with protein synthesis and imprinting. Advances in epitope-based MIPs, as demonstrated in studies on dengue virus NS1 and HPV E7, highlight the scalability and precision of this approach. Although some methods are confined to diagnostic applications, further optimization could expand their therapeutic utility, paving the way for robust

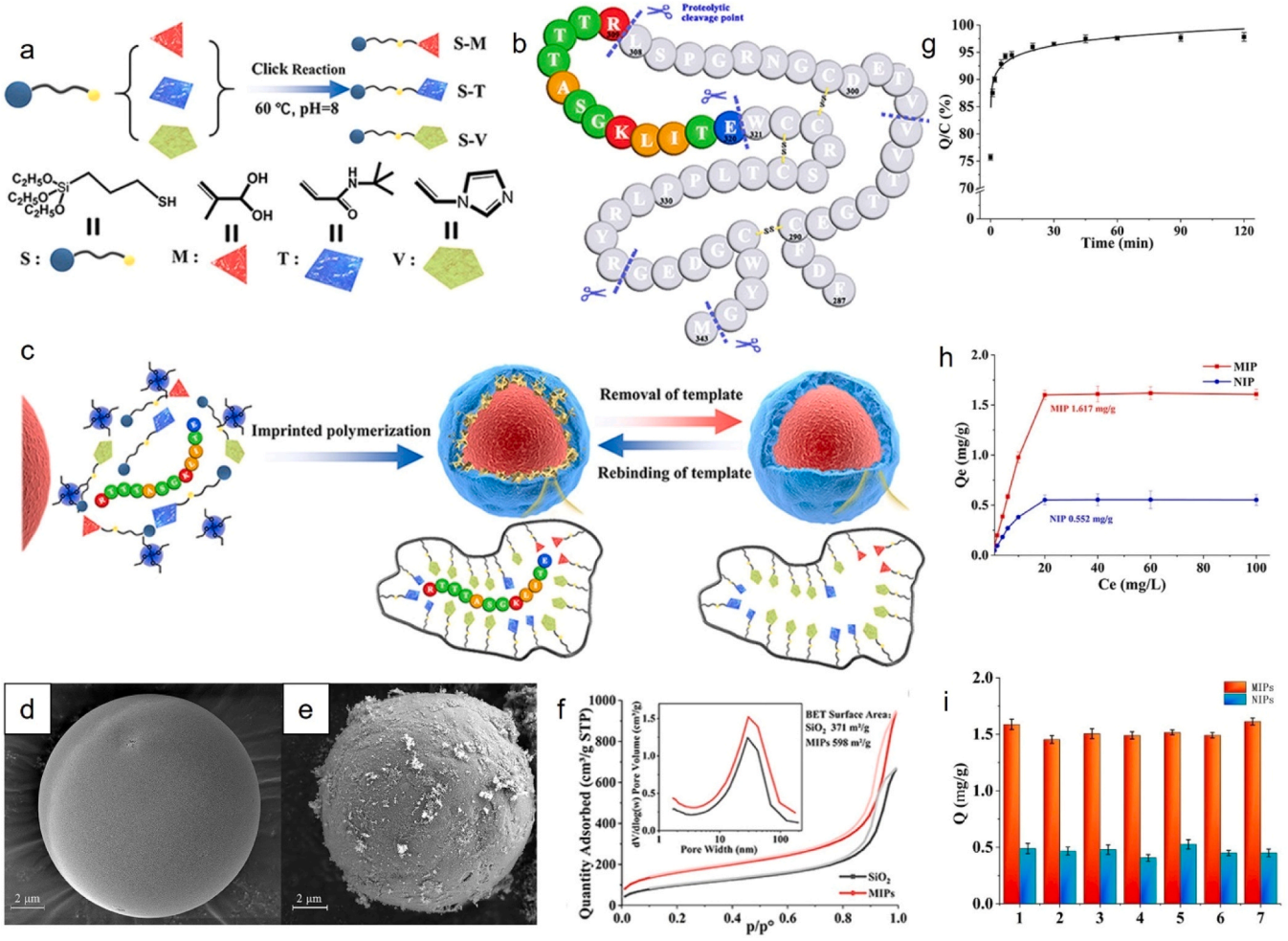

Fig. 18. a) Click reaction for synthesizing three siloxane functional monomers. b) Schematic representation of the dengue fever NS1 proteolysis site and peptide template. c) MIP polymerized on the surface of silica microspheres. SEM images of d) SiO_2 microspheres and e) MIPs. f) Thermogravimetric analysis of MIPs and NIPs, with inset showing pore size distribution calculated from adsorption data. g) Saturation adsorption curve of template peptides by MIPs and NIPs. h) Dynamic adsorption data of imprinted microspheres. i) Stability of MIPs and NIPs over repeated use. Adapted with permission from Liang *et al.* [198]. Copyright 2021, American Chemical Society.

antiviral interventions that integrate treatment and detection.

3.3. MIPs targeting viral genetic material and genome processing enzymes

Viral genetic material and genome-processing enzymes are indispensable to viral replication, providing compelling targets for MIPs. Comprising either RNA or DNA, viral genomes encode the instructions necessary for synthesizing viral proteins and assembling progeny virions [199]. Within host cells, these genomes undergo critical processing steps—including reverse transcription, integration, replication, and transcription—facilitated by specialized viral enzymes such as reverse transcriptase, integrase, and polymerase [200,201]. By selectively binding and inhibiting these molecular components, MIPs offer a promising strategy to disrupt viral replication at its most fundamental stages.

3.3.1. Targeting viral genetic intermediates

MIPs have demonstrated the capacity to recognize and bind specific nucleic acid structures, including target DNA sequences. An early study developed a DNA-imprinted polypyrrole film capable of detecting guanine oxidation signals, highlighting the feasibility of directly imprinting DNA molecules [202]. Building upon such advances, recent research has explored the application of MIPs to target viral genetic intermediates during replication.

In HIV replication, single-stranded DNA (ssDNA) serves as an essential intermediate during reverse transcription, providing a template for synthesizing double-stranded proviral DNA that integrates into the host genome—a key step in establishing persistent infection (Fig. 19) [203]. MIPs designed to target HIV ssDNA have demonstrated high specificity and affinity for this intermediate, even in complex biological matrices such as human serum [204]. By binding and sequestering ssDNA, these MIPs have the potential to interfere with its availability for second-strand synthesis, thereby preventing the formation of double-stranded proviral DNA. This stage represents a critical juncture in the HIV lifecycle: it is the moment when the virus shifts from a transient, replication-prone form (ssDNA) to a stable, long-term infection through integration into the host genome. By intercepting this transition, MIPs may block the establishment of proviral latency and prevent lifelong infection. Although further studies are required to fully elucidate the antiviral impact, these findings suggest that ssDNA-targeting MIPs could inhibit proviral integration, offering a novel therapeutic avenue. Future research should prioritize rigorous *in vitro* and *in vivo* validation to assess the feasibility of this approach and quantify its effectiveness in blocking the transition from ssDNA to double-stranded DNA (dsDNA).

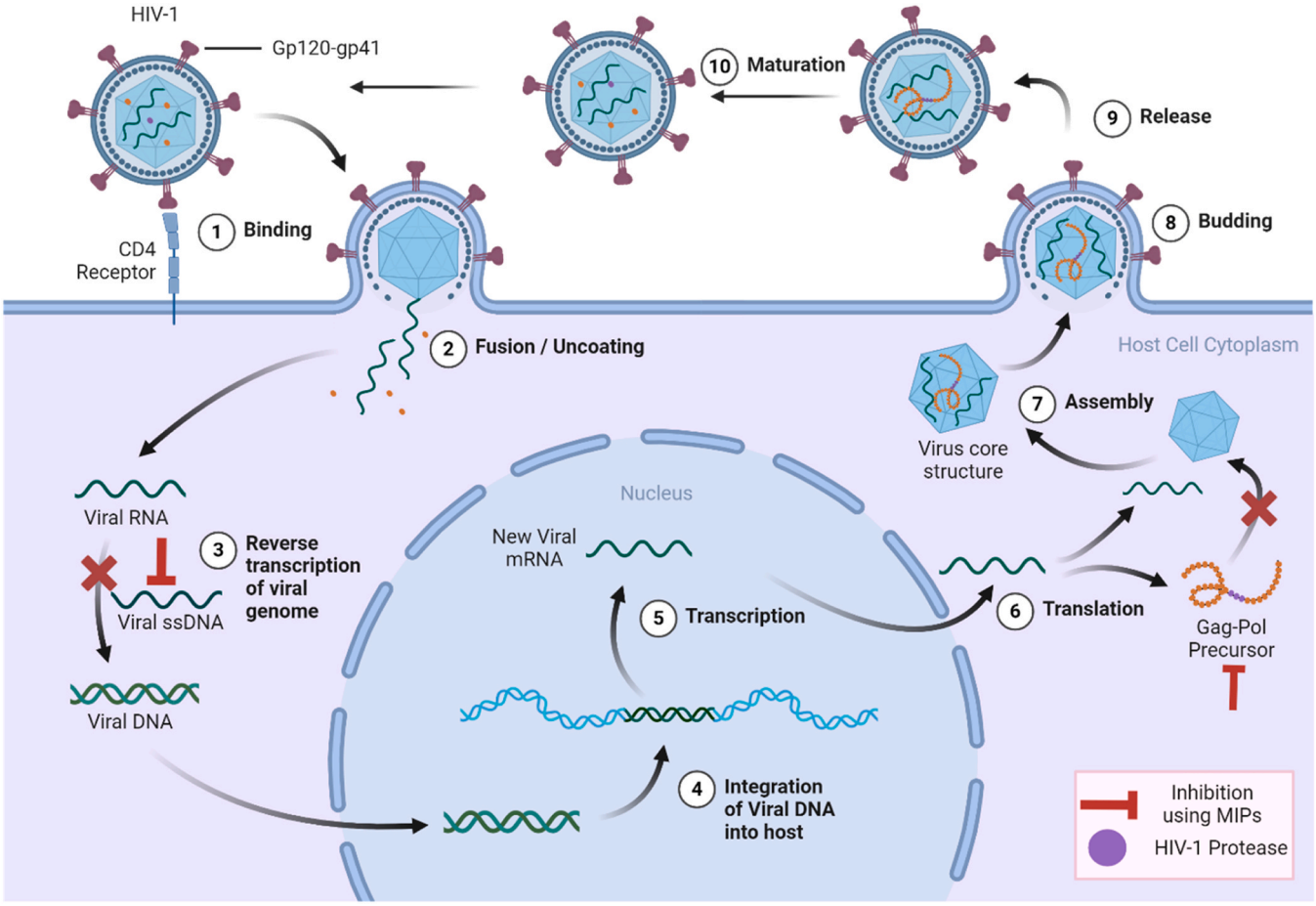

Fig. 19. The HIV-1 Lifecycle. HIV-1 infection begins when the envelope glycoprotein binds to the CD4 receptor on the host cell surface (Step 1), leading to membrane fusion and viral entry. Once inside, the viral core undergoes partial uncoating (Step 2), allowing reverse transcription in the cytoplasm to convert viral RNA into double-stranded viral DNA (Step 3). This viral DNA is transported into the nucleus and integrated into the host genome (Step 4). Transcription of the provirus produces viral mRNAs (Step 5), which are exported to the cytoplasm to serve as genome-length viral RNA or are translated into precursor proteins (Gag-pol and Gag). These precursors are cleaved by HIV-1 proteases during maturation after budding (Step 6). The genome-length viral RNA and proteins assemble into immature viral particles (Step 7), which bud from the host cell membrane (Step 8). After release (Step 9), the particles undergo protease-mediated maturation, becoming fully infectious virions (Step 10). Additionally, as indicated by the red inhibitory symbol, MIPs may exert a potential inhibitory effect on specific stages of the viral lifecycle. Created by using Biorender.com.

3.3.2. Inhibiting genome-processing enzymes

MIPs have shown potential not only with genetic intermediates but also in inhibiting genome-processing enzymes essential for viral assembly and maturation. A particularly promising target is HIV protease, which cleaves polyproteins into functional units required for assembling mature virions. Chou *et al.* developed helical epitope-imprinted MIPs (HEMIPs) targeting HIV protease using the $PR_{85–94}$ peptide segment as a template [76]. These MIPs exhibited exceptional binding specificity, achieving K_D values of 160 pM for the template peptide, 43.3 pM for His-tagged HIV protease, and 78.5 pM for native HIV protease. This high specificity allowed the MIPs to distinguish HIV protease from non-target proteins, suggesting potential for reducing infectious viral particle production by inhibiting protease activity. However, further studies are needed to confirm the functional inhibition of HIV protease in cellular environments and evaluate the stability and specificity of these MIPs under physiological conditions.

The integration of genetic intermediary targeting and enzyme inhibition represents a promising multi-layered approach to antiviral intervention. By simultaneously disrupting multiple critical stages of viral replication, MIPs could provide a robust strategy for controlling viral proliferation. For instance, combining MIPs that bind ssDNA with those targeting genome-processing enzymes could block sequential steps in the viral lifecycle, amplifying therapeutic efficacy. However, realizing the full potential of this approach requires addressing key challenges, including intracellular delivery, stability *in vivo*, and the optimization of binding kinetics for transient intermediates. Developing targeted delivery systems to enhance MIPs' intracellular localization and affinity will be crucial for their successful translation into clinical applications.

3.4. Advancing MIPs for intracellular viral replication inhibition

The studies discussed in 3.1 emphasize the potential of MIPs in recognizing viral structural and non-structural proteins, genetic material, and genome-processing enzymes with high specificity. However, these examples largely focus on thin-film MIPs designed for surface-based diagnostic applications rather than therapeutic use. Thin-film configurations, typically immobilized on sensor surfaces, excel in detecting viral markers but lack the necessary properties for intracellular targeting. For MIPs to transition from diagnostic tools to agents capable of inhibiting viral replication, they must overcome significant barriers to intracellular delivery and operation within host cells.

Effective inhibition of viral replication requires MIPs to access intracellular targets, such as ssDNA intermediates, genome-processing enzymes, and replication-associated proteins like NS1, which are located within cellular compartments. This necessitates a shift from thin-film designs to nanoparticle-based systems capable of penetrating cellular membranes. To achieve this, MIPs must be engineered with nanoscale dimensions and tailored surface properties to enhance cellular uptake. Strategies such as charge engineering, where positively charged functional groups interact with negatively charged cellular membranes, and hydrophobic surface modifications can facilitate membrane permeation through mechanisms like endocytosis, direct translocation, or receptor-mediated entry [205–207]. Functionalizing NPs with cell-penetrating peptides (CPPs), like trans-activator of transcription (TAT) peptides or polyarginine, further improves their ability to cross membranes [208–210]. Post-uptake, MIPs must escape endosomes to exert their function within the cytosol, which can be achieved through stimuli-responsive coatings such as pH-sensitive or redox-sensitive polymers that exploit intracellular conditions to enable endosomal escape [211,212].

Beyond achieving cellular internalization, replication-inhibiting MIPs must also localize to specific subcellular compartments. For example, ssDNA intermediates accumulate in the cytosol, HIV protease operates in cytoplasmic regions associated with virion maturation, and the DENV NS1 protein localizes to vesicle packets and the endoplasmic reticulum-Golgi intermediate compartment (ERGIC) [197]. To enable organelle-level precision, MIPs can be functionalized with targeting ligands such as nuclear localization signals (NLS), endoplasmic reticulum-targeting peptides, or mitochondriotropic delocalized lipophilic cations (DLC), which exploit native intracellular trafficking pathways [213–215]. These strategies have been validated in other nanoparticle platforms, for example, nucleus-targeted CPPs have improved delivery efficiency in cancer models [216]. Furthermore, tuning MIP particle size and surface charge can bias uptake toward specific endocytic pathways such as caveolae- or clathrin-mediated endocytosis, influencing organelle routing and localization [217,218]. Integrating such targeting strategies early in the design process of MIPs is essential to ensure subcellular precision, enhance efficacy, and minimize off-target effects in intracellular antiviral applications.

To ensure safe intracellular application, these replication-targeting MIPs must demonstrate compatibility with highly sensitive subcellular environments, such as the cytosol, lysosomes, and mitochondria [219]. This contrasts with extracellular MIP systems, where systemic biocompatibility suffices (as discussed in 2.3.3). Within cells, non-degradable residues, oxidative stress induction, or lysosomal overload can trigger adverse responses such as autophagy or organelle dysfunction [220]. Although several studies have explored design strategies to improve the intracellular biocompatibility of polymeric nanocarriers, including the use of degradable matrices, antioxidant modification, biomimetic surfaces, and hydrophilic coatings, these approaches remain underutilized in MIP-based systems [221–223]. Future research should prioritize integrating such principles into imprinting-compatible platforms to enable long-term, non-toxic replication inhibition *in vivo*.

Despite these challenges, the specific binding capabilities demonstrated by MIPs targeting ssDNA, NS1, and HIV protease suggest significant potential for intracellular use. By harnessing existing insights into target recognition and adapting these mechanisms to nanoparticle platforms, MIPs can move beyond diagnostics to directly disrupt viral replication. Developing such therapeutic MIPs will require the integration of advanced nanoscale engineering, intracellular delivery strategies, and biocompatibility-focused design.

4. MIPs for enhancing immune defense against viruses

Immune evasion is a strategy employed by many viruses to avoid detection and elimination by the host immune system, allowing them to establish persistent infections and enhance their replication. To achieve this, viruses use various mechanisms, such as immune suppression, latency, and glycan shielding, effectively bypassing host defenses. As highlighted in 2.3.1, when designing MIPs to inhibit viral entry, it is crucial to avoid targeting immunogenic regions essential for immune recognition, thus reducing the risk of inadvertently contributing to immune evasion. However, MIPs can also be strategically designed to counteract viral immune evasion mechanisms directly, offering an innovative pathway for antiviral intervention. By employing MIPs to disrupt these viral tactics, researchers aim to bolster the immune system's ability to detect and eliminate viral pathogens, representing a promising approach in antiviral therapy.

4.1. Targeting immune suppression in viral infections

Viruses like HIV exploit immune suppression mechanisms to deplete critical immune cell populations. Specifically, HIV weakens the immune system by selectively targeting and depleting $CD4^+$ T lymphocytes, which serve as central coordinators of adaptive immunity, leading to immune dysfunction and ultimately the onset of AIDS [224]. This chronic depletion of $CD4^+$ T cells is partly attributed to a conserved peptide motif, SWSNKS (3S), in the gp41 protein of HIV, which is exposed during viral entry and binds to gC1qR receptors on $CD4^+$ T cells [148]. This interaction induces the expression of NKp44L, a ligand that activates natural killer (NK) cells to lyse $CD4^+$ T cells, thereby contributing to immune dysfunction [133].

To counter this immunosuppressive mechanism, Xu *et al.* designed MIP NPs targeting the 3S motif using a structurally constrained cyclic peptide (CGSWSNKSC) as the template (Fig. 20) [148]. The peptide was covalently immobilized *via* its carboxyl group onto (3-aminopropyl) triethoxysilane (APTES)-modified glass beads using 1-ethyl-3-(3-dimethylaminopropyl)carbodiimide and *N*-hydroxysuccinimide (EDC/NHS) coupling chemistry, with *tert*-butyloxycarbonyl (Boc) protecting groups applied to ensure directional orientation and minimize side reactions. Solid-phase polymerization was then carried out at 38 °C using a thermo-responsive monomer mixture designed to provide complementary hydrogen bonding, electrostatic, and hydrophobic interactions. High-affinity MIP NPs were isolated by washing away low-affinity products and eluting at 6 °C.

The resulting MIP NPs exhibited strong binding to the cyclic 3S peptide, with a K_D of 79.6 nM as measured by direct fluorescence titration. Competitive binding assays yielded IC_{50} values of 85.4 nM for denatured gp41 and 69 nM for the linear 3S peptide, while unrelated competitor peptides showed no detectable inhibition even at concentrations up to 100 nM. Low cross-reactivity was observed with abundant serum proteins, with HSA and transferrin showing inhibition levels of only 1.6 % and 0.1 %, respectively. These results confirmed both sequence and conformational selectivity, attributed to imprinting around the three-dimensional structure of the target epitope. While the MIP NPs selectively bind the 3S motif under controlled conditions, their

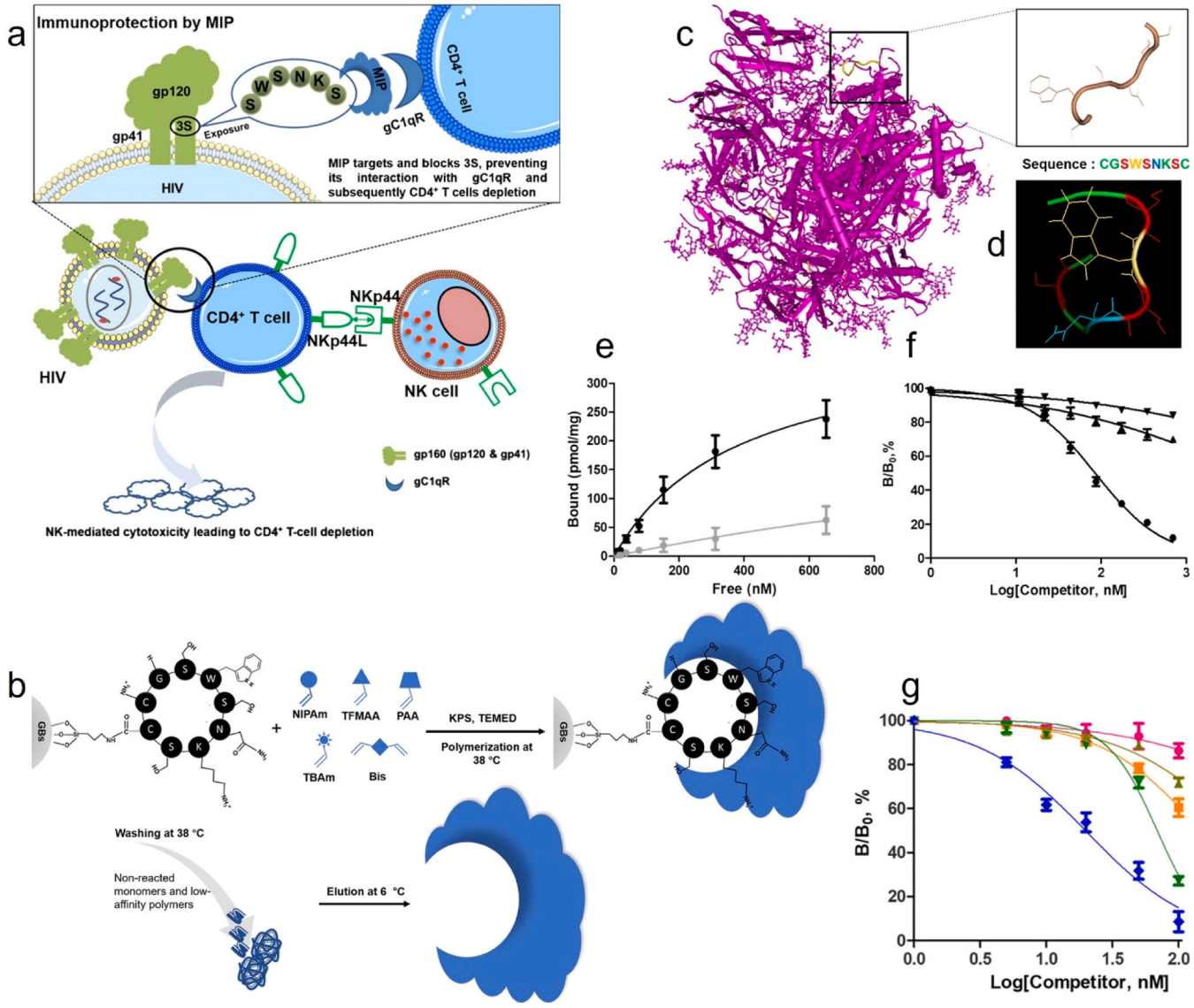

Fig. 20. a) Mechanism of $CD4^+$ T cell depletion mediated by the HIV gp41 3S motif. The inset illustrates the proposed action of MIP NPs designed to target and block the 3S motif, thereby preventing its interaction with the gC1qR receptor on $CD4^+$ T cells and halting the cascade that leads to NK cell-mediated cytotoxicity and $CD4^+$ T cell depletion. b) Solid-phase synthesis of thermo-responsive MIP NPs, using an immobilized cyclic 3S peptide as the template. Polymerization occurs at 38 °C, followed by washing to remove nonreacted monomers and low-affinity polymers. The high-affinity MIP is then eluted at 6 °C. c) 3D structure of gp160 (comprising gp120 and gp41) visualized using Protein Data Bank Europe code 5FUU, with the 3S motif highlighted in ochre; d) Structural model of the 3S peptide generated with Pepfold 2.0. e) Binding assay showing the affinity of MIP (black) and NIP (gray) to FITC-labeled gp41urea across a concentration range (10–700 nM) in 25 mM sodium phosphate buffer at pH 7. f) Competitive binding assay demonstrating inhibition of FITC-$gp41_{urea}$ (350 nM) binding to MIP (100 μg) by free denatured gp41 (circles), human serum albumin (HSA, triangles), and transferrin (inverted triangles) at 1–700 nM concentrations, with B/B_0 representing the binding ratio in the presence and absence of competitors. g) Inhibition assay for cyclic 3S peptide coupled to rhodamine 123 (pep-rho, 100 nM) binding to MIP (100 μg) by competitor 1 (circles), competitor 2 (squares), a mixture of competitors 1 and 2 (triangles), linear 3S peptide (inverted triangles), and cyclic 3S peptide (diamonds), with competitor concentrations from 1 to 100 nM. B/B_0 indicates the ratio of pep-rho binding in the presence and absence of competing ligands. Adapted with permission from Xu *et al.* [148]. Copyright 2019, American Chemical Society.

therapeutic value hinges on whether this epitope becomes sufficiently accessible during HIV infection. This limitation reinforces the need for validation in infection-relevant models to confirm target availability.

Nonetheless, the design rationale remains biologically compelling: by blocking the 3S–gC1qR interaction, these MIP NPs may reduce NKp44L expression and help preserve $CD4^+$ T cell populations. Since $CD4^+$ T cells are essential for priming cytotoxic $CD8^+$ T cells and supporting B cell–mediated antibody production, their protection may help maintain the cellular framework necessary for robust antiviral immune responses [225,226]. The downstream immunological impacts of these MIP NPs have yet to be experimentally confirmed; however, their role in protecting a central immune cell type could offer important indirect benefits to host immunity.

However, the therapeutic value of $CD4^+$ T cell preservation must be balanced against a key limitation: these cells can also serve as a long-term reservoir for latent HIV. Even under effective antiretroviral therapy, latently infected $CD4^+$ T cells, particularly those with Th1/17 polarization, which are inflammation-associated and tend to reside in tissues, and those with long-lived memory phenotypes that can survive in a resting state for years, can persist and contribute to viral rebound after treatment interruption [227,228]. The survival of these reservoir cells could undermine eradication efforts. To mitigate this risk, future approaches may explore the co-application of 3S-targeting MIPs with latency-reversing agents (LRAs), which induce antigen expression in latent cells and render them visible to immune clearance mechanisms [229]. Such combinations could enhance the selective elimination of infected cells while preserving the coordination of antiviral immune responses.

Targeting immune cell suppression is a promising strategy to preserve immune function. At the same time, addressing viral glycosylation provides an additional avenue to overcome immune evasion. The following sections will explore MIPs' potential in disrupting viral glycan shields, a key barrier to immune recognition.

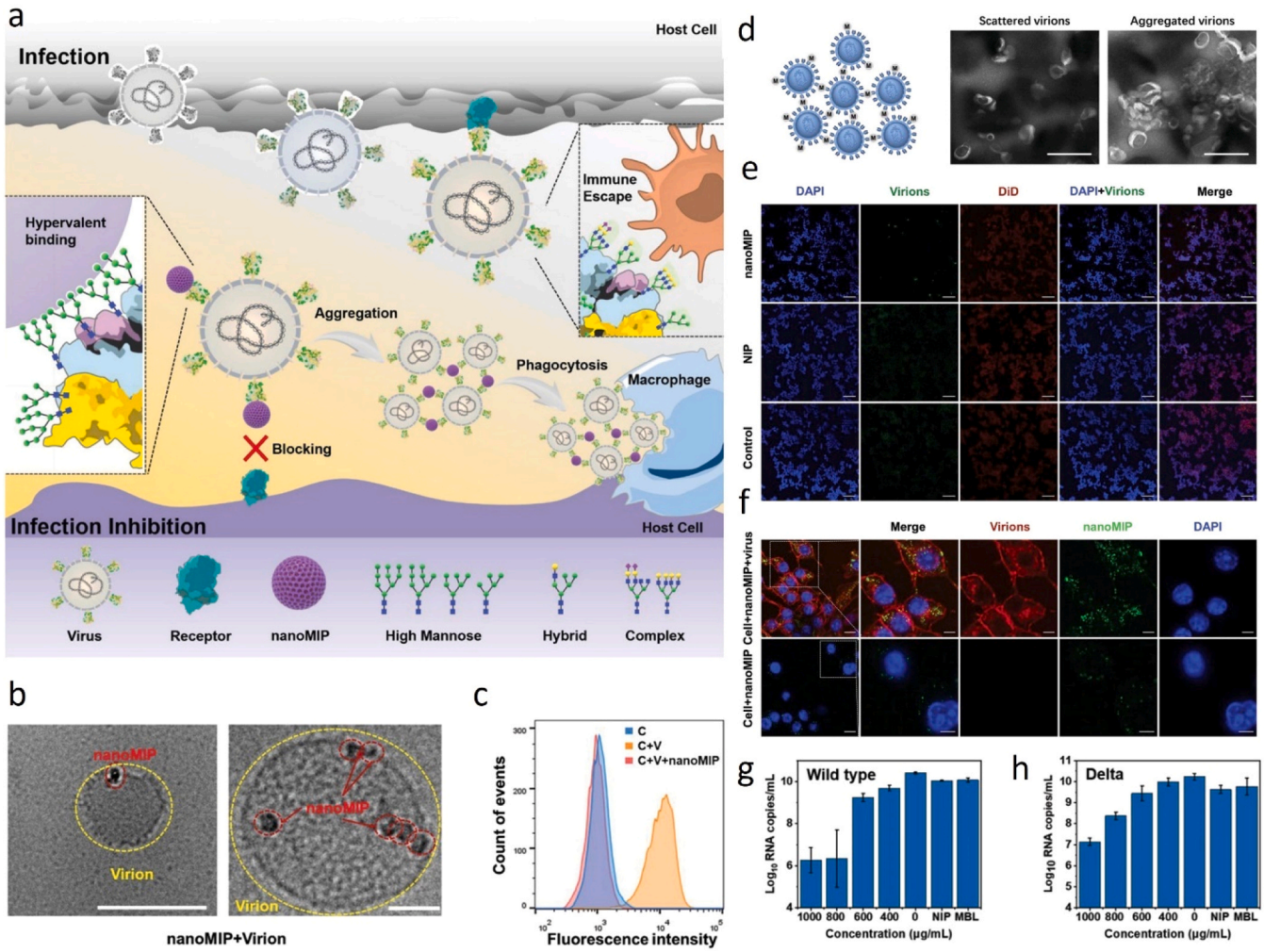

Fig. 21. a) Anti-high mannose nano molecularly imprinted polymer (nanoMIP)-mediated inhibition of SARS-CoV-2. Schematic illustrating how nanoMIPs inhibit viral infection by blocking viral attachment, promoting viral aggregation, and facilitating macrophage uptake. b) Cryo-transmission electron microscopy (Cryo-TEM) images show SARS-CoV-2 pseudovirus particles bound by nanoMIPs (25 μg/mL). Scale bars: 200 nm (left) and 50 nm (right). c) Flow cytometry analysis shows reduced pseudovirus attachment to ACE2-expressing HEK293T cells following nanoMIP treatment (1 mg/mL). d) Diagram of nanoMIP-induced virus aggregation, confirmed by negatively stained TEM images, comparing scattered and aggregated virions (200 μg/mL). Scale bars: 500 nm. e) Confocal images of pseudovirus interaction with ACE2-expressing HEK293T cells in the presence of nanoMIP, NIP, or control, showing that the nanoMIP efficiently cross-linked virions, leading to their aggregation around the cell membrane without entry, compared to the NIP and control groups. f) Confocal images showing macrophage uptake of nanoMIP-virus aggregates (200 μg/mL). g,h) SARS-CoV-2 (wild-type and Delta) RNA levels in Vero cells treated with nanoMIP, showing dose-dependent reduction, with the highest dose resulting in a significant decrease (about 3–4 orders of magnitude) comparable to neutralizing antibodies, for both variants. Adapted with permission from Li *et al.* [98]. Copyright 2023, Wiley.

4.2. Targeting viral glycosylation to enhance immune clearance

Viral glycosylation plays a dual role in infection: while facilitating viral entry into host cells (2.2.4), it also serves as a critical strategy for immune evasion[230]. Viruses like HIV-1, influenza, and SARS-CoV-2, use dense glycan shields composed of host-derived glycans to mask immunogenic epitopes, effectively preventing immune cells from recognizing viral particles. By masking these epitopes, viruses can evade immune detection, allowing them to establish persistent infections and propagate within the host environment [231]. Traditional glycan-targeting methods face limitations, such as high production costs and the limited availability of glycan ligands, which restricts their practical application in antiviral strategies [232–234]. To overcome these limitations, MIPs have emerged as a promising alternative, offering both flexibility in design and broad applicability.

4.2.1. Using glycan shields to enhance immune clearance

A recent strategy has been to utilize the properties of glycan shields to trigger an immune response. Li *et al.* developed hypervalent glycan shield-binding MIPs that bind specifically to high-mannose glycans on viral surfaces, simultaneously cross-linking multiple viral particles into tightly packed aggregates (Fig. 21) [98]. These aggregates inhibit viral entry and facilitate macrophage uptake, supporting immune-mediated viral clearance.

These MIPs demonstrated exceptional binding affinity, with a K_D of 0.85 nM for SARS-CoV-2 pseudovirus particles, reflecting strong affinity for high-mannose glycans. This binding translated into robust antiviral efficacy; the MIPs achieved inhibition efficiencies nearing 90 % against wild type and mutant SARS-CoV-2 pseudovirus, with EC_{50} values (concentration for 50 % effect) between 37 and 49 μg/mL. TEM and confocal fluorescence microscopy revealed that the MIPs cross-linked viral particles into tightly packed aggregates on the cell membrane, facilitating their uptake by macrophages through size-dependent phagocytosis. This physical clustering of viral antigens not only enhances innate immune clearance, but also increases the likelihood of efficient antigen processing and presentation by antigen-presenting cells (APCs) [235]. Such processes may in turn support downstream activation of virus-specific T cells and contribute to adaptive immune responses [236]. Furthermore, *in vitro* studies confirmed the biological impact of this aggregation, as evidenced by a significant reduction in green fluorescent protein (GFP) expression in infected cells, an indicator of diminished viral entry and infection. By exploiting the structural properties of glycan shields, these MIPs effectively block viral interactions with host cells while amplifying immune recognition, offering a promising, broad-spectrum antiviral approach.

Despite these promising results, the *in vivo* application of hypervalent glycan shield-binding MIPs raises important considerations. The formation of viral aggregates, while beneficial for immune clearance, could pose risks of clotting or precipitation in systemic circulation, particularly in cases of high viral loads. Such aggregates may obstruct microcapillaries or inadvertently activate clotting cascades, resulting in unintended side effects [210,237]. Moreover, excessive clustering of viral particles may result in highly concentrated antigenic surfaces, which can inadvertently trigger complement activation, as this innate immune pathway is sensitive to the spatial density and arrangement of antigenic determinants [238]. Overactivation of complement components such as C3a and C5a can promote inflammation by increasing vascular permeability and recruiting leukocytes, which in turn may cause bystander tissue damage [239]. Organs with high vascularity and immune sensitivity, such as the lungs, liver, and kidneys, are particularly susceptible to such effects [240]. These risks highlight the importance of optimizing MIP binding affinity and aggregation behavior to balance effective immune stimulation with safety. To mitigate these risks, further studies are needed to evaluate the behavior of MIP-induced viral aggregates under physiological conditions and to explore strategies for controlled aggregate size or targeted delivery to specific tissues. By addressing these challenges, glycan-targeting MIPs can be refined to maximize their therapeutic efficacy while ensuring safety in clinical applications.

4.2.2. MIPs as tools for selection of glycan-specific aptamers

In addition to directly targeting glycan shields, MIPs have demonstrated utility as tools for selecting glycan-specific aptamers, expanding their role in combating viral immune evasion. Researchers have combined glycan-imprinted magnetic MIP NPs with the SELEX (Systematic Evolution of Ligands by Exponential Enrichment) technique to identify short DNA or RNA sequences, known as aptamers, that bind specifically and with high affinity to glycan structures [241–243]. This innovative approach complements the direct antiviral activity of glycan-targeting MIPs by facilitating the development of aptamers tailored to complex viral glycan shields.

In this combined strategy, MIPs are employed to immobilize and stabilize viral glycan targets, such as high-mannose glycans on the HIV gp120 protein and the SARS-CoV-2 spike protein. This stable presentation of glycans allows SELEX to systematically screen diverse libraries of nucleic acid sequences, enriching for aptamers with strong specificity and binding affinity to these glycan structures. Through repeated cycles of binding, washing, and amplification, SELEX produces aptamers with K_D as low as 0.218 nM, showing their strong affinity and selectivity for viral glycan shields (Fig. 22). These aptamers are capable of independently blocking viral interactions with host cell receptors, exposing viral particles to immune surveillance and enhancing immune clearance.

Besides using aptamers alone, they can also be combined with MIPs to enhance performance [244]. This approach, which creates aptamer-based MIPs that integrate the binding precision of aptamers with the robustness of MIPs, is expected to achieve more accurate antiviral targeting.

Overall, 4 highlights the multifaceted ways in which MIPs can enhance host antiviral immunity. In immune-suppressive viral infections such as HIV, MIPs designed to target pathogenic epitopes (*e.g.*, the 3S motif in gp41) may help preserve key immune cell populations like $CD4^+$ T cells, thereby maintaining the cellular foundation for adaptive responses. Glycan-targeting MIPs, in turn, exploit viral glycan shields to trigger aggregation and promote phagocytosis, enhancing immune visibility and clearance. Beyond these direct effects, MIPs also serve as enabling platforms for selecting glycan-specific aptamers via SELEX, offering precision tools to further disrupt viral evasion strategies. As these approaches advance, future research must carefully evaluate not only the immunological benefits but also the risks: particularly those related to complement activation, inflammatory cascades, and tissue-level safety. By bridging synthetic design with immunological insight, MIPs represent a promising and programmable framework for next-generation antiviral therapies capable of both immune modulation and targeted viral disruption.

5. MIPs for improving antiviral drug systems

MIPs have emerged as versatile tools in antiviral therapy, demonstrating potential beyond their standalone antiviral activity. They play critical roles not only in enhancing drug delivery but also in supporting upstream processes such as antiviral drug detection and purification. MIPs can serve as advanced drug delivery systems (DDS) [245], addressing limitations of conventional antiviral drugs such as limited specificity, suboptimal pharmacokinetics, and adverse effects [246–248]. MIPs achieve this through sustained or stimuli-responsive release mechanisms that enhance therapeutic efficacy while minimizing systemic exposure. Simultaneously, their high specificity and selectivity enable precise isolation, quantification, and purification of antiviral agents from complex matrices, supporting pharmacokinetics studies, diagnostics, and pharmaceutical manufacturing. The following sections will explore how MIPs are integrated into both therapeutic delivery and drug processing applications, highlighting their

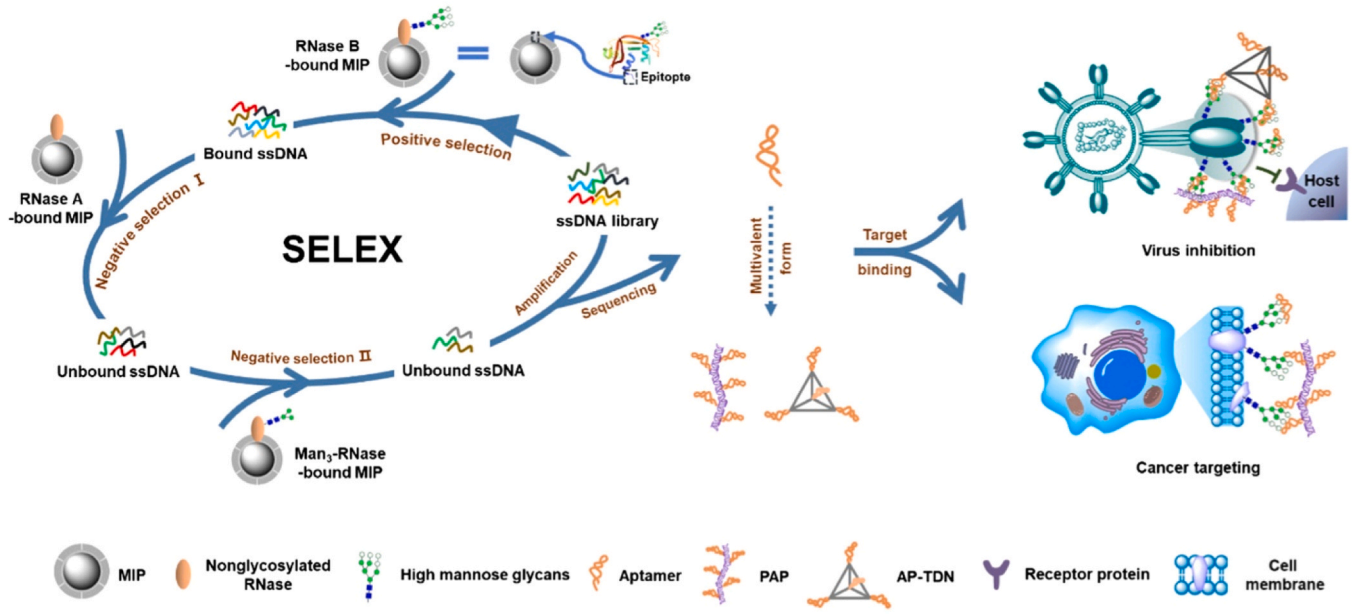

Fig. 22. Schematic illustration of the MIP-based SELEX process used to select high-affinity mannose-binding aptamers for viral inhibition and cancer targeting. In this process, MIP-coated MNPs are first bound to RNase B, a glycosylated protein carrying high mannose glycans, for positive selection, allowing binding of high mannose-specific aptamers from an ssDNA library. Non-specific sequences are then eliminated through negative selection steps involving RNase A (non-glycosylated) and Man_3-RNase (containing core mannose structures but lacking complex glycan forms). The selected ssDNA sequences are amplified, and after multiple rounds of positive and negative selection, high-affinity aptamers specific to high mannose glycans are enriched. These aptamers can bind to glycan shields on viral and cancer cell surfaces, blocking receptor interactions and enhancing immune recognition for targeted therapeutic applications, such as inhibiting virus-host cell entry and distinguishing cancer cells. Adapted with permission from Liu *et al.* [241]. Copyright 2022, Chinese Chemical Society.

multifunctional role in improving antiviral drug systems and advancing antiviral treatment strategies.

5.1. MIPs for sustained release of antiviral drugs

Sustained-release systems are a crucial application of MIPs in antiviral drug delivery, offering the potential to maintain therapeutic drug levels over extended periods, reduce dosing frequency, and enhance patient compliance. For instance, Mathieu *et al.* developed a MIP-based delivery system for Tenofovir, an FDA-approved antiviral drug [249]. The functional monomer 2-(dimethylamino)ethyl methacrylate (DMAEMA) was selected for its ability to form ion-pairing and Watson-Crick base pairing interactions with Tenofovir, resulting in a high drug-loading capacity with a maximum adsorption capacity of 2.27×10^{-5} mol/g. The MIP demonstrated controlled drug release at both 25°C (26 % released in 2 weeks) and 37°C (41 % released in 2 days), highlighting its potential to improve treatment adherence by enabling extended dosing intervals.

Sustained drug release is particularly valuable for localized infections requiring consistent therapeutic levels at the infection site. In treating ocular herpes simplex virus (HSV) keratitis, achieving prolonged drug delivery on the ocular surface is challenging due to rapid drug clearance and low bioavailability. To address this, Varela-Garcia *et al.* developed MIP hydrogels incorporated into contact lenses for sustained delivery of acyclovir (ACV) and valacyclovir (VACV), two first-line antiviral agents [250]. Computational modeling identified methacrylic acid (MAA) as the optimal functional monomer, with binding free energy values ($\Delta G_{binding}$) of −3.50 kcal/mol for ACV and −3.10 kcal/mol for VACV. VACV exhibited superior binding affinity and reloading capacity (over 4.0 mg/g compared to less than 2.5 mg/g for ACV) due to its valine side chain's stronger electrostatic interactions. Permeability tests further demonstrated the superior corneal penetration of VACV-loaded hydrogels, supporting their suitability for ocular drug delivery. These studies highlight the adaptability of MIP-based DDS, demonstrating their ability to address diverse antiviral delivery challenges, from systemic sustained-release strategies to localized, high-precision applications.

5.2. Stimuli-responsive MIP systems

Stimuli-responsive MIPs offer a targeted approach to drug delivery by releasing therapeutic agents in response to specific environmental triggers, such as temperature and pH changes. These systems enhance drug bioavailability, minimize systemic exposure, and reduce required dosages by ensuring localized and controlled release under conditions associated with viral infections.

5.2.1. Temperature-sensitive MIPs

Temperature-responsive MIPs (T-MIPs) represent an innovative strategy for drug delivery, particularly in infection scenarios where body temperature variations frequently occur. T-MIPs regulate drug release through temperature-induced phase transitions within the polymer network. The key mechanism is based on the lower critical solution temperature (LCST), where the polymer reversibly transitions between a hydrophilic swollen state and a hydrophobic collapsed state. Below the LCST, hydrogen bonding between polymer chains and water maintains the swollen state, facilitating drug diffusion. Above the LCST, hydrophobic interactions dominate, causing polymer chain association, reducing pore size, and slowing drug release [251]. The transition between these states is determined by the balance of hydrophilic and hydrophobic interactions within the polymer matrix. Selecting thermosensitive monomers, such as NIPAM, with suitable LCST values is crucial to maintain responsiveness under physiological conditions [252]. NIPAM, commonly used in T-MIPs, contains hydrophilic amide and hydrophobic isopropyl groups, with an LCST around 32°C. Copolymerization with other monomers can raise the LCST to near physiological temperature, making it widely applicable in biomedical fields [253].

Ayari *et al.* developed a T-MIP hydrogel using ribavirin, a broad-spectrum antiviral drug, as the template [254]. By optimizing the

monomer composition using NIPAM as the thermo-sensitive monomer and MBAA as the cross-linker, controlled release profiles at elevated body temperatures (*e.g.*, during fever) was achieved. At 38°C, the hydrogel exhibits reduced swelling, slowing down ribavirin release compared to the release rate at 25°C, thus preventing a sudden drug burst under febrile conditions. *In vitro* tests demonstrated that only 1–3 μg of ribavirin released from this MIP hydrogel achieved antiviral efficacy equivalent to a 30 μg/mL ribavirin solution, indicating enhanced bioavailability. This efficient and responsive release mechanism reduces the required dosage, minimizes potential toxicity, and maintains prolonged antiviral activity, making it a promising DDS for improving the therapeutic profile of antiviral drugs. Furthermore, the MIPs exhibited good biocompatibility, with no cytotoxicity or pro-inflammatory response in human lung epithelial BEAS-2B cells, further supporting their potential for safe, effective drug delivery.

5.2.2. *pH-responsive MIPs*

Viral infections often induce local pH changes due to inflammatory responses or viral ion channel activity, creating an opportunity for pH-responsive drug release [255,256]. The mechanism of pH-responsive MIPs relies on the ionization of functional groups within the polymer matrix, leading to changes in the polymer's interactions and structure in response to environmental pH variations. These functional groups typically include acidic groups (*e.g.*, carboxyl, phosphoric, sulfonic acids) and basic groups (*e.g.*, tertiary amine, pyridine, imidazole), which undergo protonation or deprotonation depending on the pH conditions. This ionization process alters electrostatic interactions and hydrogen bonding between MIPs and drug templates, affecting the binding strength [251]. Additionally, pH changes can influence the degree of polymerization and charge repulsion within the network structure of MIPs, leading to structural adjustments such as swelling or shrinking [252]. By carefully selecting combinations of acidic and basic monomers, pH-responsive MIPs can be engineered to modulate drug diffusion under different pH conditions, achieving precise control over drug release in various microenvironments.

Ge *et al.* developed pH-sensitive MIPs for delivering matrine (MAT) [257], a naturally derived alkaloid with demonstrated antiviral activity in select experimental contexts [258,259]. By integrating dopamine as a cross-linker and using carboxyl-functionalized multi-walled carbon nanotubes (MWCNs) as a support matrix, they successfully developed a system with distinct pH-dependent release profiles (Fig. 23).

For MAT-loaded MIPs in PBS, release studies demonstrated a distinct

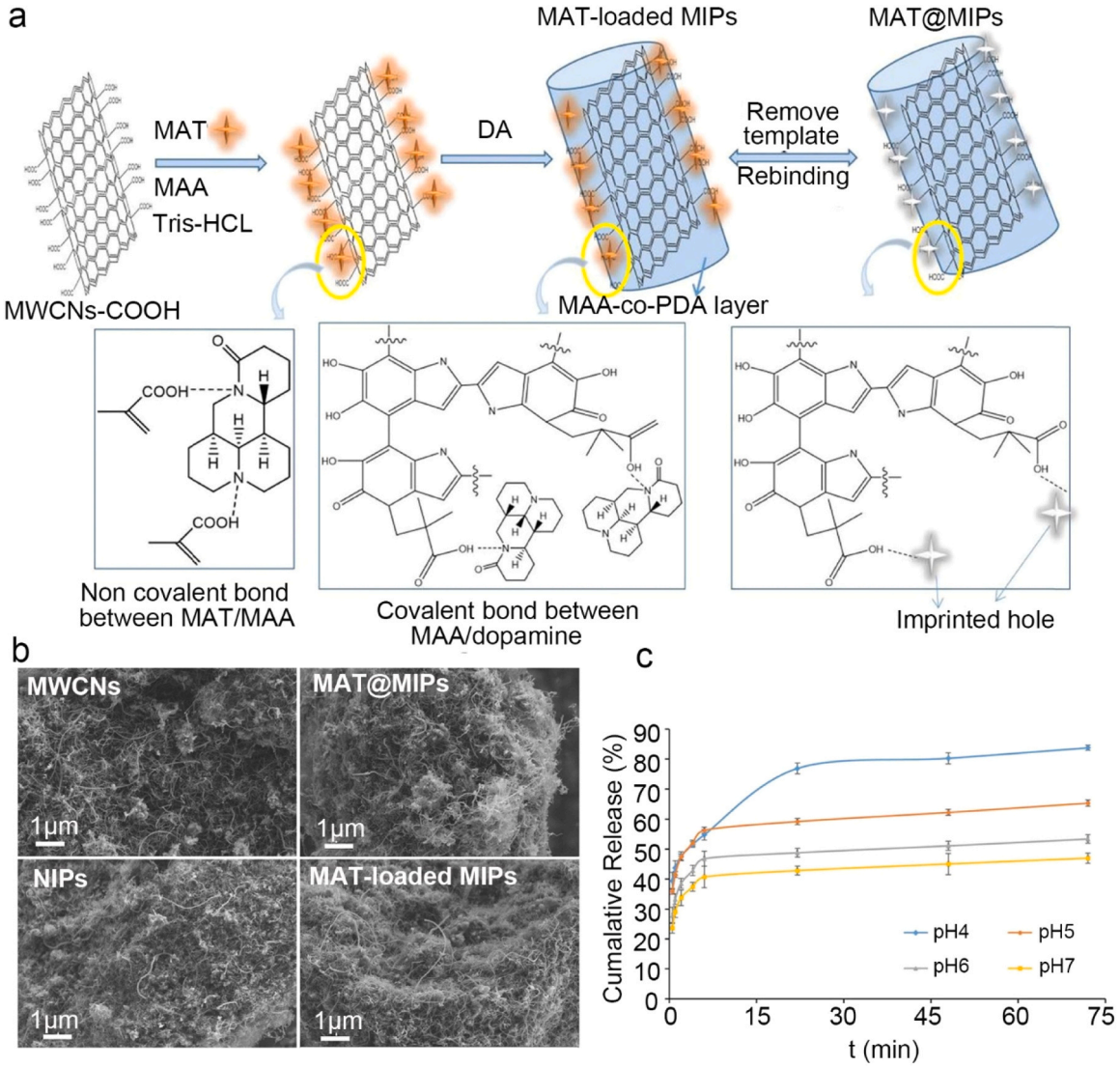

Fig. 23. a) Schematic representation of the preparation process for MAT@MIPs. b) SEM images of different materials: upper left—MWCNs; upper right—MAT@MIPs; lower left—NIPs; lower right—MAT-loaded MIPs. c) In vitro release profiles of MAT from MAT-loaded MIPs at different pH levels (4.0, 5.0, 6.0, and 7.0), demonstrating pH-responsive behavior. Adapted with permission from Ge et al. [257] under the terms of the Creative Commons CC BY license.

pH-dependent behavior. At an acidic pH of 4.0, approximately 83.73 % of MAT was released, compared to only 46.98 % at neutral pH 7.0, highlighting the responsiveness of these MIPs to environmental acidity. This selective release enhances drug concentration at infection sites, improving localized therapeutic efficacy while minimizing systemic exposure. Such precise targeting is particularly beneficial in scenarios where localized acidic microenvironments arise, resulting from inflammatory responses caused by viral infections, which can facilitate targeted drug release [260,261]. Furthermore, the biocompatibility of MWCNs has been verified, with cell survival reaching approximately 90 % at concentrations below 1 mg/mL. This design emphasizes the potential of MIPs for site-specific drug delivery, enhancing bioavailability and therapeutic outcomes in antiviral treatment.

5.2.3. *Broader stimuli-responsive MIPs*

Apart from temperature and pH, MIP DDS can be engineered to respond to a variety of stimuli, expanding their applicability in antiviral therapies. Light-responsive MIPs release drugs upon exposure to specific wavelengths, such as near-infrared light, providing controlled, on-demand release, which could be adapted for localized infections [262]. Magnetic-responsive MIPs incorporate magnetic particles to allow targeted drug release under an external magnetic field, potentially enabling focused delivery to infection sites [263]. Redox-responsive MIPs, designed to respond to oxidative stress, can release drugs in inflamed or infected tissues, making them suitable for viral diseases associated with high oxidative environments [264]. The versatility of stimuli-responsive MIPs indicates their potential to meet diverse

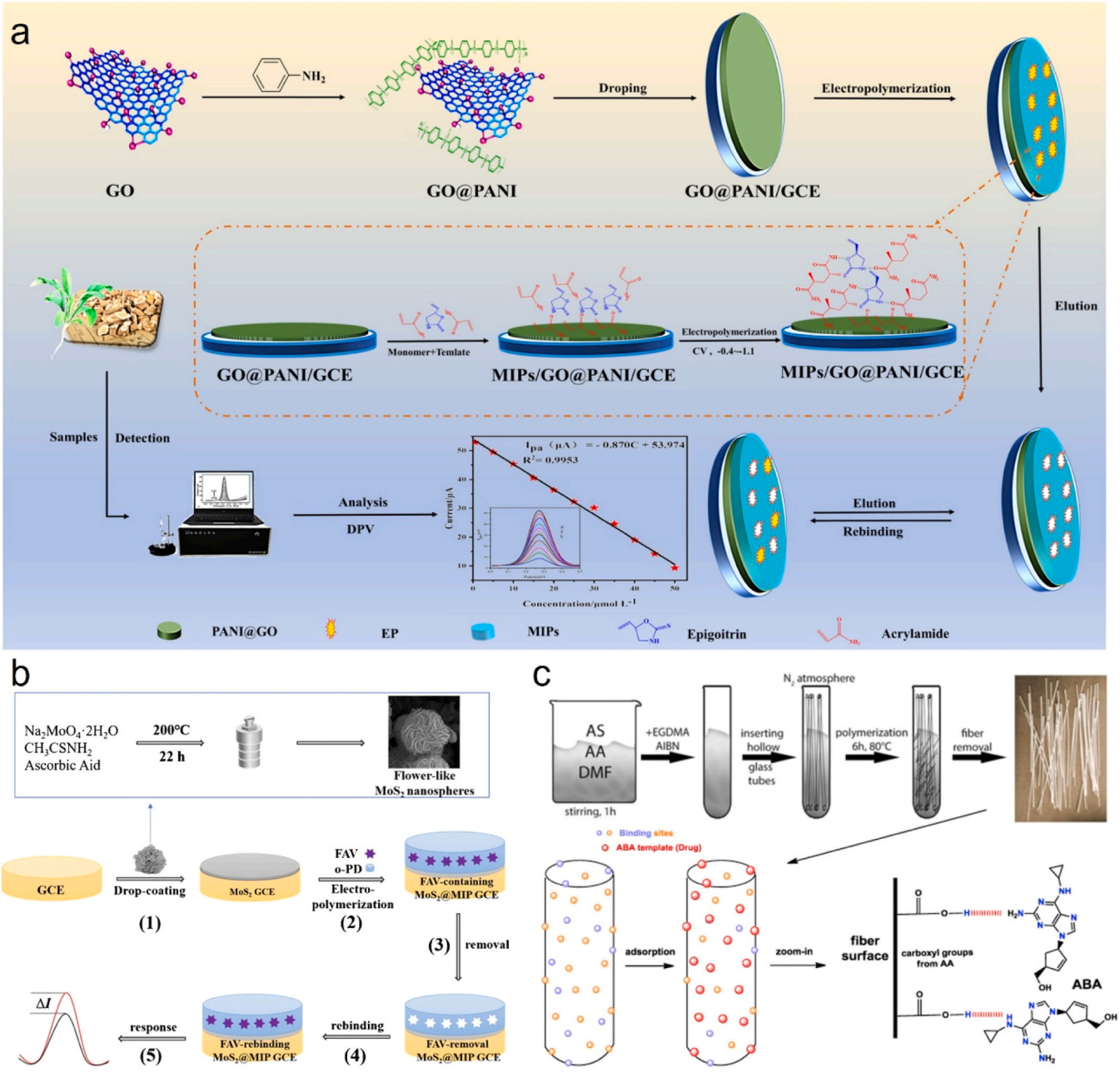

Fig. 24. a) Schematic representation of a molecularly imprinted electrochemical sensor for epigoitrin detection, utilizing MIP-coated polyaniline-functionalized graphene oxide (PANI@GO) on a glassy carbon electrode (GCE). Copyright 2022, IOP Publishing. b) Synthesis process of MoS_2@MIP core–shell nanocomposite for targeted drug detection. Copyright 2022, Springer Nature. c) Illustration of selective separation mechanisms in MIP-based systems, showcasing potential interactions for effective antiviral drug purification. Copyright 2016, Elsevier.
(a) Adapted from Sun *et al.* [268]. (b) Adapted from Wang *et al.* [267]. (c) Adapted from Terzopoulou *et al.* [270].

antiviral drug delivery needs. By tailoring MIP systems to respond to infection-specific triggers, researchers can create advanced drug delivery platforms that improve therapeutic outcomes while minimizing adverse effects, reinforcing the adaptability and innovation of MIP technology.

5.3. MIPs in antiviral drug detection and purification

MIPs play a vital role in the detection and purification of antiviral drugs, offering high specificity and selectivity for target molecules. These upstream functions complement their therapeutic applications by contributing to the overall optimization of antiviral drug systems. Beyond their potential as drug carriers, MIPs contribute to diagnostics and pharmaceutical manufacturing by enabling precise isolation, quantification, and purification of antiviral compounds in complex biological matrices [265]. As recognition elements in sensor systems and solid-phase extraction (SPE), MIPs support pharmacokinetic studies and ensure quality control in pharmaceutical production, highlighting their broader impact in advancing both clinical diagnostics and drug manufacturing processes [266].

In the realm of drug detection, Wang *et al.* developed a core–shell nanocomposite sensor featuring flower-like molybdenum disulfide (MoS_2) nanospheres coated with a MIP layer for the electrochemical detection of favipiravir, a drug used against COVID-19 [267]. The MIP was synthesized *via* electropolymerization using o-phenylenediamine as the monomer and favipiravir as the template, enabling selective binding through hydrogen bonding and π-π stacking interactions. Molecular dynamics simulations indicated a binding energy of −4.8 kcal/mol, supporting the high affinity for favipiravir. This sensor achieved a wide detection range (0.01–100 nM) and a low detection limit (0.002 nM), showing its potential for monitoring favipiravir in biological fluids like urine and plasma with precision and reliability.

In another example, Sun *et al.* constructed a MIP sensor on functionalized graphene oxide for the detecting Epigoitrin, a sulfur-containing antiviral alkaloid from *Isatidis Radix* (Fig. 24) [268,269]. By optimizing polymerization variables, they developed a sensor with high sensitivity and selectivity for Epigoitrin in complex matrices, showcasing the utility of MIPs in pharmaceutical quality control and pharmacokinetic studies. This application highlights the adaptability of MIPs in detecting both synthetic and natural antiviral compounds.

MIPs have also demonstrated their efficacy in drug purification. Chianella *et al.* designed an itaconic acid-based MIP for the selective extraction of abacavir hemi-sulfate, a key antiviral used in HIV treatment, from complex pharmaceutical solutions and biological matrices [271]. The purpose of this extraction was to support drug purification and concentration during pharmaceutical production, addressing the

Table 5
Application of MIPs for antiviral drugs.

Drug template	Targeted disease	Type of MIP	Application of MIP	Reference
Abacavir	AIDS	Molecularly imprinted solid-phase microextraction fiber (MIP-SPMEf)	Sorbent for selective removal and extraction of abacavir	[270]
	AIDS	MIP microparticles (MIP MPs)	Sorbent for concentration and purification of abacavir	[271]
Acyclovir	Diseases caused by HSV types 1 and 2, varicella-zoster virus, epstein-barr virus, cytomegalovirus and human herpesvirus 6	MIP MPs	Sorbent for recognition and selective extraction of acyclovir from urine	[272]
Acyclovir and valacyclovir (prodrug)	HSV ocular keratitis	Molecularly imprinted hydrogels	Soft contact lenses DDS for sustained release of ACV and VACV	[250]
Adefovir dipivoxil	viral infection chronic hepatitis B	MIP NPs	Sorbent for the selective extraction and purification of adefovir from human serum and urine	[273]
Efavirenz	AIDS	MIP MPs	Sorbent for the extraction of efavirenz from wastewater influent and effluent as well as surface water	[274]
	AIDS	MIP NPs	Sorbent for extraction and purification of efavirenz from serum and urine	[275]
Epigoitrin	Influenza and other viral respiratory infections	MIP-coated polyaniline-functionalized graphene oxide on a glassy carbon electrode (MIPs/PANI@GO/GCE)	Electrochemical sensor for epigoitrin detection	[268]
Famciclovir	HSV−1, HSV−2 and varicella zoster virus	MIP MPs	Electrochemical sensor for famciclovir detection	[276]
Favipiravir	COVID−19	Flower-like MoS2@MIP core-shell nanocomposite	Electrochemical sensor for favipiravir detection	[267]
	COVID−19	Water-dispersible MIP-Co/Ni@metal–organic framework (MOF)-based nanosheets	Electrochemical sensor for favipiravir detection	[277]
Lamivudine	AIDS	MIP NPs	Sorbent for extraction and separation of lamivudine from serum and urine	[278]
Oseltamivir	Influenza	MIP MPs	Sorbent for enrichment and separation oseltamivir from the complex matrix	[279]
	Influenza	Silica gel microspheres coated with MIP layer	Chromatographic column material for the analysis of oseltamivir	[280]
Ribavirin	Diseases caused by RNA and DNA viruses	Biochar-based boronate affinity MIPs (C@H@B-MIPs)	Adsorbing material for the enrichment and analysis of ribavirin	[281]
	Diseases caused by RNA and DNA viruses	Boric acid-functionalized lanthanide MOF coupled with MIP (BA-LMOFs@MIP)	Fluorescence sensor for monitoring trace ribavirin	[282]
	Diseases caused by RNA and DNA viruses	Molecularly imprinted hydrogels	DDS for the sustained release of ribavirin	[254]
Sofosbuvir	Hepatitis C	Polymerized p-aminothiophenol on N,S co-doped graphene quantum dots in presence of Au NPs	Electrochemical sensor for sofosbuvir detection	[49]
Tenofovir	AIDS	MIP-based nanocomposites	Electrochemical sensor for tenofovir detection	[283]
Valganciclovir	Cytomegalovirus retinitis in patients with AIDS	MIP-based nanocomposites	Electrochemical sensor for valganciclovir detection	[284]

challenges posed by traditional methods like chromatography, which are often expensive and time-consuming. This MIP exhibited a binding capacity of approximately 15.7 % in Na-acetate buffer (pH 4.0) and was successfully applied in SPE to concentrate abacavir from various samples. Similarly, Terzopoulou *et al.* fabricated MIP fibers capable of purifying abacavir from complex biological and environmental matrices with extraction efficiencies of 88–99 %, even in challenging conditions like wastewater and urine [270]. These examples emphasize the potential of MIPs to ensure the precise isolation and purification of antiviral drugs, enhancing both the efficiency and scalability of pharmaceutical production.

Collectively, these studies demonstrate the versatility of MIPs in antiviral drug detection and purification. By integrating advanced recognition elements with optimized synthesis protocols, MIPs address key challenges in isolating and monitoring antiviral agents, enabling high-performance diagnostics and manufacturing solutions. Table 5 summarizes various MIP-based DDS, detection, and purification systems for small-molecule antiviral drugs, showcasing the breadth of their applications and potential for future innovation.

5.4. Challenges and strategies of MIPs in antiviral drug systems

Although MIPs have achieved notable progress in the controlled release, stimuli-responsive activation, and purification of antiviral drugs, their clinical translation as DDS still faces multifaceted challenges. These challenges involve not only precise control over drug release kinetics but also coordinated regulation of in vivo targeting, intracellular delivery, and long-term biocompatibility, making the overall system design of MIPs more complex and tightly coupled [245, 285].

A unique challenge for drug-loaded MIPs arises from the "double-edged sword effect" of their molecular recognition mechanism. For example, antiviral nucleoside analogs such as acyclovir and zidovudine are designed to mimic endogenous nucleosides for intracellular activation [286]. However, their structural similarity also increases the risk that MIP binding sites may unintentionally capture native nucleosides in blood or tissues, leading to premature drug release in non-target regions, reduced drug concentration at infection sites, and potential toxicity associated with interference in DNA replication. To mitigate such off-target effects, molecular modeling strategies have been widely adopted in recent years. By comparing the binding behaviors of target drugs and endogenous analogs with various functional monomers, researchers can identify and exclude monomers that exhibit high affinity but low specificity, thereby improving the molecular selectivity of the imprinting process [287,288].

Another key challenge lies in achieving efficient *in vivo* targeting and intracellular delivery. Unmodified MIPs often exhibit passive distribution throughout the body and are prone to clearance by macrophage-rich organs such as the liver and spleen, resulting in low drug concentration at infection sites and increased systemic side effects [289,290]. To enhance drug accumulation at target lesions, strategies such as grafting virus-targeting aptamers onto MIP surfaces (active targeting), or using microenvironment-responsive triggers (*e.g.*, acidic pH, oxidative stress) to activate local release, have been employed to reduce non-specific uptake and toxicity exposure [291–293].

For drugs like protease inhibitors and nucleoside reverse transcriptase inhibitors (NRTIs) that act on intracellular targets, tissue-level targeting alone is insufficient [294]. These drugs must traverse cellular membranes, reach the cytosol, and escape endosomes before exerting therapeutic effects, posing additional structural demands on MIPs. Coping strategies include constructing dual-imprinted MIPs (*e.g.*, simultaneously targeting the drug and membrane receptors such as ERα) to promote receptor-mediated endocytosis [295], modifying surface charge or introducing CPPs to enhance membrane transport, and designing redox- or pH-responsive shells to enable endosomal escape [296,297]. As discussed in Section 3.4, these functional enhancements not only increase cellular uptake but also improve intracellular bioavailability while maintaining biocompatibility.

For MIPs used as antiviral DDS, biocompatibility optimization must not only follow the basic strategies outlined in 2.3.3, such as the use of biodegradable monomers and hydrophilic surface modifications, but also involve a systematic assessment of safety after drug loading. This includes assessing how MIPs affect drug stability, release kinetics, and *in vivo* metabolism, as well as their potential to cause combination effects. While MIPs may be biocompatible, drug incorporation can alter their biological behavior and introduce unexpected or synergistic toxicity. Recent studies have proposed the integration of multi-component pharmacokinetic/pharmacodynamic (PK/PD) modeling and toxicity prediction frameworks to assess potential long-term risks such as immune activation, off-target organ accumulation, or pharmacodynamic anomalies [298,299]. Only through coordinated optimization of materials, release behavior, and pharmacological mechanisms can both therapeutic efficacy and safety be ensured.

For MIPs used in antiviral drug detection and purification, their applications are primarily limited to *in vitro* diagnostics, pharmaceutical manufacturing, and quality control workflows. Since these do not involve *in vivo* use, biocompatibility is not a concern; instead, evaluation focuses on target selectivity, operational stability, and reusability [300].

In summary, MIPs in antiviral drug systems face multiple challenges including targeting precision, off-target recognition, and biocompatibility. However, through rational molecular design, functional surface engineering, and systemic safety assessment, they have demonstrated strong engineering controllability and translational potential. With continued integration of design strategies and scalable fabrication technologies, MIPs are poised to become next-generation platforms for safe and effective antiviral drug delivery.

6. Conclusion and future outlook

The advancement of MIPs has introduced a synthetic strategy with unique value in antiviral therapy, particularly where traditional approaches struggle with precision and efficacy. These engineered materials are capable of highly selective recognition of viral components, supported by inherent physicochemical robustness, synthetic adaptability and cost-effective synthesis. Such characteristics enable their incorporation into diverse therapeutic mechanisms aimed at neutralizing viruses with greater targeting specificity and functional versatility. This review has systematically highlighted their potential across four therapeutic axes. First, they can obstruct viral entry by binding to viral structures ranging from intact viral particles to refined targets such as surface proteins, binding domains, epitopes, and glycans. Second, they hold promise for interfering with genome synthesis and viral replication by selectively recognizing viral enzymes, genetic intermediates (*e.g.*, ssDNA), and replication-associated proteins. Third, they offer new approaches to modulate immune evasion, through binding immunosuppressive motifs and clustering glycan-shielded virions to facilitate immune clearance. Fourth, they have been integrated into advanced antiviral delivery systems, offering controlled release kinetics and supporting efforts to achieve tissue-selective drug distribution. In addition, MIPs serve as platforms for aptamer screening, drug detection and purification, broadening their utility in antiviral technology. These capabilities position MIPs as a therapeutically versatile and functionally cohesive solution, complementing and alternating current antiviral strategies and offering promising avenues for targeted, resilient, and customizable interventions.

Despite their multifunctional promise, the clinical translation of antiviral molecularly imprinted systems is still in an early stage, with several key challenges that continue to shape ongoing research. One central consideration is their biological adaptability *in vivo*. Risks such as off-target interactions, insufficient biodegradability, and unintended immune responses may compromise therapeutic precision and long-term safety. Some studies have reported low cytotoxicity and

hemolysis *in vitro*; however, comprehensive *in vivo* validation is still needed to confirm these findings, particularly for systemic or intracellular applications. Manufacturing scalability and standardization also remain under active development. Small-batch synthesis enables structural versatility and rapid iteration, but clinical-scale translation requires refined control over imprinting conditions and biosafety-compliant template processing, particularly for complex targets like viruses and proteins. Compared to conventional biologics, MIPs offer advantages in cost and design flexibility, though industrial-scale implementation still depends on application-specific optimization. The diversity of antiviral MIP implementations, including virus-capturing hydrogels, nanoscale formulations, and drug delivery systems, highlights their adaptability while simultaneously introducing complexity for regulatory integration. In the absence of unified standards, each system often requires bespoke development workflows, making the establishment of Good Manufacturing Practice (GMP)-compliant production routes more complex. These regulatory challenges are further compounded by the fragmented nature of oversight frameworks, as MIP-based technologies frequently span pharmaceutical, diagnostic, and medical device domains, complicating classification and approval processes.

To bridge these translation gaps, future research should focus on optimizing MIP materials for safety and efficacy. A key strategy involves using biodegradable and non-toxic polymer matrices, and adjusting their physicochemical properties such as structure, size, crosslinking density, surface charge, and hydrophilicity based on the administration route. This aims to balance specific recognition with efficient *in vivo* clearance. Meanwhile, appropriate surface modification strategies (like hydrophilic coatings, biomimetic surface, or functional ligands) can also enhance their biostability and specific targeting capabilities. Equally important is the development of standardized *in vivo* evaluation systems, including validation in relevant animal models, to support stepwise clinical translation.

Building upon these considerations, it is also important to recognize that biocompatibility requirements vary significantly across different antiviral MIP application scenarios. For in vitro virus capture, including applications in diagnostics, surface disinfection, or mucosal cleansing, MIPs typically contact biological systems only briefly. In these settings, the primary concern is to minimize acute cytotoxicity caused by unreacted monomers or surface reactivity. This can be effectively managed through rigorous post-synthesis purification techniques, such as Soxhlet extraction or supercritical fluid extraction, as well as careful selection of monomers and crosslinkers with low inherent toxicity. Since these materials are often rinsed off or removed shortly after application, long-term tissue accumulation and systemic toxicity are generally not major concerns.

In contrast, MIPs intended for *in vivo* use, such as intravenous nanocarriers or intracellular inhibitors, face more stringent safety demands. These systems must demonstrate sufficient degradability, immune neutrality, and compatibility at the subcellular level. Inadequate degradation may result in accumulation within organs such as the liver or spleen, potentially provoking macrophage activation, fibrotic responses, or complement system engagement. Material properties including particle size and surface charge directly affect biodistribution and clearance, with larger or highly charged particles being more likely to induce immune reactions. To mitigate these risks, researchers have employed biodegradable polymers such as PLA, PCL, and chitosan, along with surface functionalization using PEG, zwitterionic coatings, or biomimetic membranes. For intracellular applications, compatibility with organelles and avoidance of oxidative or lysosomal stress is crucial. Furthermore, in drug-loaded systems, one must consider both the intrinsic toxicity of the cargo and any synergistic cytotoxicity arising from the combined system. These application-specific challenges highlight the need for biocompatibility assessment frameworks that are adapted to the intended mode of use and informed by *in vivo* data. A comparative summary of key application scenarios, safety challenges, and mitigation strategies for different antiviral MIP types is provided in Supplementary Table S1.

Furthermore, the "intelligent design" of MIPs is increasingly vital for enhancing their functionality. Computational-assisted methods such as molecular docking, molecular dynamics, and density functional theory can predict monomer-template interactions and optimize recognition sites before imprinting, thereby improving imprinting efficiency and binding affinity [301,302]. Machine learning-based models are also being progressively introduced to efficiently screen functional monomer combinations, predict the impact of viral mutation sites on recognition interfaces, and even integrate viral evolution data to guide rapid adaptation for variants [303,304]. Beyond computational strategies, intelligent MIP systems have also incorporated post-imprinting feedback mechanisms that enable real-time cavity quality assessment, thereby enhancing recognition specificity and selectivity in complex targets [305]. In parallel, incorporating responsive functionalities allows MIPs to achieve conditionally triggered recognition or release behaviors based on external stimuli (like *pH*, temperature, redox state, or enzymatic activity), thereby boosting their therapeutic precision and timeliness in complex physiological environments.

When addressing the challenges of large-scale production, research is increasingly focusing on developing standardized processes and synthesis platforms. This will enable an efficient transition from structural design to clinical application. Green synthesis concepts have become a significant development direction, including the use of low-toxicity solvents, aqueous polymerization systems, biodegradable monomers, and reusable solid-phase templates. The goal here is to reduce environmental impact while also improving template utilization and reaction controllability [306]. Existing research indicates that continuous flow synthesis technology can achieve continuous preparation of MIPs through microreactors. By precisely controlling reaction time, temperature, and flow rate, this method effectively enhances material structural consistency and batch stability [307,308]. Furthermore, automated synthesis systems have been employed for the standardized preparation of protein-imprinted MIPs, demonstrating good reproducibility [309]. Although AI-based high-throughput optimization strategies and modular preparation platforms are still in their exploratory stages, their potential in automating synthesis processes and regulating reaction parameters is creating new opportunities for the large-scale production and personalized application of antiviral MIPs [310]. In particular, recent studies have demonstrated that continuous flow microreactors, when combined with AI-guided optimization, can translate predicted reaction inputs into GMP-compatible automated synthesis parameters. For example, Raza *et al.* developed a machine-learning-assisted microreactor platform capable of rapidly mapping complex polymerization designs and adjusting high-throughput production parameters in real time, dramatically reducing chemical waste and accelerating discovery [311]. This approach shows strong potential for application in MIP synthesis, where AI-predicted monomer combinations could be seamlessly translated into precise microreactor settings such as flow rate, temperature, and residence time to support automated, scalable, and reproducible production [312]. To meet GMP requirements, integrating in-line monitoring tools and digital batch records can facilitate validation, traceability, and robust quality control during scale-up. The next step should involve deeper alignment with regulatory frameworks by defining Critical Quality Attributes (CQA), establishing Process Analytical Technology (PAT), and reaching consensus on material evaluation standards, all of which will boost the accessibility and operability of MIPs in clinical applications [313].

To enhance the regulatory feasibility of antiviral MIPs in diverse applications, future considerations could include integrating approval processes by referencing the "combination product" pathway [314]. This should be accompanied by promoting the development of classification guidelines based on use and risk [315]. Concurrently, there should be greater emphasis on standardized collection and sharing of key

performance data. This will facilitate mutual recognition of information among regulatory agencies, streamline approval pathways, and improve translation efficiency [316].

As these technical and regulatory obstacles are progressively overcome, the clinical application prospects for antiviral MIPs are becoming increasingly clear. Leveraging their diverse capabilities in molecular recognition, targeted delivery, and responsive control, MIPs could realistically be deployed in several future scenarios. For instance, MIPs designed for viral clearance might be developed as nasal sprays or nebulized inhalants to offer early intervention in respiratory infections [317]. Functional MIPs for replication inhibition could be incorporated into oral medications or injectable formulations to systematically interfere with critical points in the viral life cycle. Furthermore, MIPs with immunomodulatory potential might be further developed as subcutaneous adjuvants or mucosal immune enhancers, boosting antigen presentation efficiency [318,319]. Their controlled release and targeting characteristics also promise to drive more precise applications of injectable nanomedicines for drug delivery. Lastly, diagnostic MIPs could serve as platforms for test strips, chips, or sensors, assisting in the highly sensitive enrichment and detection of viral molecules. While these concepts still require extensive validation, their clinical value is gradually emerging as synthesis methods, material properties, and translational platforms continue to advance. It is important to note that these application pathways not only hold intrinsic value but can also complement existing antiviral drugs and vaccines. For example, they could expand the functional boundaries of current treatment options by improving tissue targeting, prolonging drug action, mitigating drug resistance, or enhancing immune activation.

Overall, antiviral MIPs, as an engineered platform integrating recognition, intervention, and delivery functions, are constructing a highly integrated new paradigm for antiviral intervention. Their designability, adaptability, and modular characteristics are expected to support future integrated, customizable strategic systems for addressing viral threats, accelerating the realization of next-generation precise and scalable antiviral solutions.

CRediT authorship contribution statement

Xiaohan Ma: Writing – original draft, Visualization, Methodology, Formal analysis, Data curation. **Alessandro Poma:** Writing – review & editing, Supervision, Project administration, Funding acquisition, Conceptualization. **Jonathan C. Knowles:** Writing – review & editing, Supervision, Project administration, Funding acquisition, Conceptualization. **Gareth R. Williams:** Writing – review & editing, Supervision, Project administration, Funding acquisition, Conceptualization. **Chau David Y. S.:** Writing – review & editing, Supervision, Project administration, Funding acquisition, Conceptualization. **Myrto Dimoula:** Writing – original draft, Visualization, Methodology, Formal analysis, Data curation. **Yingqi Ma:** Writing – original draft, Visualization, Methodology, Formal analysis, Data curation. **Ren Yang:** Writing – original draft, Visualization, Methodology, Formal analysis, Data curation. **Latifa W. Allahou:** Writing – original draft, Visualization, Methodology, Formal analysis, Data curation.

Consent for publication

Not applicable.

Ethics approval and consent to participate

Not applicable.

Funding

This work was supported by grants from the Royal Society of Chemistry, the Wellcome Trust (ISSF3), the National Institute for Health and Care Research, the Rosetrees Trust, the Great Britain-China Educational Trust, the Kuwait University and the University College London.

Declaration of Competing Interest

The authors declare the following financial interests/personal relationships which may be considered as potential competing interests: Alessandro Poma reports financial support was provided by Royal Society of Chemistry. Alessandro Poma reports financial support was provided by Wellcome Trust. Alessandro Poma reports financial support was provided by NIHR University College London Hospitals Biomedical Research Centre. Latifa W. Allahou reports financial support was provided by Kuwaiit University. Xiaohan Ma reports financial support was provided by University College London. If there are other authors, they declare that they have no known competing financial interests or personal relationships that could have appeared to influence the work reported in this paper.

Acknowledgement

The authors acknowledge Miss Tingting Peng for her help with the graphics.

Appendix A. Supporting information

Supplementary data associated with this article can be found in the online version at doi:10.1016/j.mser.2025.101099.

Data availability

No data was used for the research described in the article.

References

[1] J. Louten, Chapter 1 - the world of viruses, in: J. Louten (Ed.), Essential Human Virology, Academic Press, Boston, 2016, pp. 1–18.
[2] S.J. Flint, V.R. Racaniello, G.F. Rall, T. Hatziioannou, A.M. Skalka, Principles of virology, 2, John Wiley & Sons, 2020.
[3] D. Kaul, Curr. Med. Res. Pract. 10 (2020) 54–64.
[4] WHO, Number of COVID-19 cases reported to WHO (cumulative total), vol 2025, 2025.
[5] J. Louten, Chapter 2 - virus structure and classification, in: J. Louten (Ed.), Essential Human Virology, Academic Press, Boston, 2016, pp. 19–29.
[6] A. Tselis, J. Booss, Viral vaccines and antiviral therapy, in: M.J. Aminoff, R. B. Daroff (Eds.), Encyclopedia of the Neurological Sciences (Second Edition), Academic Press, Oxford, 2014, 659-669.
[7] G. Andrei, Front. Virol. 1 (2021).
[8] A.R. Hinman, Vaccine 16 (1998) 1116–1121.
[9] D.R. Tompa, A. Immanuel, S. Srikanth, S. Kadhirvel, Int. J. Biol. Macromol. 172 (2021) 524–541.
[10] R.B. Kennedy, I.G. Ovsyannikova, P. Palese, G.A. Poland, Front. Immunol. 11 (2020).
[11] E. Moysi, R.M. Paris, R. Le Grand, R.A. Koup, C. Petrovas, Expert Rev. Vaccin. 21 (2022) 633–644.
[12] E.E. Walsh, K. Ilangovan, A. Zareba, Q. Jiang, G.P. Marc, T. Verbeek, J. Breedt, H. Stacey, A. Uchiyama, J. Ojanperä, E.N. DeHaan, M. Patton, Y. Kan, D.P. Eiras, T. Mikati, E. Kalinina, D. Cooper, A.S. Anderson, K.A. Swanson, W.C. Gruber, A. C. Gurtman, B. Schmoele-Thoma, Open Forum Infect. Dis. 10 (2023).
[13] F. Krammer, Semin Immunopathol. 45 (2024) 451–468.
[14] D. Sharma, S. Sharma, N. Akojwar, A. Dondulkar, N. Yenorkar, D. Pandita, S. K. Prasad, M. Dhobi, Vaccines 11 (2023) 206.
[15] D. Lembo, R. Cavalli, Antivir. Chem. Chemother. 21 (2010) 53–70.
[16] X. Huang, W. Xu, M. Li, P. Zhang, Y.S. Zhang, J. Ding, X. Chen, Matter 4 (2021) 1892–1918.
[17] D. Hughes, D.I. Andersson, Nat. Rev. Genet 16 (2015) 459–471.
[18] K.K. Irwin, N. Renzette, T.F. Kowalik, J.D. Jensen, Virus, Evolution 2 (2016).
[19] L. Chen, S. Xu, J. Li, Chem. Soc. Rev. 40 (2011) 2922–2942.
[20] J.J. BelBruno, Chem. Rev. 119 (2019) 94–119.
[21] Y.H. Wen, D.N. Sun, X.Y. Fu, Y.M. Jin, J.L. Yu, L.Z. Xu, Z.H. Song, L.X. Chen, J. H. Li, Acs Appl. Nano Mater. 7 (2024) 9565–9575.
[22] X. Chen, A. Ostovan, M. Arabi, Y. Wang, L. Chen, J. Li, Anal. Chem. 96 (2024) 6417–6425.
[23] W. Lu, S. Fu, X. Lang, H. Zhao, D. Zhu, S. Cao, L. Chen, J. Li, J. Chromatogr, A 1731 465196 (2024).

[24] K. Haupt, P.X. Medina Rangel, B.T.S. Bui, Chem. Rev. 120 (2020) 9554–9582.
[25] K. Haupt, Anal. Chem. 75 (2003) 376A–383A.
[26] G. Vasapollo, R.D. Sole, L. Mergola, M.R. Lazzoi, A. Scardino, S. Scorrano, G. Mele, Int. J. Mol. Sci. 12 (2011) 5908–5945.
[27] B. Tse Sum Bui, T. Auroy, K. Haupt, Angew Chem Int, 61, Engl, 2022 e202106493.
[28] A.N. Hasanah, N. Safitri, A. Zulfa, N. Neli, D. Rahayu, Molecules 26 (2021) 5612.
[29] T. Sajini, B. Mathew, Talanta Open 4 (2021) 100072.
[30] L. Resina, C. Alemán, F.C. Ferreira, T. Esteves, Biotechnol. Adv. 68 (2023) 108220.
[31] M. Diaz-Alvarez, E. Turiel, A. Martin-Esteban, J. Sep Sci 46 (2023) e2300157.
[32] A. Poma, A.P. Turner, S.A. Piletsky, Trends Biotechnol. 28 (2010) 629–637.
[33] M.S. Amorim, M.G.F. Sales, M.F. Frasco, Biosens. Bioelectron. X 10 (2022) 100131.
[34] X. Guo, J. Li, M. Arabi, X. Wang, Y. Wang, L. Chen, A.C.S. Sens 5 (2020) 601–619.
[35] N.W. Turner, C.W. Jeans, K.R. Brain, C.J. Allender, V. Hlady, D.W. Britt, Biotechnol. Prog. 22 (2006) 1474–1489.
[36] M. Gast, H. Sobek, B. Mizaikoff, TrAC Trends Anal. Chem. 114 (2019) 218–232.
[37] M. Dabrowski, P. Lach, M. Cieplak, W. Kutner, Biosens. Bioelectron. 102 (2018) 17–26.
[38] S. Ramanavicius, A. Jagminas, A. Ramanavicius, Polymers 13 (2021) 974.
[39] M.E. Byrne, K. Park, N.A. Peppas, Adv. Drug Deliv. Rev. 54 (2002) 149–161.
[40] M.E. Byrne, V. Salian, Int J. Pharm. 364 (2008) 188–212.
[41] L.D. Bolisay, J.N. Culver, P. Kofinas, Biomaterials 27 (2006) 4165–4168.
[42] L.D. Bolisay, P. Kofinas, Imprinted Polymer Hydrogels for the Separation of Viruses. 19th Polymer-Networks-Group Meeting, Wiley-VCH, Verlag Gmbh, Larnaca, 2008, pp. 291–292. VOL 302. (CYPRUS).
[43] W. Bai, D.A. Spivak, Angew Chem Int, 53, Engl, 2014, pp. 2095–2098.
[44] G. Erturk, B. Mattiasson, Sensors 17 (2017) 288.
[45] C. Dong, H. Shi, Y. Han, Y. Yang, R. Wang, J. Men, Eur. Polym. J. 145 (2021) 110231.
[46] L. Luo, J. Yang, K. Liang, C. Chen, X. Chen, C. Cai, Talanta 202 (2019) 21–26.
[47] A. Mujahid, N. Iqbal, A. Afzal, Biotechnol. Adv. 31 (2013) 1435–1447.
[48] H.F. El Sharif, S.R. Dennison, M. Tully, S. Crossley, W. Mwangi, D. Bailey, S. P. Graham, S.M. Reddy, Anal. Chim. Acta 1206 (2022) 339777.
[49] A.M. Mahmoud, M.M. El-Wekil, M.H. Mahnashi, M.F.B. Ali, S.A. Alkahtani, Mikrochim Acta 186 (2019) 617.
[50] E. Brazys, V. Ratautaite, E. Mohsenzadeh, R. Boguzaite, A. Ramanaviciute, A. Ramanavicius, Adv. Colloid Interface Sci. 337 (2025) 103386.
[51] S. Ramanavicius, A. Ramanavicius, Adv. Colloid Interface Sci. 305 (2022) 102693.
[52] A. Poma, A. Guerreiro, M.J. Whitcombe, E.V. Piletska, A.P. Turner, S.A. Piletsky, Adv. Funct. Mater. 23 (2013) 2821–2827.
[53] Z. Altintas, M. Gittens, A. Guerreiro, K.A. Thompson, J. Walker, S. Piletsky, I. E. Tothill, Anal. Chem. 87 (2015) 6801–6807.
[54] C. Unger, P.A. Lieberzeit, React. Funct. Polym. 161 (2021) 104855.
[55] T. Muhammad, D.N. Zhao, A. Guerreiro, I. Muhammad, M. Aimaitiniyazi, B. Ding, Y. Zheng, T. Yimamumaimaiti, L.X. Chen, S.A. Piletsky, TracTrends Anal. Chem. 184 (2025) 118134.
[56] T. Karasu, F. Çalışır, S. Pişkin, E. Özgür, C. Armutcu, M.E. Çorman, L. Uzun, J. Pharm. Biomed. Anal. Open 4 (2024) 100041.
[57] E. Mohsenzadeh, V. Ratautaite, E. Brazys, S. Ramanavicius, S. Zukauskas, D. Plausinaitis, A. Ramanavicius, TrAC Trends Anal. Chem. 171 (2024) 117480.
[58] L. Levi, V. Raim, S. Srebnik, J. Mol Recognit 24 (2011) 883–891.
[59] X. Yu, J. Mo, M. Yan, J. Xin, X. Cao, J. Wu, J. Wan, Polymers 16 (2024) 2257.
[60] E. Mohsenzadeh, V. Ratautaite, E. Brazys, S. Ramanavicius, S. Zukauskas, D. Plausinaitis, A. Ramanavicius, Wiley Interdiscip. Rev. Comput. Mol. Sci. 14 (2024) e1713.
[61] L. Chen, X. Wang, W. Lu, X. Wu, J. Li, Chem. Soc. Rev. 45 (2016) 2137–2211.
[62] J.M. Pan, W. Chen, Y. Ma, G.Q. Pan, Chem. Soc. Rev. 47 (2018) 5574–5587.
[63] M. Jia, Z. Zhang, J. Li, X. Ma, L. Chen, X. Yang, TrAC Trends Anal. Chem. 106 (2018) 190–201.
[64] R. Yang, X. Ma, M. Xuan, Y. Ma, J. Ding, D.Y.S. Chau, J.C. Knowles, F. Peng, A. Poma, Chem. N./a (2025) e2500127.
[65] S.A. Zaidi, Biosensors 11 (2021) 89.
[66] J. Li, D. Sun, Langmuir 38 (2022) 13305–13312.
[67] T. Wangchareansak, A. Thitithanyanont, D. Chuakheaw, M.P. Gleeson, P. A. Lieberzeit, C. Sangma, Medchemcomm 5 (2014) 617–621.
[68] T. Wangchareansak, A. Thitithanyanont, D. Chuakheaw, M.P. Gleeson, P. A. Lieberzeit, C. Sangma, J. Mater. Chem. B 1 (2013) 2190–2197.
[69] D.F. Tai, C.Y. Lin, T.Z. Wu, J.H. Huang, P.Y. Shu, Clin. Chem. 52 (2006) 1486–1491.
[70] D.F. Tai, C.Y. Lin, T.Z. Wu, L.K. Chen, Anal. Chem. 77 (2005) 5140–5143.
[71] P.A. Lieberzeit, S. Chunta, K. Navakul, C. Sangma, C. Jungmann, Procedia Eng. 168 (2016) 101–104.
[72] C.E. Buensuceso, B.D.B. Tiu, L.P. Lee, P.M.G. Sabido, G.M. Nuesca, E.B. Caldona, F.R. Del Mundo, R.C. Advincula, Anal. Bioanal. Chem. 414 (2022) 1347–1357.
[73] C. Liang, H. Wang, K. He, C. Chen, X. Chen, H. Gong, C. Cai, Talanta 160 (2016) 360–366.
[74] K. He, C.Y. Chen, C.S. Liang, C. Liu, B. Yang, X.M. Chen, C.Q. Cai, Sens. Actuators BChem. 233 (2016) 607–614.
[75] C.H. Lu, Y. Zhang, S.F. Tang, Z.B. Fang, H.H. Yang, X. Chen, G.N. Chen, Biosens. Bioelectron. 31 (2012) 439–444.
[76] C.Y. Chou, C.Y. Lin, C.H. Wu, D.F. Tai, Sensors 20 (2020) 3592.
[77] B. Yang, H. Gong, C. Chen, X. Chen, C. Cai, Biosens. Bioelectron. 87 (2017) 679–685.
[78] L. Luo, F. Zhang, C. Chen, C. Cai, Anal. Chem. 91 (2019) 15748–15756.
[79] Y.T. Wang, Z.Q. Zhang, V. Jain, J.J. Yi, S. Mueller, J. Sokolov, Z.X. Liu, K. Levon, B. Rigas, M.H. Rafailovich, Sens. Actuators BChem. 146 (2010) 381–387.
[80] D. Cai, L. Ren, H. Zhao, C. Xu, L. Zhang, Y. Yu, H. Wang, Y. Lan, M.F. Roberts, J. H. Chuang, M.J. Naughton, Z. Ren, T.C. Chiles, Nat. Nanotechnol. 5 (2010) 597–601.
[81] C. Tancharoen, W. Sukjee, C. Thepparit, T. Jaimipuk, P. Auewarakul, A. Thitithanyanont, C. Sangma, A.C.S. Sens 4 (2019) 69–75.
[82] A. Raziq, A. Kidakova, R. Boroznjak, J. Reut, A. Opik, V. Syritski, Biosens. Bioelectron. 178 (2021) 113029.
[83] A.G. Ayankojo, R. Boroznjak, J. Reut, A. Opik, V. Syritski, Sens Actuators B Chem. 353 (2022) 131160.
[84] F.L. Dickert, O. Hayden, R. Bindeus, K.J. Mann, D. Blaas, E. Waigmann, Anal. Bioanal. Chem. 378 (2004) 1929–1934.
[85] A. Ramanaviciene, A. Ramanavicius, Biosens. Bioelectron. 20 (2004) 1076–1082.
[86] V. Liustrovaite, V. Ratautaite, A. Ramanaviciene, A. Ramanavicius, Biosens. Bioelectron. 272 (2025) 117092.
[87] V. Ratautaite, R. Boguzaite, E. Brazys, D. Plausinaitis, S. Ramanavicius, U. Samukaite-Bubniene, M. Bechelany, A. Ramanavicius, Talanta 253 (2023) 123981.
[88] V. Ratautaite, R. Boguzaite, E. Brazys, A. Ramanaviciene, E. Ciplys, M. Juozapaitis, R. Slibinskas, M. Bechelany, A. Ramanavicius, Electro Acta 403 (2022) 139581.
[89] A. Karthik, K. Margulis, K. Ren, R.N. Zare, L.W. Leung, Nanoscale 7 (2015) 18998–19003.
[90] J. Yang, W. Feng, K. Liang, C. Chen, C. Cai, Talanta 212 (2020) 120744.
[91] W.B. Feng, C.S. Liang, H. Gong, C.Q. Cai, N. J. Chem. 42 (2018) 3503–3508.
[92] L. Luo, W. Feng, W. Hu, C. Chen, H. Gong, C. Cai, Methods Appl. Fluor. 7 (2018) 015006.
[93] L. Luo, F. Zhang, C. Chen, C. Cai, Mikrochim Acta 187 (2020) 140.
[94] N. Li, Y.J. Liu, F. Liu, M.F. Luo, Y.C. Wan, Z. Huang, Q. Liao, F.S. Mei, Z.C. Wang, A.Y. Jin, Y. Shi, B. Lu, Acta Biomater. 51 (2017) 175–183.
[95] S.P. Graham, H.F. El-Sharif, S. Hussain, R. Fruengel, R.K. McLean, P.C. Hawes, M. V. Sullivan, S.M. Reddy, Front Bioeng. Biotechnol. 7 (2019) 115.
[96] O.I. Parisi, M. Dattilo, F. Patitucci, R. Malivindi, S. Delbue, P. Ferrante, S. Parapini, R. Galeazzi, M. Cavarelli, F. Cilurzo, S. Franze, I. Perrotta, V. Pezzi, F. Selmin, M. Ruffo, F. Puoci, Nanoscale 13 (2021) 16885–16899.
[97] J. Zhou, L. Wang, X. Liu, Y. Gai, M. Dong, C. Wang, M.M. Ali, M. Ye, X. Yu, L. Hu, Nano Lett. 24 (2024) 4423–4432.
[98] Y. Li, S. Xu, Q. Ye, H. Chi, Z. Guo, J. Chen, M. Wu, B. Fan, B. Li, C.F. Qin, Z. Liu, Adv. Sci. (Weinh.) 10 (2023) e2202689.
[99] F. Ding, Y. Ma, W. Fan, J. Xu, G. Pan, Trends Biotechnol. 42 (2024) 1097–1111.
[100] A.F. Nahhas, T.J. Webster, J. Nanobiotechnology 19 (2021) 305.
[101] F. Puoci, J. Funct Biomater 11 (2020).
[102] N. Sankarakumar, Y.W. Tong, J. Mater. Chem. B 1 (2013) 2031–2037.
[103] V. Mirshafiee, R. Kim, M. Mahmoudi, M.L. Kraft, Int J. Biochem Cell Biol. 75 (2016) 188–195.
[104] Y. Hoshino, H. Koide, T. Urakami, H. Kanazawa, T. Kodama, N. Oku, K.J. Shea, J. Am Chem Soc 132 (2010) 6644–6645.
[105] R.R. Tian, M.B. Luo, J.Y. Li, Phys. Chem. Chem. Phys. 20 (2018) 68–74.
[106] S.M. Gheibi Hayat, V. Bianconi, M. Pirro, A. Sahebkar, Int. J. Pharm. 569 (2019) 118628.
[107] L. Li, C. Zhang, Z. Cao, L. Ma, C. Liu, X. Lan, C. Qu, P. Fu, R. Luo, Y. Wang, Biomaterials 305 (2024) 122423.
[108] M. Gast, S. Kühner, H. Sobek, P. Walther, B. Mizaikoff, Anal. Chem. 90 (2018) 5576–5585.
[109] S. Dietl, P. Walther, H. Sobek, B. Mizaikoff, Materials 14 (2021) 7692.
[110] L.D. Bolisay, J.N. Culver, P. Kofinas, Biomacromolecules 8 (2007) 3893–3899.
[111] R. Randriantsilefisoa, C. Nie, B. Parshad, Y. Pan, S. Bhatia, R. Haag, Chem. Commun. 56 (2020) 3547–3550.
[112] R. Wang, Y. Li, Biosens. Bioelectron. 42 (2013) 148–155.
[113] T.E. Torres, E. Lima Jr, M.P. Calatayud, B. Sanz, A. Ibarra, R. Fernández-Pacheco, A. Mayoral, C. Marquina, M.R. Ibarra, G.F. Goya, Sci. Rep. 9 (2019) 3992.
[114] P. Paul, K.L. Edmonds, K.C. Baldridge, D. Bhattacharyya, T. Dziubla, R.E. Dutch, J.Z. Hilt, A.C.S. Appl Bio Mater 5 (2022) 5140–5147.
[115] B. Adams, H. Bak, A.D. Tustian, Biotechnol. Bioeng. 117 (2020) 3199–3211.
[116] A.A. Malik, C. Nantasenamat, T. Piacham, C. Mater Sci Eng, Mater. Biol. Appl. 77 (2017) 1341–1348.
[117] P. Trischitta, M.P. Tamburello, A. Venuti, R. Pennisi, Int J. Mol. Sci. 25 (2024) 5188.
[118] M. Gast, F. Wondany, B. Raabe, J. Michaelis, H. Sobek, B. Mizaikoff, Anal. Chem. 92 (2020) 3050–3057.
[119] K. Lothert, M.W. Wolff, Membranes 13 (2023) 770.
[120] L. Crowley, J.J. Labisch, M. Leskovec, M. Tajnik Sbaizero, K. McLaughlin, P. Nestola, A. Boulais, Purifying viral vectors: a review of chromatography solutions, in: S. Gautam, A.I. Chiramel, R. Pach (Eds.), Bioprocess and Analytics Development for Virus-based Advanced Therapeutics and Medicinal Products (ATMPs), Springer International Publishing, Cham, 2023, pp. 171–202.
[121] A. Bajaj, J. Trimpert, I. Abdulhalim, Z. Altintas, Chemosensors 10 (2022) 459.
[122] B. Sellergren, Molecularly Imprinted Polymers: Man-made Mimics of Antibodies and Their Application in Analytical Chemistry, Elsevier, 2000.
[123] G. Fibriansah, T.-S. Ng, V.A. Kostyuchenko, J. Lee, S. Lee, J. Wang, S.-M. Lok, J. Virol. 87 (2013) 7585–7592.
[124] J.M. Casasnovas, Virus-Receptor interactions and Receptor-Mediated virus entry into host cells, in: M.G. Mateu (Ed.), Structure and Physics of Viruses: An Integrated Textbook, Springer, Netherlands, Dordrecht, 2013, pp. 441–466.

[125] Y. Wang, Z. Zhang, L. Shang, H. Gao, X. Du, F. Li, Y. Gao, G. Qi, W. Guo, Z. Qu, T. Dong, Front Microbiol 12 (2021) 717047.
[126] M. Gast, H. Sobek, B. Mizaikoff, C. Mater Sci Eng, Mater. Biol. Appl. 99 (2019) 1099–1104.
[127] A. Kumar, T.C. Rohe, E.J. Elrod, A.G. Khan, A.D. Dearborn, R. Kissinger, A. Grakoui, J. Marcotrigiano, Nat. Commun. 14 (2023) 433.
[128] M.C. Metcalf, B.M. Janus, R. Yin, R. Wang, J.D. Guest, E. Pozharski, M. Law, R. A. Mariuzza, E.A. Toth, B.G. Pierce, T.R. Fuerst, G. Ofek, Nat. Commun. 14 (2023) 3980.
[129] M. Antipchik, J. Reut, A.G. Ayankojo, A. Opik, V. Syritski, Talanta 250 (2022) 123737.
[130] C.B. Jackson, M. Farzan, B. Chen, H. Choe, Nat. Rev. Mol. Cell Biol. 23 (2022) 3–20.
[131] Y. Huang, C. Yang, X.F. Xu, W. Xu, S.W. Liu, Acta Pharm. Sin. 41 (2020) 1141–1149.
[132] X.D. Wu, B. Shang, R.F. Yang, H. Yu, Z.H. Ma, X. Shen, Y.Y. Ji, Y. Lin, Y.D. Wu, G. M. Lin, L. Tian, X.Q. Gan, S. Yang, W.H. Jiang, E.H. Dai, X.Y. Wang, H.L. Jiang, Y. H. Xie, X.L. Zhu, G. Pei, L. Li, J.R. Wu, B. Sun, Cell Res 14 (2004) 400–406.
[133] B. Tse Sum Bui, A. Mier, K. Haupt, Small 19 (2023) 2206453.
[134] J. Lan, J. Ge, J. Yu, S. Shan, H. Zhou, S. Fan, Q. Zhang, X. Shi, Q. Wang, L. Zhang, X. Wang, Nature 581 (2020) 215–220.
[135] S. Brindha, Y. Kuroda, Int. J. Mol. Sci. 23 (2022) 1703.
[136] F. Li, W. Li, M. Farzan, S.C. Harrison, Science 309 (2005) 1864–1868.
[137] C. Yi, X. Sun, J. Ye, L. Ding, M. Liu, Z. Yang, X. Lu, Y. Zhang, L. Ma, W. Gu, A. Qu, J. Xu, Z. Shi, Z. Ling, B. Sun, Cell. Mol. Immunol. 17 (2020) 621–630.
[138] O.I. Parisi, M. Dattilo, F. Patitucci, R. Malivindi, V. Pezzi, I. Perrotta, M. Ruffo, F. Amone, F. Puoci, BioRxiv (2020), 2020.2005. 2028.120709.
[139] W. van Oeveren, Scientifica (Cairo) 2013 (2013) 392584.
[140] R. Luna-Vazquez-Gomez, M.E. Arellano-Garcia, J.C. Garcia-Ramos, P. Radilla-Chavez, D.S. Salas-Vargas, F. Casillas-Figueroa, B. Ruiz-Ruiz, N. Bogdanchikova, A. Pestryakov, Materials 14 (2021) 2792.
[141] M. Dattilo, F. Patitucci, M.F. Motta, S. Prete, R. Galeazzi, S. Franze, I. Perrotta, M. Cavarelli, O.I. Parisi, F. Puoci, Colloids Surf. B Biointerfaces 247 (2025) 114408.
[142] N.L. Miller, R. Raman, T. Clark, R. Sasisekharan, Front. Immunol. 13 (2022) 904609.
[143] S. Piletsky, F. Canfarotta, A. Poma, A.M. Bossi, S. Piletsky, Trends Biotechnol. 38 (2020) 368–387.
[144] T. Khumsap, A. Corpuz, L.T. Nguyen, R.S.C. Adv 11 (2021) 11403–11414.
[145] M. Siqueira Silva, A.P. Moreira Tavares, L.F. Leomil Coelho, L.E. Morganti Ferreira Dias, R.M. Chura-Chambi, F. Guimaraes da Fonseca, M.G. Ferreira Sales, E. Costa figueiredo, Biosens. Bioelectron. 191 (2021) 113419.
[146] A. Mier, I. Maffucci, F. Merlier, E. Prost, V. Montagna, G.U. Ruiz-Esparza, J. V. Bonventre, P.K. Dhal, B. Tse Sum Bui, P. Sakhaii, K. Haupt, Angew Chem Int, 60, Engl, 2021, pp. 20849–20857.
[147] E. Sehit, G. Yao, G. Battocchio, R. Radfar, J. Trimpert, M.A. Mroginski, R. Sussmuth, Z. Altintas, A.C.S. Sens 9 (2024) 1831–1841.
[148] J. Xu, F. Merlier, B. Avalle, V. Vieillard, P. Debre, K. Haupt, B. Tse Sum Bui, A.C. S. Appl Mater, Interfaces 11 (2019) 9824–9831.
[149] B. Fresco-Cala, S. Rajpal, T. Rudolf, B. Keitel, R. Gross, J. Munch, A.D. Batista, B. Mizaikoff, Nanomater. 11 (2021) 2985.
[150] J. McClements, L. Bar, P. Singla, F. Canfarotta, A. Thomson, J. Czulak, R. E. Johnson, R.D. Crapnell, C.E. Banks, B. Payne, S. Seyedin, P. Losada-Perez, M. Peeters, A.C.S. Sens 7 (2022) 1122–1131.
[151] Z. Bognar, E. Supala, A. Yarman, X. Zhang, F.F. Bier, F.W. Scheller, R. E. Gyurcsanyi, Chem. Sci. 13 (2022) 1263–1269.
[152] A.D. Batista, S. Rajpal, B. Keitel, S. Dietl, B. Fresco-Cala, M. Dinc, R. Gross, H. Sobek, J. Munch, B. Mizaikoff, Adv. Mater. Interfaces 9 (2022) 2101925.
[153] V. Hariharan, R.S. Kane, Biotechnol. Bioeng. 117 (2020) 2556–2570.
[154] K.O. Francois, J. Balzarini, J. Biol Chem 286 (2011) 42900–42910.
[155] B. Cosar, Z.Y. Karagulleoglu, S. Unal, A.T. Ince, D.B. Uncuoglu, G. Tuncer, B. R. Kilinc, Y.E. Ozkan, H.C. Ozkoc, I.N. Demir, A. Eker, F. Karagoz, S.Y. Simsek, B. Yaşar, M. Pala, A. Demir, I.N. Atak, A.H. Mendi, V.U. Bengi, G. Cengiz Seval, E. Gunes Altuntas, P. Kilic, D. Demir-Dora, Cytokine Growth Factor Rev. 63 (2022) 10–22.
[156] A.J. Thompson, J.C. Paulson, J. Biol Chem 296 (2021) 100017.
[157] J. Wee, G.W. Wei, Virus evol, veaf026 (11 () (2025).
[158] Z.W. Nie, X.D. Liu, J. Chen, Z.N. Wang, Y.T. Liu, H.R. Si, T.Y. Dong, F. Xu, G. L. Song, Y. Wang, P. Zhou, W. Gao, Y.H. Tian, Nat. Mach. Intell. 7 (2025) 131–144.
[159] W.J. Choi, J. Park, D.Y. Seong, D.S. Chung, D. Hong, Genom. Inf. 22 (2024) 15.
[160] X. Li, Y. Li, X. Shang, H. Kong, Front Microbiol 15 (2024) 1345794.
[161] J.G. Liu, Y.L. Xue, X.M. Dong, Y.S. Fan, H.Q. Hao, X.Z. Wang, Int. J. Adhes. Adhes. 126 (2023) 103446.
[162] V. Mocharko, P. Mascarenhas, A.M. Azul, A.H.S. Delgado, Biomedicines 10 (2022) 3104.
[163] H.Q. Zhang, Adv. Mater. 32 (2020) 23.
[164] J. Szczepanska, T. Poplawski, E. Synowiec, E. Pawlowska, C.J. Chojnacki, J. Chojnacki, J. Blasiak, Mol. Biol. Rep. 39 (2012) 1561–1574.
[165] A. Bielecka-Kowalska, P. Czarny, P. Wigner, E. Synowiec, B. Kowalski, M. Szwed, R. Krupa, M. Toma, M. Drzewiecka, I. Majsterek, J. Szemraj, T. Sliwinski, M. Kowalski, Toxicol. Vitr. 47 (2018) 8–17.
[166] P.A. Baldion, M.L. Velandia-Romero, J.E. Castellanos, Chem. Biol. Inter. 333 (2021) 109336.
[167] J. Zuo, X.Y. Zhang, X.Y. Li, Z.W. Li, Z.R. Li, H.H. Li, W.C. Zhang, Rsc Adv. 9 (2019) 19712–19719.
[168] F. Canfarotta, A. Waters, R. Sadler, P. McGill, A. Guerreiro, D. Papkovsky, K. Haupt, S. Piletsky, Nano, Research 9 (2016) 3463–3477.
[169] M. Gagliardi, A. Bertero, A. Bifone, Sci. Rep. 7 (2017) 40046.
[170] S. Yedgar, G. Barshtein, A. Gural, Micromachines 13 (2022) 2091.
[171] Q. Shi, X. Xu, Q. Fan, J. Hou, W. Ye, J. Yin, J. Mater. Chem. B 3 (2015) 2119–2126.
[172] N. Mina, V.S. Guido, A.F. Lima, M.L.V. Oliva, A.A. Sousa, Part. Part. Syst. Charact. 41 (2023) 2300107.
[173] S. Tenzer, D. Docter, J. Kuharev, A. Musyanovych, V. Fetz, R. Hecht, F. Schlenk, D. Fischer, K. Kiouptsi, C. Reinhardt, K. Landfester, H. Schild, M. Maskos, S. K. Knauer, R.H. Stauber, Nat. Nanotechnol. 8 (2013) 772–781.
[174] S. Panico, S. Capolla, S. Bozzer, G. Toffoli, M. Dal Bo, P. Macor, Pharmaceutics 14 (2022) 2605.
[175] L.E. Gonzalez-Garcia, M.N. MacGregor, R.M. Visalakshan, A. Lazarian, A. A. Cavallaro, S. Morsbach, A. Mierczynska-Vasilev, V. Mailander, K. Landfester, K. Vasilev, Nanomaterials 12 (2022) 682.
[176] C.F. Adhipandito, S.H. Cheung, Y.H. Lin, S.H. Wu, Int. J. Mol. Sci. 22 (2021) 11182.
[177] K.S. Lee, D.S. Kim, B.S. Kim, Biotechnol. Bioprocess Eng. 12 (2007) 152–156.
[178] X. Ma, J.C. Knowles, A. Poma, Pharmaceutics 15 (2023) 1440.
[179] I. Göktürk, K.Ç. Güler, F. Yılmaz, C. Oktar, G.E. Yılmaz, A. Denizli, Biomed. Mater. Devices 3 (2024) 299–316.
[180] D. Makharadze, L.J. Del Valle, R. Katsarava, J. Puiggali, Int J. Mol. Sci. 26 (2025) 3102.
[181] J.Y. Wen, S.S. Huang, Q.Y. Hu, W. He, Z.J. Wei, L. Wang, J.H. Lu, X.T. Yue, S. Men, C.X. Miao, Z.J. He, X.Y. Yang, G.X. Zhai, J.J. Li, L. Ye, Materials today, Chemistry 40 (2024) 102232.
[182] M. Guo, C. Xia, Y. Wu, N. Zhou, Z. Chen, W. Li, Front Bioeng. Biotechnol. 9 (2021) 772522.
[183] S. Sunoqrot, J. Bugno, D. Lantvit, J.E. Burdette, S. Hong, J. Control Release 191 (2014) 115–122.
[184] S. Kassem, S.S. Piletsky, H. Yesilkaya, O. Gazioglu, M. Habtom, F. Canfarotta, E. Piletska, A.C. Spivey, E.O. Aboagye, S.A. Piletsky, Polymers 14 (2022) 4582.
[185] M. Xu, Y. Qi, G. Liu, Y. Song, X. Jiang, B. Du, A.C.S. Nano 17 (2023) 20825–20849.
[186] P. Lulinski, C. Mater Sci Eng, Mater. Biol. Appl. 76 (2017) 1344–1353.
[187] W. Wu, Y. Cheng, H. Zhou, C. Sun, S. Zhang, J. Virol 20 (2023) 6.
[188] M. Sinha, S. Pandit, P. Singh, S.S. Chauhan, R. Parthasarathi, Visualizing chemical functionality and structural insights into SARS-CoV-2 proteins, in: Y.K. Verma, N. K. Satija, P.K. Raghav, N. Tyagi, S. Kumar (Eds.), Stem Cells, Academic Press, 2024, pp. 257–275.
[189] M. Drobysh, V. Ratautaite, E. Brazys, A. Ramanaviciene, A. Ramanavicius, Biosens. Bioelectron. 251 (2024) 116043.
[190] T. Zhang, L. Sun, Y. Zhang, Anal. Methods 13 (2021) 5772–5776.
[191] S. Urata, J. Yasuda, Viruses 4 (2012) 2049–2079.
[192] Z.Y. Low, N.Z. Zabidi, A.J.W. Yip, A. Puniyamurti, V.T.K. Chow, S.K. Lal, Viruses 14 (2022) 1991.
[193] D. Marc, J. Gen Virol 95 (2014) 2594–2611.
[194] P.M. Mishra, N.C. Verma, C. Rao, V.N. Uversky, C.K. Nandi, Chapter one - intrinsically disordered proteins of viruses: involvement in the mechanism of cell regulation and pathogenesis, in: V.N. Uversky (Ed.), Progress in Molecular Biology and Translational Science, 174, Academic Press, 2020, pp. 1–78.
[195] P. Bhatt, S.P. Sabeena, M. Varma, G. Arunkumar, Curr. Microbiol 78 (2021) 17–32.
[196] R. Arshad, A. Rhouati, A. Hayat, M.H. Nawaz, M.A. Yameen, A. Mujahid, U. Latif, Appl. Biochem Biotechnol. 191 (2020) 1384–1394.
[197] G. Lebeau, A. Lagrave, E. Ogire, L. Grondin, S. Seriacaroupin, C. Moutoussamy, P. Mavingui, J.J. Hoarau, M. Roche, P. Krejbich-Trotot, P. Despres, W. Viranaicken, Vaccines 9 (2021) 946.
[198] J. Wu, S. Huang, L. Tan, Y. Li, X. Wu, Y. Liang, Anal. Chem. 93 (2021) 14106–14112.
[199] S.A.o.P.T.b.B. German Advisory Committee Blood, Transfus. Med Hemother 43 (2016) 203–222.
[200] F. Kirchhoff, (2013).
[201] S.S. Tekeste, T.A. Wilkinson, E.M. Weiner, X. Xu, J.T. Miller, S.F. Le Grice, R. T. Clubb, S.A. Chow, J. Virol. 89 (2015) 12058–12069.
[202] V. Ratautaite, S.N. Topkaya, L. Mikoliunaite, M. Ozsoz, Y. Oztekin, A. Ramanaviciene, A. Ramanavicius, Electroanalysis 25 (2013) 1169–1177.
[203] S. Kim, C.M. Schroeder, X.S. Xie, J. Mol. Biol. 395 (2010) 995–1006.
[204] B. Babamiri, A. Salimi, R. Hallaj, Biosens. Bioelectron. 117 (2018) 332–339.
[205] S. Kralj, M. Rojnik, R. Romih, M. Jagodič, J. Kos, D. Makovec, J. Nanopart. Res. 14 (2012) 1151.
[206] S. Jeon, J. Clavadetscher, D.K. Lee, S.V. Chankeshwara, M. Bradley, W.S. Cho, Nanomaterials 8 (2018) 1028.
[207] S. Wang, H. Guo, Y. Li, X. Li, Nanoscale 11 (2019) 4025–4034.
[208] X. Quan, D. Sun, J. Zhou, Phys. Chem. Chem. Phys. 21 (2019) 10300–10310.
[209] J. Hu, Y. Lou, F. Wu, J. Phys. Chem. B 123 (2019) 2636–2644.
[210] X. Ma, Y. Tian, R. Yang, H. Wang, L.W. Allahou, J. Chang, G. Williams, J. C. Knowles, A. Poma, J. Nanobiotechnology 22 (2024) 715.
[211] S. Rayamajhi, J. Marchitto, T.D.T. Nguyen, R. Marasini, C. Celia, S. Aryal, Colloids Surf. B Biointerfaces 188 (2020) 110804.
[212] A. Ibrahim, E. Twizeyimana, N. Lu, W. Ke, J.F. Mukerabigwi, F. Mohammed, A. Japir, Z. Ge, A.C.S. Appl Bio Mater 2 (2019) 5099–5109.
[213] Y. Nie, G. Fu, Y. Leng, Cells 12 (2023) 1637.
[214] Y. Shi, S. Wang, J. Wu, X. Jin, J. You, J. Control Release 329 (2021) 337–352.

[215] S.S. Liew, X. Qin, J. Zhou, L. Li, W. Huang, S.Q. Yao, Angew Chem Int, 60, Engl, 2021, pp. 2232–2256.
[216] H. Gao, Q. Zhang, Y. Yang, X. Jiang, Q. He, Int J. Pharm. 478 (2015) 240–250.
[217] M. Ekkapongpisit, A. Giovia, C. Follo, G. Caputo, C. Isidoro, Int J. Nanomed. 7 (2012) 4147–4158.
[218] S. Mazumdar, D. Chitkara, A. Mittal, B. Acta Pharm Sin 11 (2021) 903–924.
[219] G.C. Porter, W.J. Duncan, A. Jude, D. Abdelmoneim, R.A. Easingwood, D. E. Coates, Nanomedicine 33 (2021) 102355.
[220] B. Halamoda Kenzaoui, C. Chapuis Bernasconi, S. Guney-Ayra, L. Juillerat-Jeanneret, J. Biochem 441 (2012) 813–821.
[221] J. Deng, C. Gao, Nanotechnology 27 (2016) 412002.
[222] R. Samadarsi, D. Dutta, Int J. Biol. Macromol. 151 (2020) 36–46.
[223] K. Gopal, N. Nandakumar, R.R.C., R. Babu, S.V. Nair, B.N. Sathy, D. Menon, ACS Appl. Bio Mater. 6 (2023) 3143–3152.
[224] S.K. Masenga, B.C. Mweene, E. Luwaya, L. Muchaili, M. Chona, A. Kirabo, Cells 12 (2023) 1351.
[225] S.L. Swain, K.K. McKinstry, T.M. Strutt, Nat. Rev. Immunol. 12 (2012) 136–148.
[226] A.A. Okoye, L.J. Picker, Immunol. Rev. 254 (2013) 54–64.
[227] H. Sun, D. Kim, X. Li, M. Kiselinova, Z. Ouyang, L. Vandekerckhove, H. Shang, E. S. Rosenberg, X.G. Yu, M. Lichterfeld, J. Virol 89 (2015) 11284–11293.
[228] C.S. McGary, C. Deleage, J. Harper, L. Micci, S.P. Ribeiro, S. Paganini, L. Kuri-Cervantes, C. Benne, E.S. Ryan, R. Balderas, S. Jean, K. Easley, V. Marconi, G. Silvestri, J.D. Estes, R.P. Sekaly, M. Paiardini, Immunity, 776788 47 (2017) e775.
[229] R. Fromentin, S. DaFonseca, C.T. Costiniuk, M. El-Far, F.A. Procopio, F.M. Hecht, R. Hoh, S.G. Deeks, D.J. Hazuda, S.R. Lewin, J.P. Routy, R.P. Sekaly, N. Chomont, Nat. Commun. 10 (2019) 814.
[230] C.A. Reis, R. Tauber, V. Blanchard, J. Mol. Med. 99 (2021) 1023–1031.
[231] Z.T. Berndsen, S. Chakraborty, X. Wang, C.A. Cottrell, J.L. Torres, J.K. Diedrich, C.A. Lopez, J.R. Yates, 3rd, M.J. Van Gils, J.C. Paulson, S. Gnanakaran, A.B. Ward, Proc. Natl. Acad. Sci. 117 (2020) 28014–28025.
[232] R.K. Gupta, G.R. Apte, K.B. Lokhande, S. Mishra, J.K. Pal, Curr. Protein Pept. Sci. 21 (2020) 1085–1096.
[233] R. Pejchal, K.J. Doores, L.M. Walker, R. Khayat, P.S. Huang, S.K. Wang, R. L. Stanfield, J.P. Julien, A. Ramos, M. Crispin, R. Depetris, U. Katpally, A. Marozsan, A. Cupo, S. Maloveste, Y. Liu, R. McBride, Y. Ito, R.W. Sanders, C. Ogohara, J.C. Paulson, T. Feizi, C.N. Scanlan, C.H. Wong, J.P. Moore, W. C. Olson, A.B. Ward, P. Poignard, W.R. Schief, D.R. Burton, I.A. Wilson, Science 334 (2011) 1097–1103.
[234] D. Mannar, K. Leopold, S. Subramaniam, Sci. Rep. 11 (2021) 12448.
[235] L. Chen, C. Shang, Z. Wang, M. Zheng, C. Zhang, D. Li, Z. Yang, Y. Dong, Y. Xu, Y. Yuan, S. Fan, W. Zhong, J. Lin, X. Li, MedComm 6 (2025) (2020) e70045.
[236] L.M. Wakim, M.J. Bevan, Nature 471 (2011) 629–632.
[237] X. Ma, A. Poma, Clinical translation and envisioned impact of nanotech for infection control: economy, government policy and public awareness, in: A. Poma, L. Rizzello (Eds.), Nanotechnology Tools for Infection Control, Elsevier, 2025, pp. 299–392.
[238] C.A. Diebolder, F.J. Beurskens, R.N. de Jong, R.I. Koning, K. Strumane, M. A. Lindorfer, M. Voorhorst, D. Ugurlar, S. Rosati, A.J. Heck, J.G. van de Winkel, I. A. Wilson, A.J. Koster, R.P. Taylor, E.O. Saphire, D.R. Burton, J. Schuurman, P. Gros, P.W. Parren, Science 343 (2014) 1260–1263.
[239] B.P. Morgan, C.L. Harris, Nat. Rev. Drug Discov. 14 (2015) 857–877.
[240] P. Macor, P. Durigutto, A. Mangogna, R. Bussani, L. De Maso, S. D'Errico, M. Zanon, N. Pozzi, P.L. Meroni, F. Tedesco, Biomedicines 9 (2021) 1003.
[241] W. Li, S.X. Xu, Y. Li, J.R. Chen, Y.Y. Ma, Z. Liu, Ccs, Chemistry 5 (2023) 497–509.
[242] C. Tuerk, L. Gold, Science 249 (1990) 505–510.
[243] A.D. Ellington, J.W. Szostak, Nature 346 (1990) 818–822.
[244] A. Poma, H. Brahmbhatt, H.M. Pendergraff, J.K. Watts, N.W. Turner, Adv. Mater. 27 (2015) 750–758.
[245] R. Liu, A. Poma, Molecules 26 (2021) 3589.
[246] U. Bulbake, S. Doppalapudi, N. Kommineni, W. Khan, Pharmaceutics 9 (2017) 12.
[247] Y. Abo-zeid, G. Mantovani, W.L. Irving, M.C. Garnett, J. Drug Deliv. Sci. Technol. 46 (2018) 354–364.
[248] K. Kaneko, T. Ishihara, Cogent, Medicine 4 (2017) 1418133.
[249] T. Mathieu, P. Favetta, L.A. Agrofoglio, Pharmaceutics 16 (2024) 965.
[250] A. Varela-Garcia, J.L. Gomez-Amoza, A. Concheiro, C. Alvarez-Lorenzo, Polymers 12 (2020) 2026.
[251] Z. Li, J. Deng, P. Ma, H. Bai, Y. Jin, Y. Zhang, A. Dong, M. Burenjargal, J. Sep Sci 47 (2024) e202400441.
[252] V. Lawai, Z. Ngaini, S. Farooq, R. Wahi, S.A. Bhawani, Polym. Adv. Technol. 35 (2024) e6317.
[253] M.V. Sullivan, P. Lasserre, C. Blackburn, N.W. Turner, B. Sellergren, Responsive, Materials 3 (2025) e20240032.
[254] M.G. Ayari, P. Favetta, D. Warszycki, V. Vasseur, V. Herve, P. Degardin, B. Carbonnier, M. Si-Tahar, L.A. Agrofoglio, Macromol. Biosci. 22 (2022) e2100291.
[255] H. Liu, H. Maruyama, T. Masuda, A. Honda, F. Arai, Front Microbiol 7 (2016) 1127.
[256] F.W. Charlton, H.M. Pearson, S. Hover, J.D. Lippiat, J. Fontana, J.N. Barr, J. Mankouri, Virus 12 (2020) 844.
[257] Y. Ge, L. Ding, Y. Liu, X. Li, e-Polymers 24 (2024).
[258] J. Liu, C. Chen, H. Du, D.X. Wang, H.X. Ma, G.X. Wang, T. Liu, E.R. Wang, Aquaculture 561 (2022) 738662.
[259] W.T. Qiao, X. Yao, W.H. Lu, Y.Q. Zhang, K.K. Malhi, H.X. Li, J.L. Li, Int J. Biol. Macromol. 270 (2024) 132408.
[260] F. Erra Diaz, E. Dantas, J. Geffner, Mediat. Inflamm. 2018 (2018) 1218297.
[261] X. Mo, F. Wei, Y. Tong, L. Ding, Q. Zhu, S. Du, F. Tan, C. Zhu, Y. Wang, Q. Yu, Y. Liu, E.S. Robertson, Z. Yuan, Q. Cai, J. Virol 92 (2018), https://doi.org/10.1128/jvi.00033-00018.
[262] L.T. Liu, M.J. Chen, H.L. Yang, Z.J. Huang, Q. Tang, C.F. Chow, C.B. Gong, M. H. Zu, B. Xiao, C. Mater Sci Eng, Mater. Biol. Appl. 106 (2020) 110253.
[263] N. Sanadgol, J. Wackerlig, Pharmaceutics 12 (2020) 831.
[264] H. Lu, S. Xu, Z. Guo, M. Zhao, Z. Liu, A.C.S. Nano 15 (2021) 18214–18225.
[265] T. Kubo, K. Otsuka, J. Pharm Biomed Anal 130 (2016) 68–80.
[266] S. Ansari, M. Karimi, TrAC Trends Anal. Chem. 89 (2017) 146–162.
[267] S. Wang, C. Wang, Y. Xin, Q. Li, W. Liu, Microchim. Acta 189 (2022) 125.
[268] B.L. Sun, C.Y. Gao, L. Yang, H.X. Shi, L. Kan, Q.H. Ma, X.F. Shi, J. Electrochem. Soc. 169 (2022).
[269] Z. Luo, L.F. Liu, X.H. Wang, W. Li, C. Jie, H. Chen, F.Q. Wei, D.H. Lu, C.Y. Yan, B. Liu, H. Kurihara, Y.F. Li, R.R. He, Front. Pharmacol. 10 (2019) 12.
[270] Z. Terzopoulou, M. Papageorgiou, G.Z. Kyzas, D.N. Bikiaris, D.A. Lambropoulou, Anal. Chim. Acta 913 (2016) 63–75.
[271] I. Chianella, K. Karim, E.V. Piletska, C. Preston, S.A. Piletsky, Anal. Chim. Acta 559 (2006) 73–78.
[272] H. Yan, M. Wang, Y. Han, F. Qiao, K.H. Row, J. Chromatogr A 1346 (2014) 16–24.
[273] M. Pourfarzib, R. Dinarvand, B. Akbari-adergani, A. Mehramizi, H. Rastegar, M. Shekarchi, J. Sep. Sci. 38 (2015) 1755–1762.
[274] S.P. Mtolo, P.N. Mahlambi, L.M. Madikizela, Water Sci. Technol. 79 (2019) 356–365.
[275] M. Pourfarzib, M. Shekarchi, H. Rastegar, B. Akbari-Adergani, A. Mehramizi, R. Dinarvand, J. Chromatogr. BAnal. Technol. Biomed. Life Sci. 974 (2015) 1–8.
[276] N.A. El Gohary, A. Madbouly, R.M. El Nashar, B. Mizaikoff, Biosens. Bioelectron. 65 (2015) 108–114.
[277] N. Erk, M. Mehmandoust, M. Soylak, Biosensors 12 (2022) 769.
[278] M. Shekarchi, M. Pourfarzib, B. Akbari-Adergani, A. Mehramizi, M. Javanbakht, R. Dinarvand, J. Chromatogr, B. Analyt Technol Biomed Life Sci 931 (2013) 50–55.
[279] Y. Yang, J. Li, Y. Liu, J. Zhang, B. Li, X. Cai, Anal. Bioanal. Chem. 400 (2011) 3665–3674.
[280] Y.J. Yang, X.W. Liu, X.J. Kong, Z. Qin, Z.H. Jiao, S.H. Li, J.Y. Li, Molecules 23 (2018) 1881.
[281] J. Chai, J. Zheng, Y. Tong, F. Chai, M. Tian, Environ. Res 236 (2023) 116756.
[282] X. Hu, Y. Guo, T. Wang, C. Liu, Y. Yang, G. Fang, J. Hazard Mater 421 (2022) 126748.
[283] M. Mehmandoust, M. Soylak, N. Erk, Talanta 253 (2023) 123991.
[284] M.B. Gholivand, M. Torkashvand, C. Mater Sci Eng, Mater. Biol. Appl. 59 (2016) 594–603.
[285] A.I. Baraian, B.C. Iacob, A.E. Bodoki, E. Bodoki, Int J. Mol. Sci. 23 (2022) 14071.
[286] D. Deville-Bonne, C. El Amri, P. Meyer, Y. Chen, L.A. Agrofoglio, J. Janin, Antivir. Res 86 (2010) 101–120.
[287] E. Rajaee, M. Izadyar, M.R. Housaindokht, J. Polym. Res. 30 (2023) 450.
[288] T. Cowen, K. Karim, S. Piletsky, Anal. Chim. Acta 936 (2016) 62–74.
[289] K.G. Shevchenko, I.S. Garkushina, F. Canfarotta, S.A. Piletsky, N.A. Barlev, Rsc Adv. 12 (2022) 3957–3968.
[290] D. Chenthamara, S. Subramaniam, S.G. Ramakrishnan, S. Krishnaswamy, M. M. Essa, F.H. Lin, M.W. Qoronfleh, Biomater. Res 23 (2019) 20.
[291] A. Kumar, S. Kashyap, F. Mazahir, R. Sharma, A.K. Yadav, Drug Discov. Today 29 (2024) 104164.
[292] X.L. Wang, H.F. Yao, X.Y. Li, X. Wang, Y.P. Huang, Z.S. Liu, Rsc Adv. 6 (2016) 94038–94047.
[293] G.K. Ali, K.M. Omer, Talanta 236 (2022) 122878.
[294] C. Bazzoli, V. Jullien, C. Le Tiec, E. Rey, F. Mentre, A.M. Taburet, Clin. Pharm. 49 (2010) 17–45.
[295] P. Singla, T. Broughton, M.V. Sullivan, S. Garg, R. Berlinguer-Palmini, P. Gupta, K.J. Smith, B. Gardner, F. Canfarotta, N.W. Turner, E. Velliou, S. Amarnath, M. Peeters, Adv. Sci. 11 (2024) e2309976.
[296] V.P. Torchilin, Biopolymers 90 (2008) 604–610.
[297] P. Chen, H. Cabral, ChemMedChem 19 (2024) e202400274.
[298] H. Zou, P. Banerjee, S.S.Y. Leung, X. Yan, Front Pharm. 11 (2020) 997.
[299] S. Schmidt, A. Barbour, M. Sahre, K.H. Rand, H. Derendorf, Curr. Opin. Pharm. 8 (2008) 549–556.
[300] Y. Li, L. Luo, Y. Kong, Y. Li, Q. Wang, M. Wang, Y. Li, A. Davenport, B. Li, Biosens. Bioelectron. 249 (2024) 116018.
[301] S. Rajpal, B. Mizaikoff, J. Mater. Chem. B 10 (2022) 6618–6626.
[302] S. Jin, Y. Zhang, R. Liu, Z. Liu, L. Gong, L. Zhang, T. Zhao, S. Chen, H. Fa, L. Niu, W. Yin, Colloids Surf. A Physicochem. Eng. Asp. 705 (2025) 135572.
[303] B. Yarahmadi, S.M. Hashemianzadeh, S.M.Milani Hosseini, Sci. Rep. 13 (2023) 12111.
[304] B. Hie, E.D. Zhong, B. Berger, B. Bryson, Science 371 (2021) 284–288.
[305] M. Arabi, A. Ostovan, Y. Wang, R. Mei, L. Fu, J. Li, X. Wang, L. Chen, Nat. Commun. 13 (2022) 5757.
[306] A. Ostovan, M. Arabi, Y. Wang, J. Li, B. Li, X. Wang, L. Chen, Adv. Mater. 34 (2022) e2203154.
[307] O. Erdem, I. Es, Y. Saylan, M. Atabay, M.A. Gungen, K. Olmez, A. Denizli, F. Inci, Nat. Commun. 14 (2023) 4840.
[308] N. Zaquen, M. Rubens, N. Corrigan, J.T. Xu, P.B. Zetterlund, C. Boyer, T. Junkers, Prog. Polym. Sci. 107 (2020) 101256.
[309] C. Caceres, E. Moczko, I. Basozabal, A. Guerreiro, S. Piletsky, Polymers 13 (2021) 314.
[310] J.-M. Lu, J.-Z. Pan, Y.-M. Mo, Q. Fang, Artificial intelligence, Chemistry 2 (2024) 100057.

[311] B.A. Rizkin, A.S. Shkolnik, N.J. Ferraro, R.L. Hartman, Nat. Mach. Intell. 2 (2020) 200–209.
[312] T. Sato, K. Masuda, C. Sano, K. Matsumoto, H. Numata, S. Munetoh, T. Kasama, R. Miyake, Micromachines 15 (2024) 1064.
[313] L. Chemmalil, T. Prabhakar, J. Kuang, J. West, Z. Tan, V. Ehamparanathan, Y. Song, J. Xu, J. Ding, Z. Li, Biotechnol. Bioeng. 117 (2020) 3757–3765.
[314] D.K. Gupta, A. Tiwari, Y. Yadav, P. Soni, M. Joshi, Front Med Technol. 6 (2024) 1377443.
[315] F.D. Rodriguez-Gomez, O. Penon, D. Monferrer, P. Rivera-Gil, Front Med. 10 (2023) 1212949.
[316] F. Caputo, G. Favre, G. Borchard, L. Calzolai, P. Fisicaro, E. Frejafon, N. Gunday-Tureli, D. Koltsov, C. Minelli, B.C. Nelson, J. Parot, A. Prina-Mello, S. Zou, F. X. Ouf, Drug Deliv. Transl. Res. 14 (2024) 2578–2588.
[317] H.A. Parray, S. Shukla, R. Perween, R. Khatri, T. Shrivastava, V. Singh, P. Murugavelu, S. Ahmed, S. Samal, C. Sharma, S. Sinha, K. Luthra, R. Kumar, Appl. Microbiol Biotechnol. 105 (2021) 6315–6332.
[318] Z. Jin, S. Gao, X. Cui, D. Sun, K. Zhao, Int, J. Pharm. 572 (2019) 118731.
[319] A.L.Z. Lee, C. Yang, S. Gao, Y. Wang, J.L. Hedrick, Y.Y. Yang, A.C.S. Appl Mater, Interfaces 12 (2020) 52285–52297.

Xiaohan Ma is a Ph.D. candidate and UCL Research Excellence Scholar at the Eastman Dental Institute, University College London. His research focuses on antimicrobial molecularly imprinted polymers for infection control and biomedical applications. Before joining UCL, he carried out translational research at the Shanghai Institute of Ceramics, Chinese Academy of Sciences, where he led projects on advanced medical coatings and biointeractive surfaces. He holds a B.Eng. in Materials Science and Engineering from Jinling Institute of Technology. His work bridges polymer nanotechnology and clinical translation, with the goal of developing next-generation therapeutic materials and diagnostic technologies.

Latifa Allahou holds an MPharm degree from the University of Nottingham and an MSc in Nanotechnology and Regenerative Medicine from University College London (UCL). She is currently pursuing a PhD in nanomedicine at UCL under the supervision of Dr Alessandro Poma, supported by a scholarship from Kuwait University. Her research focuses on the development of nanoparticle-based platforms for immunotherapeutic applications in oncology, with broader interests in drug delivery, cancer immunotherapy, and biomedical nanotechnology.

Ren Yang currently works as a research assistant at the Department of Orthopedics Laboratory at Guangdong Provincial People's Hospital. She holds a Master of Science in Pharmaceutics from University College London (UCL), where she completed her dissertation at the UCL Eastman Dental Institute under the supervision of Dr. Alessandro Poma. Her research interests center on molecularly imprinted polymers (MIPs) and the design of functional biomaterials for regenerative medicine and antimicrobial applications. She will shortly commence her PhD study at the UCL Eastman Dental Institute, continuing her work on innovative biomaterial strategies for clinical translation.

Yingqi Ma earned her BSc in Pharmacology (2023) and MSc in Pharmaceutics (2024) from University College London. Her academic journey has focused on pioneering cancer therapies through biodegradable molecular imprinting techniques. Her research interests include nanoparticle-based drug delivery systems, biodegradable polymer development, and targeted oncology treatment modalities. Motivated by a commitment to pharmaceutical innovation, Yingqi aspires to play a leading role in future drug development, dedicated to bridging cutting-edge delivery technologies with real-world clinical impact to improve patient outcomes and address critical unmet medical needs.

Myrto Dimoula works at OFET Group of Pharmaceutical companies as a Research and Development Analyst. She graduated from University College London with a master of science in Pharmaceutics, where she conducted her dissertation at the UCL Eastman Dental Institute with the supervision of Dr. Alessandro Poma. She is a licensed Pharmacist, having completed her MPharm at the National and Kapodistrian University of Athens. Her job mainly focuses on conducting and validating analytical methods to produce data allowing new products to enter the pharmaceutical market. She aspires to be a principled formulation scientist committed to developing impactful pharmaceutical solutions that improve patient outcomes and address unmet medical needs.

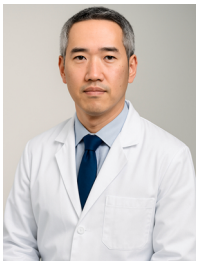

David Chau is Associate Professor at UCL specialising in regenerative medicine, and biotechnology. David originally trained as a (bio)chemical engineer (BEng, MSc) before gaining a PhD in the field of Tissue Engineering, and then several postdoc roles at the Universities of Nottingham and Cambridge during which he generated > 18 scientific articles and an international patent. David started his academic career as a Lecturer/Senior Lecturer in Pharmaceutics at the University of Hertfordshire before progressing to his current position at UCL. David is a firm believer of the concept "to make things better, you first need to know how it works", and the application of a "benchside-to-bedside approach. He also believes that you should "think big" as "people don't build planes, if they don't dream of flying". David's main research interest focuses on biotechnology- in particular its use for regenerative medicine and drug delivery. Previous outputs have centred on developing novel therapeutic modalities with an emphasis of applications to skin, the eye and the brain. Current interests include the development of novel (bio)mimetic materials, sustainable biotechnology, and the development of immortalised (stem) cells. He is also the Founder and CSO of a spin-out company that repurposes waste eggshells to develop novel wound dressings, and sustainable alternative packaging materials.

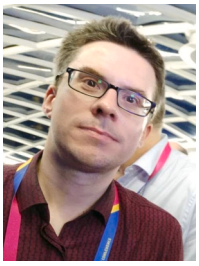

Gareth received a MChem (Hons) degree from the University of Oxford in 2002. He remained in Oxford for a DPhil (PhD), supervised by Prof Dermot O'Hare, which was completed in 2005. Gareth's PhD work was focused on the use of synchrotron techniques to monitor intercalation reactions in situ. After graduation, he worked as a post-doctoral researcher and in science program management. In September 2010 he joined London Metropolitan University as a Senior Lecturer in Pharmaceutical Science, and in November 2012 was appointed to the UCL School of Pharmacy as a Lecturer in Pharmaceutics. He was promoted to Associate Professor in 2016 and to full Professor in 2020, when he also became Head of Pharmaceutics. Gareth leads a group of around 15 researchers applying inorganic and polymer-based nanomaterials to overcome drug delivery challenges. He greatly enjoys fine cheeses.

Jonathan Knowles is Professor of Biomaterials Science at University College London. His work mainly focusses on degradable materials for a wide range of clinical applications including repair of musculoskeletal tissues and drug delivery. He has had funding from a wide range of agencies and this has culminated in nearly 500 publications and over 38,000 citations and an h index of over 100. During his career he has also been a visiting Professor at the University of Aveiro and Dankook University as part of the World Class Universities program and subsequent funding. He is a Fellow of the Institute of Materials Mineral and Mining and the Royal Society of Chemistry.

Dr Alessandro Poma received his MSc in Pharmaceutical Technology and Chemistry from the University of Palermo (Italy) in 2009. He then joined Cranfield University to undertake a PhD in Biosensors and Nanomaterials (2013). He moved to UCL in 2014, first as an NC3Rs David Sainsbury Fellow and subsequently in other roles, and in 2019 he has been appointed Lecturer in Biomaterials and Allied Subjects in the Division of Biomaterials and Tissue Engineering. His key research area is the development of nanomaterials as synthetic antibodies as well as gene/drug delivery systems, and their biodegradable composites for diagnostic, therapeutic and tissue engineering applications.